ELECTROCHEMICAL MACHINING

Anthony Christopher Baxter

A Thesis submitted to the

UNIVERSITY OF WARWICK

for the degree of

Doctor of Philosophy.

1967

PREFACE

The work reported here is, except where acknowledged by the citing of references, my own work. It is, as far as I am aware, original, and the detailed description of the fundamental phenomena of electrochemical machining represents a considerable advance in the understanding of the process.

I wish to thank my supervisor, Professor Shercliff, for his interest and many valuable suggestions and criticisms, and for keeping my feet firmly on the ground. I should also like to thank the workers at the Universities of Nottingham and Leicester with whom I have had much useful contact. I wish to record my gratitude to the Science Research Council and Shell International Petroleum company whose financial support made it possible for me to pursue this study. Last, but far from least, I must thank Mr. Webb, who has helped me enormously by his criticism of my apparatus, and then nevertheless producing a perfect job.

SUMMARY.

The thesis describes an investigation into the fundamental phenomena governing the electrochemical machining process. It excludes a detailed investigation of the electrochemistry of the anode surface, work on which is in hand at the University of Nottingham.

Photographs have been obtained of both electrode surfaces during machining in a two dimensional channel, showing the important role of gas evolution both at currents below the limit and in limiting the current density achievable. The distribution of electrical potential across the gap has been measured, clearly showing that the limiting current phenomenon is governed by a process occurring very close to the cathode. Measurements have been made of the streamwise current distribution; the distribution is essentially uniform at low currents, but as the limit is approached the current at the downstream end falls, and this fall then propagates upstream to fill about two-thirds of the channel. It has been found that the limiting current is proportional to $(\text{absolute pressure})^{\frac{1}{3}}$, that the size of bubbles produced is inversely proportional to $(\text{absolute pressure})^{\frac{1}{3}}$, and that reduction of the surface tension of the electrolyte leads to a marked fall in limiting current. The efficiency of the process has been investigated by a technique involving the measurement of the gas evolved during machining.

An analysis of these results leads to the formulation of an explanation of the cell voltage-current characteristic, a hypothesis to explain the current limiting process, and a suggestion of the detailed mechanism of the latter.

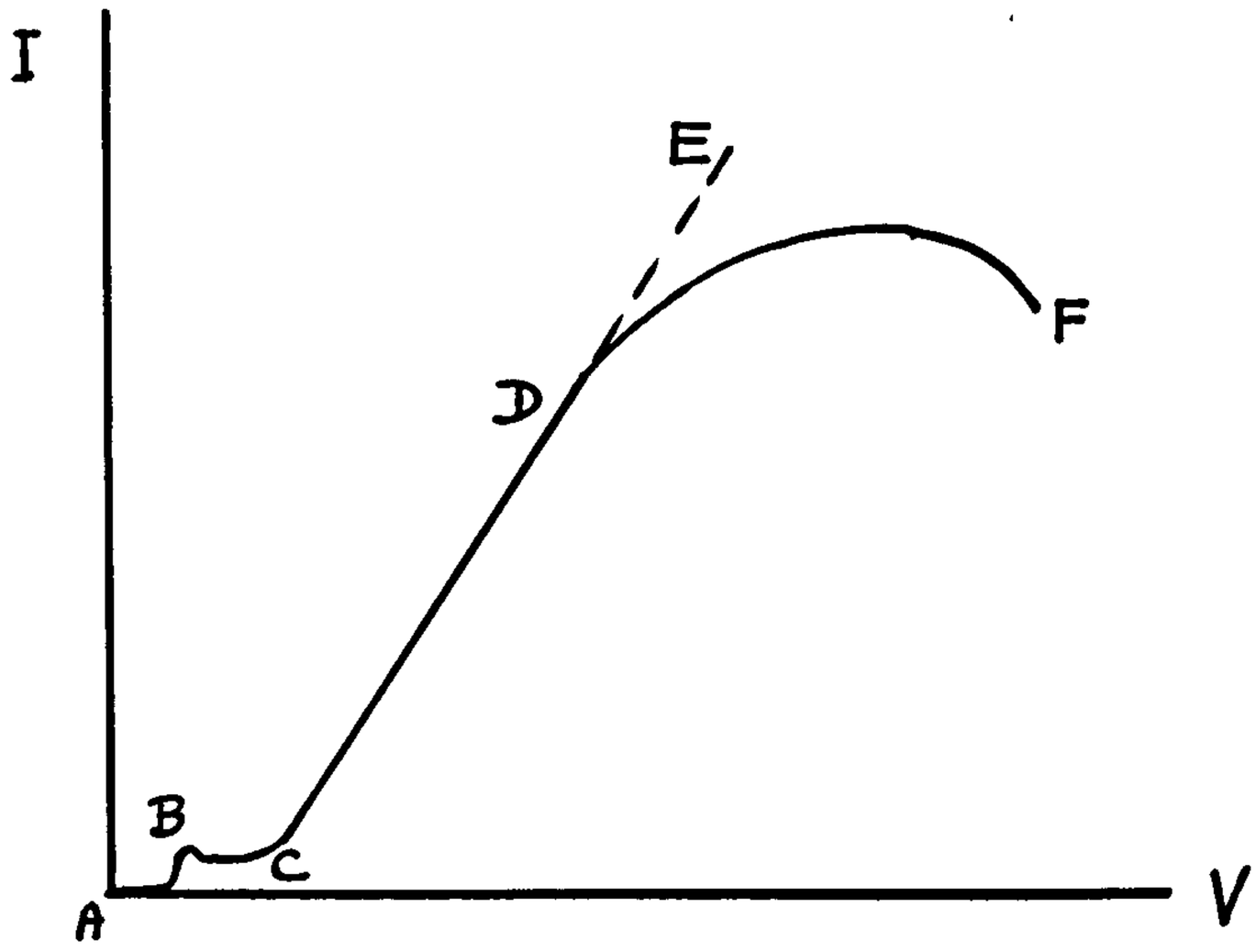

The cell voltage-current curve (above) can be explained as follows:- AB is equilibrium dissolution with etching, BC is caused by the formulation of a solid (impure oxide?) film on the anode surface. The rise in current from C to D is caused by the anodic evolution of a gas (oxygen?), causing better mixing conditions in the diffusion layer near the anode and hence a higher metal dissolution rate. The ratio of current used for metal dissolution to current used for gas evolution appears to be a constant for this region. This process would be expected to continue along DE, but the current is limited by the achievement of a maximum rate of cathodic hydrogen evolution which brings about the reduction in current to F.

This limiting current crisis has been analysed in terms of the mechanics of bubble formation, and a detailed explanation in terms of various mechanisms has been attempted. The experimental data is fitted by a model in which the hydrodynamic conditions give a velocity at which bubbles can be removed from a fixed number of nucleation sites. The limiting current is then predicted to be proportional to (surface tension)^{2} x (absolute pressure)$^{\frac{1}{3}}$.

Several proposals are made for further experiments to investigate these proposals, and for data needed to extend the industrial application of the theory developed.

CONTENTS.

LIST OF FIGURES

LAYOUT

The thesis can be divided into three main sections.

The first part, consisting of Chapters 1 to 3, is an introduction to the subject and a discussion of the methods and apparatus involved in the investigation.

Chapters 4 to 8 contain the results of the planned experiments, including the development of the instrumentation involved; Chapter 9 is a discussion of these results leading to a hypothesis of the controlling processes.

Further experiments were performed to check and expand this hypothesis, these are reported in Chapter 10 and discussed in Chapter 11. Chapter 12 includes an extension of convective mass transfer theory to include variations in viscosity and diffusion coefficient. The thesis ends with some proposals for further research brought to light by this investigation.

Figures are bound in the relevant position in the text.

INTRODUCTION

1.

1.1 BACKGROUND

Electrochemical machining (E.C.M.) is at the same time both a new and an old process. Its development can be traced from its origin in the laws of electrolysis as stated by Faraday. As applied to metals these laws are industrially most familiar in the cathodic process of electroplating.

This process generally takes place under conditions of natural convection or in "stirred" tanks, with well separated electrodes, as does the similar process of electro-refining of copper; the anodic reaction of electro-dissolution being a subsidiary one in these processes.

The only industrial application of anodic dissolution has been electropolishing. This has been used in the laboratory for many years, and the industrial application dates back nearly as far. In most cases the process is simply one of finishing, the production of a very smooth, reflecting surface, the amount of metal removed being of secondary importance.

A recent application of polishing, called electrolytic super-finishing, was reported in 1955 in France (1) where gear wheels for high speed locomotives were finished to produce an accurate, polished profile. The electrolyte velocity was low and the gaps large.

About 1950 there was a sudden increase in interest in the E.C.M. process due to the advent of modern aerospace materials, the machining of which was proving to be slow and expensive.

These materials are used particularly in the hot spots of gas turbine engines, the machining of the turbine stators and rotors being particularly difficult due to the aerodynamic shape of the components. The alternative process of spark machining is slow, and produces a rather

rough finish. A new process was required for cutting these materials. This led naturally to the interest in electro-machining, the rate of which is independent of material hardness, and which lends itself naturally to operations which are difficult by conventional means, such as turbine blades, deep hole drilling and diesinking.

1-2

1.2 ELECTROCHEMICAL MACHINING.(E.C.M.) in 1965

By 1965 much experience had been gained in operating the process, particularly in the United States. The published literature contained little beyond advertising and any data published was so incomplete as to be useless. The most useful of these are referred to in the list of references.

An exception must be made in the work of Bayer (2) whose report contains much of interest.

At that time the state of electrochemical machining can be summarised as a collection of local experimental experience held by each concern; all development aimed at producing a product using existing techniques, modified if necessary. There was no understanding of the basic processes at work, conflicting data as to the effect of varying various parameters and no evidence of any attempt to correlate E.C.M. with related phenomena such as electropolishing.

1-3

1.3 PROPOSALS FOR INVESTIGATION

Three problems were evident at the time the present work was started. They were:-

(1) The electrochemistry of the electrode reactions

(2) The 'Physicochemical Hydrodynamics' (Levich) of the process

(3) The development of control methods and instrumentation for this purpose.

Work on (1) was proceeding at the University of Nottingham and B.S.A. research centre; much was being done by Industrial research laboratories such as Associated Engineering, Bristol Siddeley, M.T.I.R.A., P.E.R.A. and Rolls-Royce, mainly on practical aspects and control methods. Work at the University of Glasgow (now at Leicester) was being done on the effect of the flow on surface finish and metal removal rates(3). It was,therefore, decided to investigate the controlling phenomena involved and to concentrate mainly on the fluid aspects.

2. OUTLINE OF RESEARCH PROPOSED.

2.1 As has been mentioned, there existed a lack of information on the basic processes involved, and it was decided to investigate these under the simplest possible geometrical conditions using four experimental methods; external voltage-current characteristics, electric potential distribution across the gap, streamwise current density variation, and photographic observations. Approaching from the theoretical angle, it was decided to attempt to extend the theory of mass transfer to the conditions existing in E.C.M. The results of the experiments eventually showed that the extension of the theory was made in the wrong direction and hence it was dropped.

An outline of this work is included in Chapter 12 for completeness.

Faraday's original work on electrolysis involved low current densities on well separated electrodes. To be economic, E.C.M. must remove metal reasonably fast, and, therefore, the current density must be raised. Accuracy is also a requirement, and to achieve this a tool of nearly the same form as the required final work shape is separated from the work by a small gap. The high current densities now produced lead to Joule heating of the electrolyte and hydrogen evolution at the cathode(tool). To alleviate these effects a fast flow of electrolyte is required.

The present state of E.C.M., therefore, involves a narrow channel containing a high velocity flow of electrolyte; metal being removed from the anode, hydrogen being generated at the cathode and Joule heat being evolved throughout.

Since the investigation was to be essentially a basic one, no attempt was made to make the experiments conform to actual E.C.M. practice where there was reasonable evidence that the difference was basically unimportant. The important changes decided on were as follows:-

(1) A Two dimensional channel was chosen with a width of $\frac{1}{2}$ inch and a flow length of 2 inches (sometimes 1 inch) This allowed the inclusion of nonconducting side windows to enable photographic observations to be made, and reduced the complexity of the hydrodynamic situation, though introducing edge effects.

(2) A stationary cathode was employed. Though a motor drive was included, it was used for positioning rather than maintaining a dynamically constant gap. This is justified as the ratio between the flow and electrode advance velocities is of the order of 10^6

(3) The investigation was restricted in the main to one material for both electrodes, copper, and one electrolyte, phosphoric acid of specific gravity 1.2 to 1.25.

The reasons for this last choice were as follows:-

(a) The combination of electrode/electrolyte has to allow the process to proceed at the required high rates. As a result of reading papers on the anodic dissolution of metals; the most important of which were those of Hoar(4a, b, c,) and his workers at Cambridge; I formed the hypothesis that E.C.M. was a process similar to electropolishing , in that a solid film on the anode surface was involved and that, therefore, a good electropolishing electrolyte would be a good E.C.M. electrolyte. A large amount of literature is available on the copper/phosphoric acid system for electropolishing; and indeed most fundamental work on these phenomena was and is being done using

this system because of its comparative simplicity.

(b) Bayer(2) reported some attempts to photograph E.C.M. using neutral salt electrolytes and attributed his failure to obtain results to the scatterings of light by the suspended metal hydroxide. This favoured the adoption of an acid electrolyte in which the metal goes into solution, despite the disadvantage that eventually it has to be discarded when metal deposition as a powder on the cathode leads to short circuiting of the gap.

(c) For the potential distribution investigation the problem of reference electrodes arises and in phosphoric acid copper is a suitable reference electrode (Hoar.4a).

(d) Mineral acids have higher conductivities than salts because of the high mobility of the hydrogenion, and they will thus produce less Joule heating under similar conditions.

(e) Phosphoric acid is the least corrosive of the mineral acids, being neither a 'strong' acid nor a powerful oxidising agent.

3. APPARATUS

3.1. Working Section.

Figure 3.1 shows the working section which was designed to provide a flow channel 2" long, $\frac{1}{2}$" wide with a gap variable up to $\frac{1}{4}$". It was stressed to withstand a pressure of 500p.s.i. over the area inside the sealing 'O' ring, and made of two blocks of P.V.C., with copper and bronze fittings to permit the entry of the electrodes, one electrode being fixed and the other moveable, $\frac{1}{4}$" thick glass windows were let into the sides of the channel to allow optical observations to be made. All joints were sealed with rubber 'O' rings with the exception of the fluid couplings which were sealed with Dowty bonded seals. Setting chambers were provided at entry and exit

from the working channel; Pressure tappings were made in each of these chambers and in the entry and exit areas of the actual machining channel. Provision was made for the introduction of sheathed thermocouples in the settling chambers, though in practice the sheathing proved incapable of withstanding the environment and no useful temperature measurements were made.

Figures 3.2 and 3.3 show the general arrangement of the apparatus.

3.2

3.2 ELECTRICAL CIRCUIT.

D.C. Power was provided by a motor generator set producing up to 60V and up to 1000A; a ballast resistor was included to protect the apparatus generally from short circuits in the working section. A 'Witton' Potentiostat producing 10 Amps. was also used as a power source in some experiments to investigate the low current phenomena involved. For this a copper wire reference electrode was fitted in the working section just upstream of the anode. The current was carried by solid copper bus bars and flexible braid leads to the working section. Provision was made for measuring the current and voltage across the working section.

3.3

3.3 FLUID CIRCUIT.

A tank farm of four 35 gallon polythene tanks was provided with selection by ball valve to inlet and outlet manifolds. A mains water inlet was provided for flushing the apparatus and a drainage connection to the outlet manifold. A strainer was provided before the pump, and a ceramic filter after it. The flow rate was governed by a variable spring relief valve acting as a by-pass, and measured with rotameters. Provision was also included for back flushing the filter with mains water.

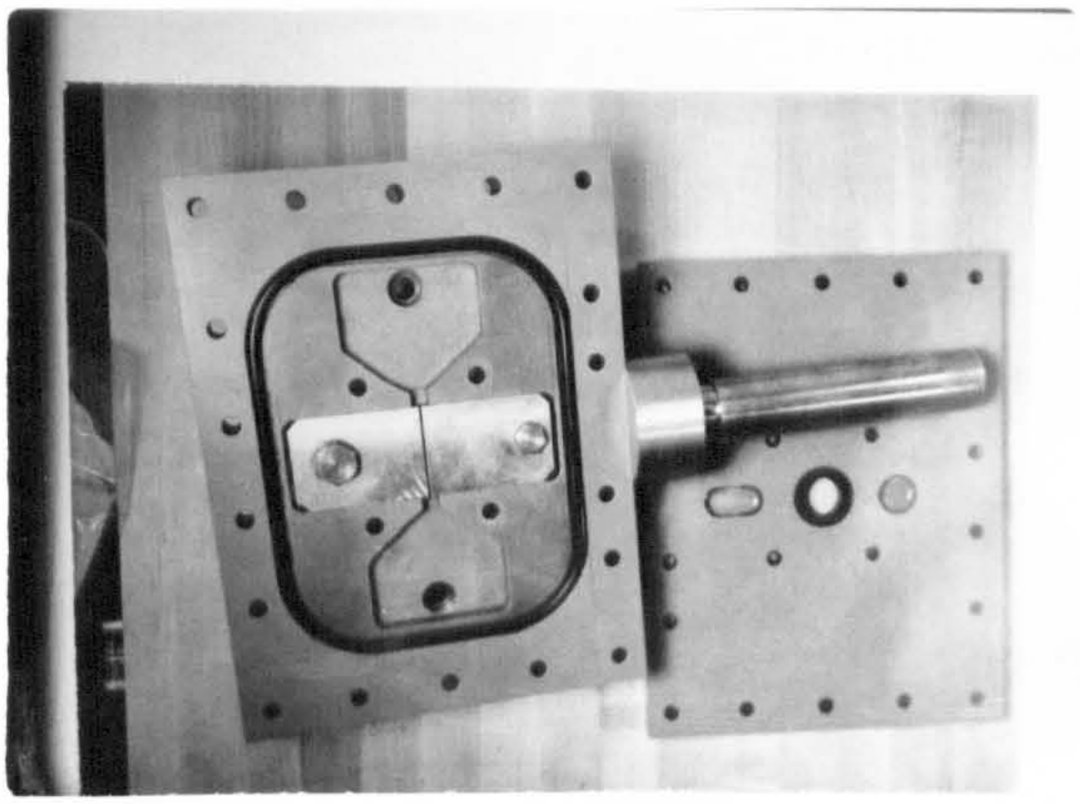

Figure 3.1 Working section.

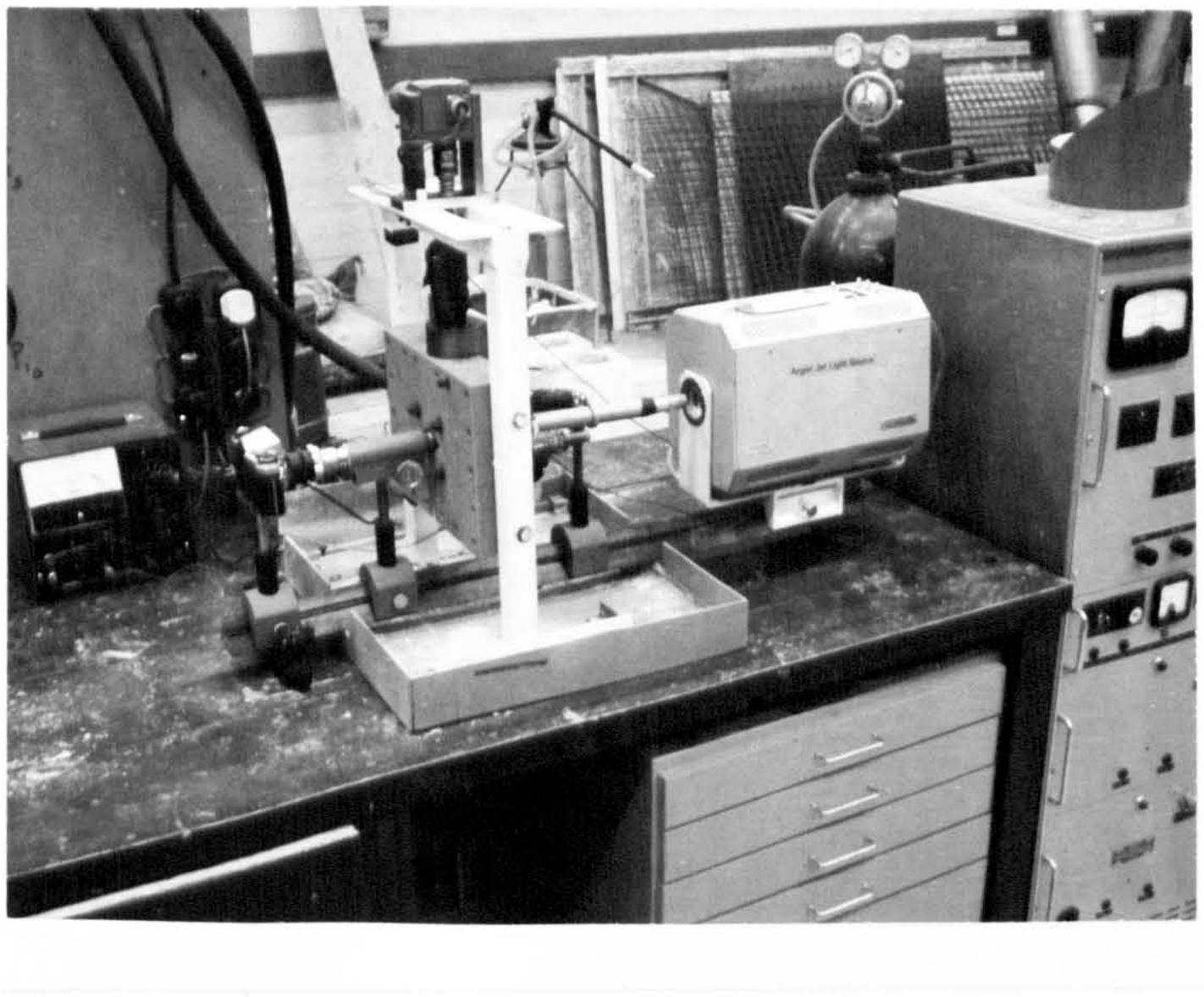

Figure 3.2 Working bench area.

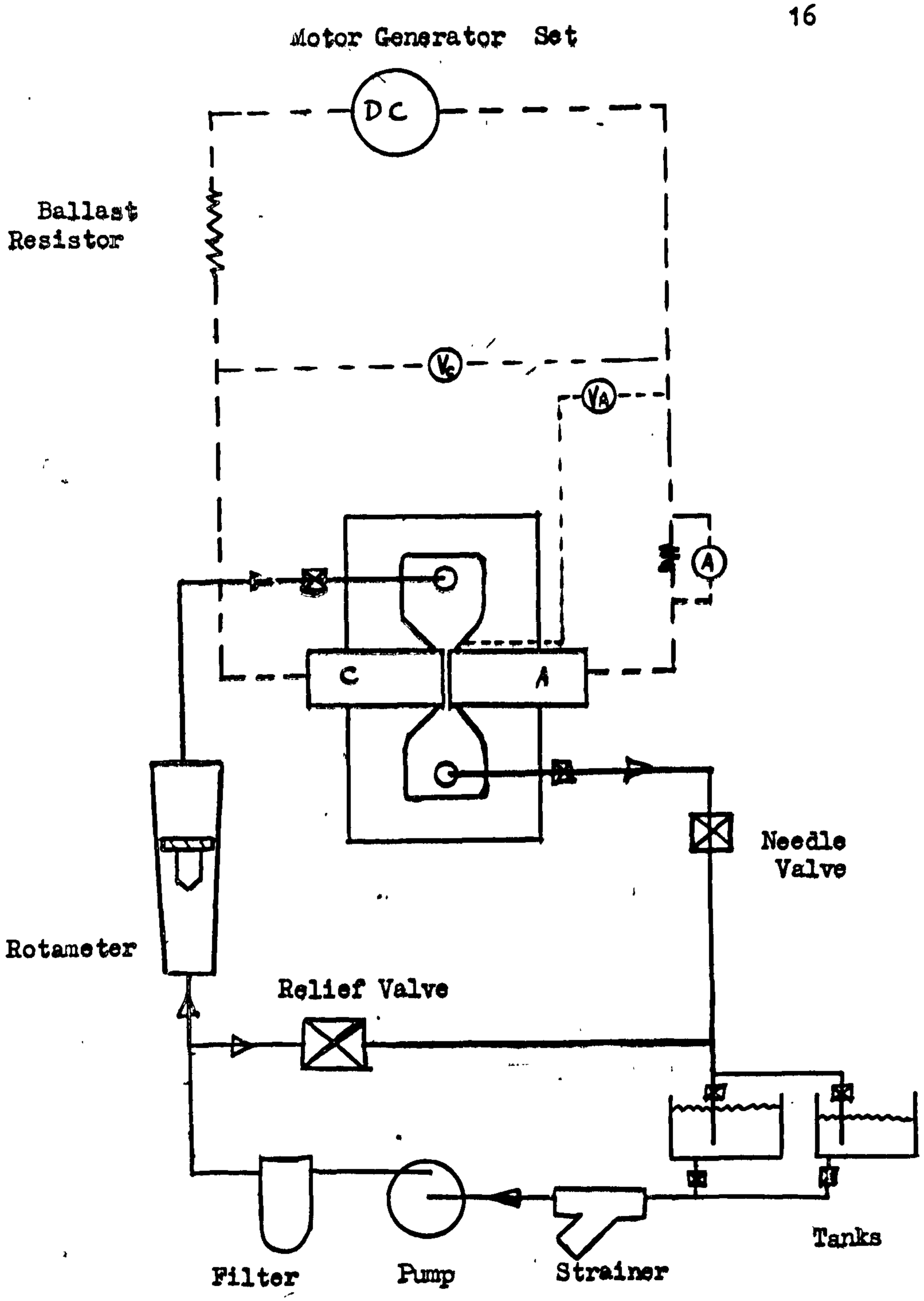

Electrical and fluid circuits.

Figure 3.3

The pump initially installed was a 'Gyrobloc' pump in cast iron with a bronze impeller made by Holden and Brooke,Ltd., but the seal of this gave unending trouble due to misalignment and it was eventually discarded when the rotor and casing became corroded and worn due to fouling.. It was replaced by a 'Handipump' made by Stainless Steel Pumps,Ltd., that has since given good service, though only a limited pressure performance. The plumbing of the low pressure side of the apparatus was in $\frac{3}{4}$" rigid P.V.C. pipe and fittings and the high pressure side was copper pipe connected with bronze fittings copied from standard 'Keelaring' components. Wire reinforced rubber hose was used to convey the fluid to and from the working section.

This arrangement has proved successful and little corrosion was noted at stainless steel/bronze/copper connections.

3.4 Working Area.

The working section was mounted in a steel framework which also supported the electrode drive mechanism. The frame was stood in a P.V.C. tray on a bench with sufficient clearance between the working section and the tray to allow an optical bench to be placed there to support the optical apparatus. A transparent cover was made to enclose the working section for additional safety when high pressures were in use.

3.5 Optical apparatus.

The layout is shown in Figure 3.2.

The light source was an Argon Jet spark source made by Lunartron Electronics,Ltd. of Luton and supplied by Optical Works,Ltd. of Ealing. It has an output of 3 Joules in 0.2 micro seconds and is triggered by the flash contacts on the camera.

This was chosen after consideration of the results of Bayer(2) who failed to obtain useful results with cine-photography. He reported that about 0.1 Joules gave no image on 250 ASA film at 1/2000 second exposure, about .3 Joules gave a faint blurred image on 250 ASA film at 1/640 second; and indicated that 100 microsecond exposure should freezethe motion. The combination of 3 Joules in 0.2 microseconds with 800 ASA film and acid electrolyte was considered to be likely to produce results.

This was in fact the case and the combination has proved very successful.

The light from the source was concentrated on the area of interest by a bench microscope working backwards and the transmitted light obs rved with a microscope at x 25 magnification on the film of a 'Pentax' camera coupled to it.

3.6 Enclosure

The tanks, pump, valves etc., were mounted inside a P.V.C. 'house' 8' x 4' x 6' to contain any spillage due to leaks or bursts. The instruments were mounted on the front panel of this house and the working area bench placed in front of it as shown in Figure 3.2 A fan was fitted to the house to remove the hydrogen evolved to the outside air.

3.7 Various special pieces of apparatus and instrumentation were constructed and used during the course of the investigation and these are described as they occur.

4. EXTERNAL CURRENT- VOLTAGE MEASUREMENTS

The external current- voltage characteristic was measured, by two methods, for a range of gaps from .025" to .1", and for a range of electrolyte flow rates from 0.4 to 20 cubic ins/second.

Initially the technique was to note current and voltage readings as the voltage was increased in steps, adjusting the relief valve as needed to maintain the flow rate.

The gap was set at about .002" less than the nominal value for the run and allowed to increase to .002" more than the nominal value. This entails introducing a scatter of up to $\pm$ 12% in the worst case, but any attempt to move the cathode to keep the gap constant would involve either much trial and error to find the correct feed rate, by which time the preferential attack at the edges of the anode would require it to be replaced or some method of measuring the actual gap during machining. Such a measurement must be regarded as highly desirable and is worthy of great effort to find a solution, which at present appears remote.

Later an X-Y recorder became available and this was used to record the characteristic directly, the voltage being increased steadily and the flow rate maintained with the relief valve. This method, still with stationary electrodes, allowed faster measurements, but still permitted the gap to increase by up to .004", or 12% of the smallest gap. For larger gaps, normally involving lower current densities, the problem of gap accuracy is much reduced and is normally within 5%. The lower limit of gap of .025" was in fact mainly determined by this factor, though arcing due to copper deposition on the cathode when old electrolyte was used was also a factor in fixing this lower limit.

Figure 4.1 shows a typical trace from the X-Y recorder experiments. It shows several interesting features, the most important of which is the fact that eventually a limiting value of current is reached, further increase in voltage leading to a reduced current.

This limiting current was investigated using both manual and X-Y recorder methods and the results are contained in Table 4.2 and Figure 4.3

The layout of Table 4.2 is as follows;- single lines divide the results obtained in different series of experiments; those above the double line were obtained by the initial technique, while those below it were obtained by the X-Y recorder method.

The heavy upper line in Figure 4.3 is drawn through the early results, and the three short lines show the variation due to gap found later for smaller gaps, the late results for larger gaps fall near the main line.

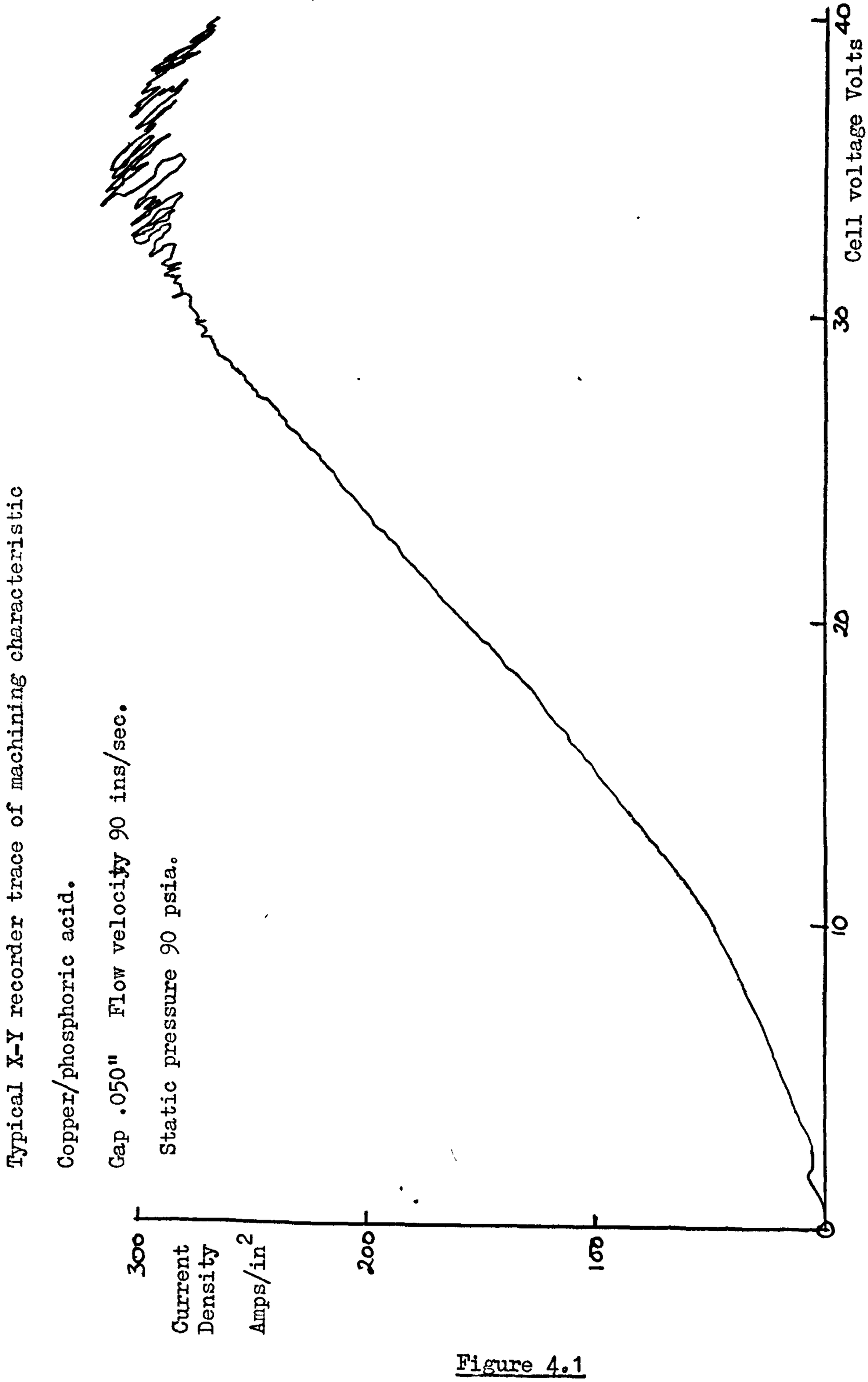
Typical X-Y recorder trace of machining characteristic
Copper/phosphoric acid.
Gap .050" Flow velocity 90 ins/sec.
Static pressure 90 psia.
Current Density Amps/in^2
300
200
100
0
10
20
30
40
Cell voltage Volts

Figure 4.1

TABLE 4.2

Acid S.G.	Temperature of Tank (°C)	I lim Amps/in²	Gap ins	Mean flow velocity Ins/ Sec
1.225	20	138	.050	82
1.225	24	203	.025	164
1.21	24	120	.025	79
1.20	16	202	.025	122
1.20	16	80	.025	32
1.20	18	260	.025	220
1.19	20	130	.075	74
1.19	22	165	.040	104
1.19	22	180	.040	138
1.19	23	135	.040	77
1.19	24	100	.040	50
1.19	25	120	.060	70
1.20	15	136	.030	84
1.20	17	205	.030	138
1.20	19	232	.030	183
1.165	22	212	.025	223
1.215	19	232	.030	182
1.215	20	224	.025	237
1.215	24	227	.050	181
1.245	14	122	.050	82
1.245	14	72	.050	39
1.245	23	145	.050	82
1.18	18	225	.025	625
1.18	25	300	.050	590
1.17	27	185	.025	450
1.17	17	135	.025	222
1.225	22	200	.024	455
1.22	24	270	.025	790
1.22	21	290	.050	398
1.22	21	180	.050	89
1.20	21	116	.050	39
1.20	21	72	.050	38
1.205	21	70	.025	78
1.205	21	85	.050	39
1.203	21	290	.075	330
1.205	26	40	.025	32
1.205	28	210	.100	202
1.205	18	180	.042	265
1.205	18	157	.030	240
1.205	18	127	.029	187
1.205	18	169	.042	220
1.205	18	180	.032	290
1.205	18	185	.032	290
1.205	18	202	.032	350

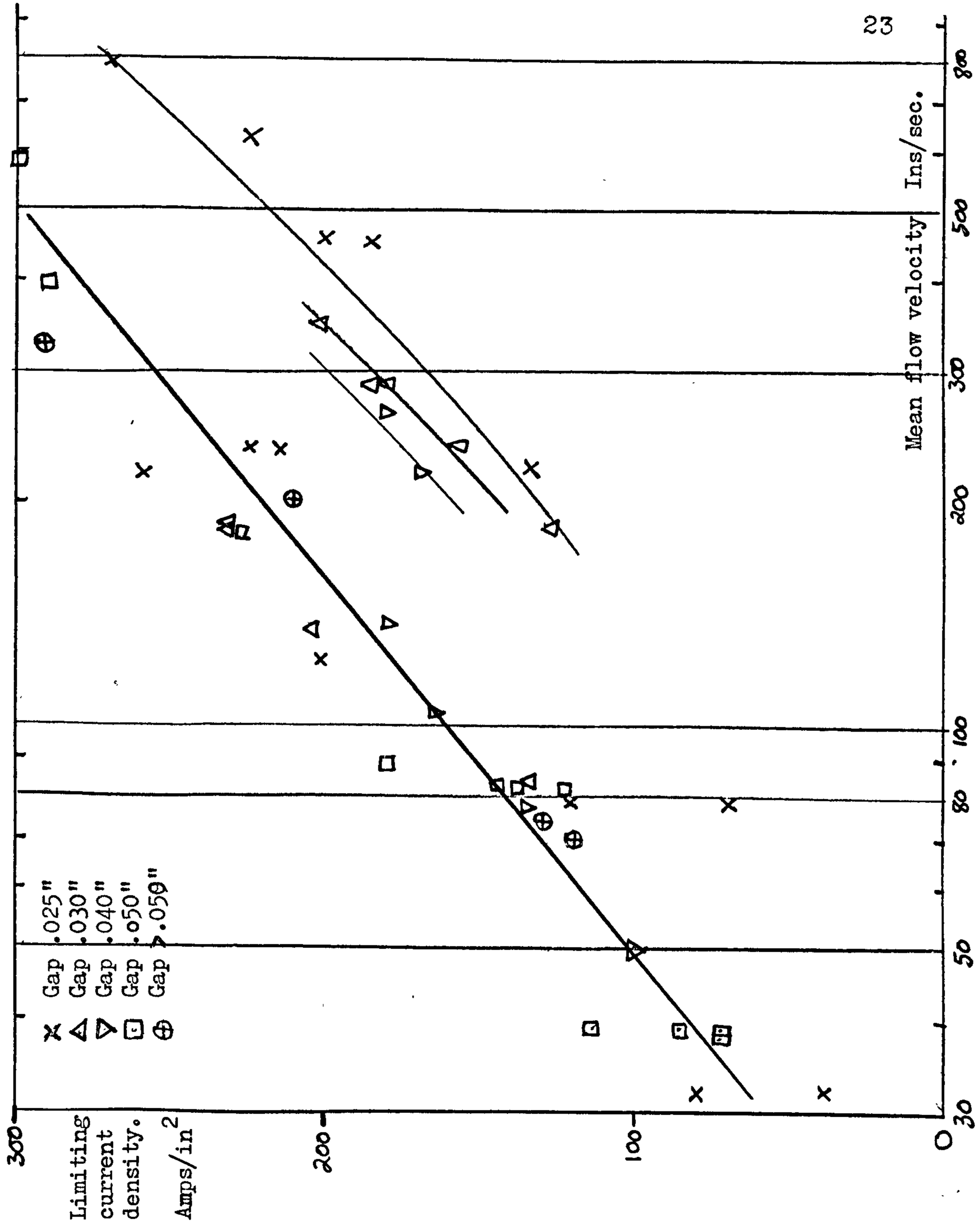

Variation of limiting current density with mean flow velocity.

Copper/ phosphoric acid

Figure 4.3.

5. Photographic Experiments

Photomicrographs have been obtained using the 0.2 microsecond spark source at x 25 and x 4 magnification on 35mm film.

The optical setup can be seen in Figure 3.2.

The light from the spark source was concentrated on the machining area with a bench microscope, and the camera fixed to the back of another bench microscope. This latter was focused as close to the centre of the channel as possible and the illuminating microscope adjusted to produce the maximum illumination. All photographs shown in this chapter were obtained with $\frac{1}{2}$" wide channels.

Figures 5.1 to 5.3 show the bubble boundary layers on both electrodes for a gap of .045" at x 10 magnification at currents up to the limiting value.

They show the entry regions of a channel of 1" flow path. The gross eddies in the last frame are suspected to be due to trapping of hydrogen evolved on the front edge of the cathode in the entry section, followed by its ingestion as large bubbles.

Figures 5.4 to 5.7 show, at magnification x 50, the entry section of a copper anode with the upstream portion filled with perspex.

These two series of photographs indicate clearly the importance of the anodic evolution of a gas. In particular in Figure 5.6 it can be seen that the bubbles are moving copper saturated acid into the bulk of the fluid much more rapidly than diffusion. This is clearly shown by the streaks, trailing from the bubbles, which indicate areas of higher density.

A series of photographic experiments was also conducted to measure the size of bubbles evolved. In this case photographs were obtained at low current densities so that individual bubbles free from interference

Figures 5.1 to 5.3.
Copper/Phosphoric acid.
Gap .o45"
Flow 90 ins/sec.
x10

GEOMETRY.

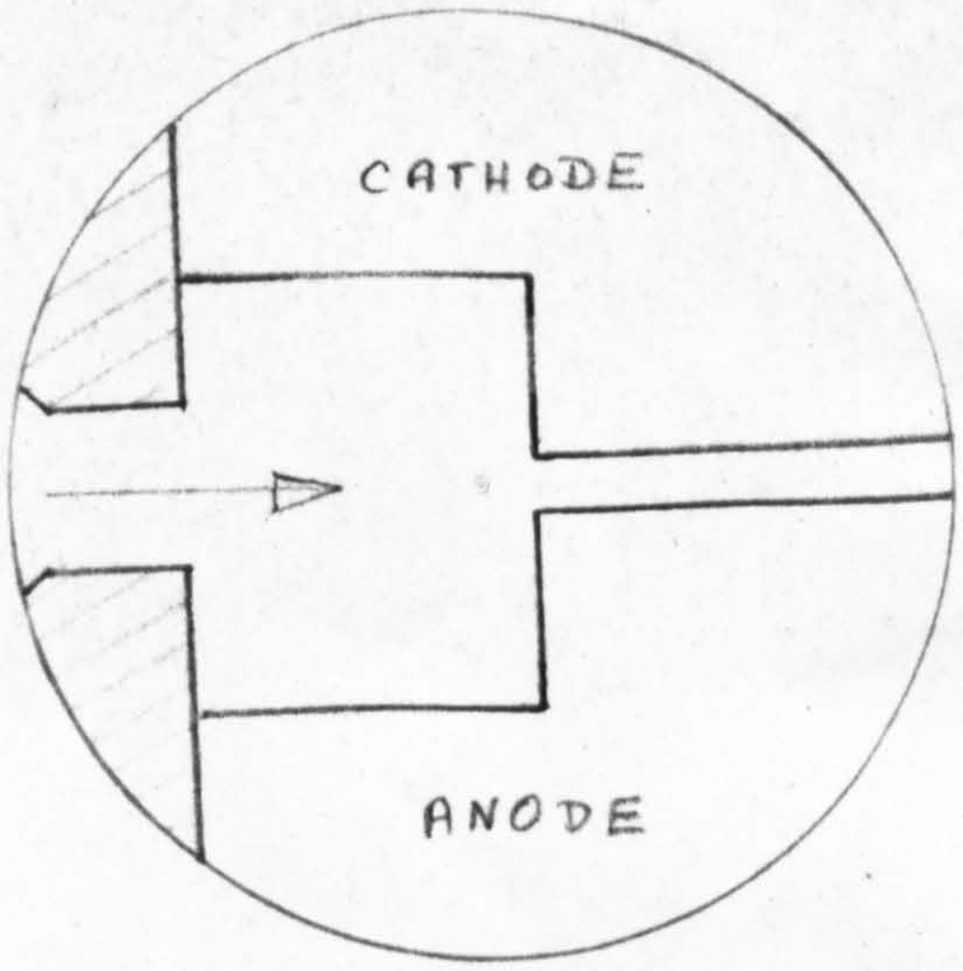

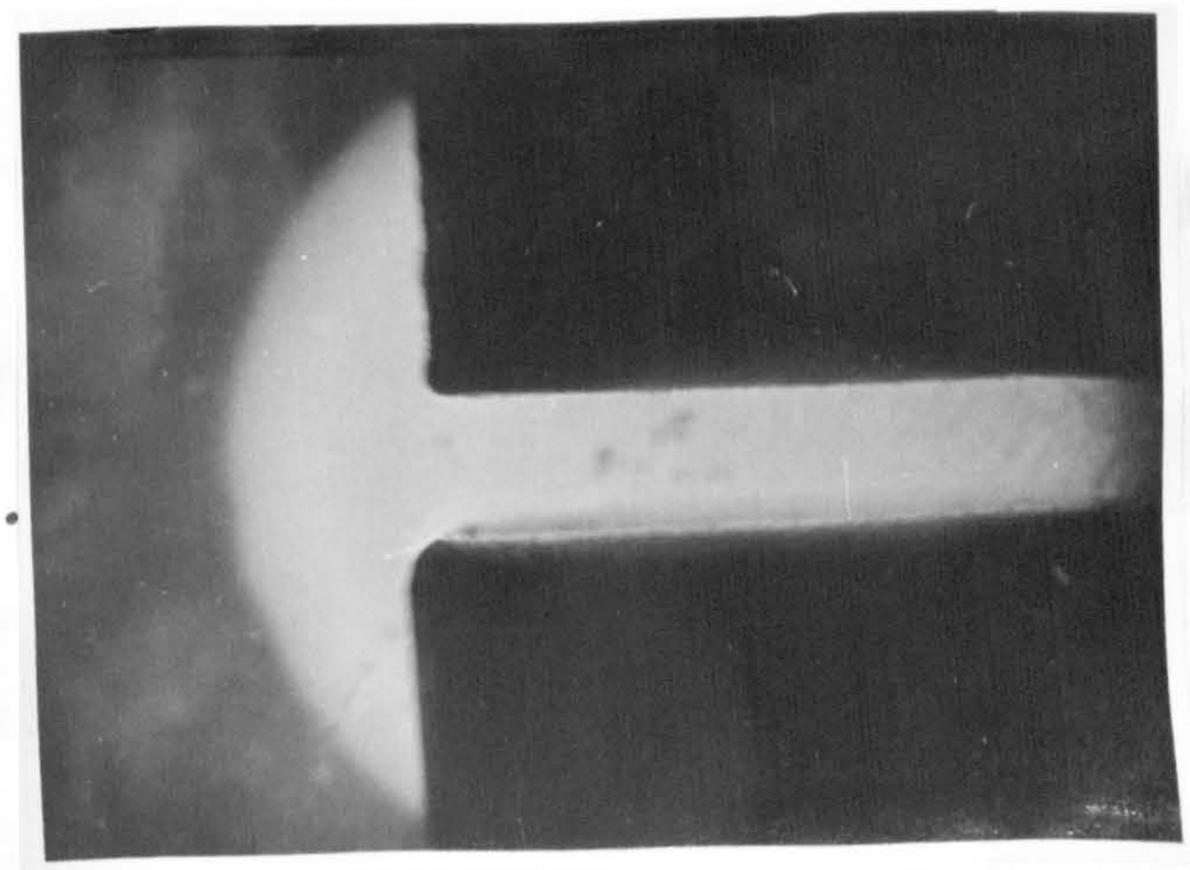

5.1 No current.

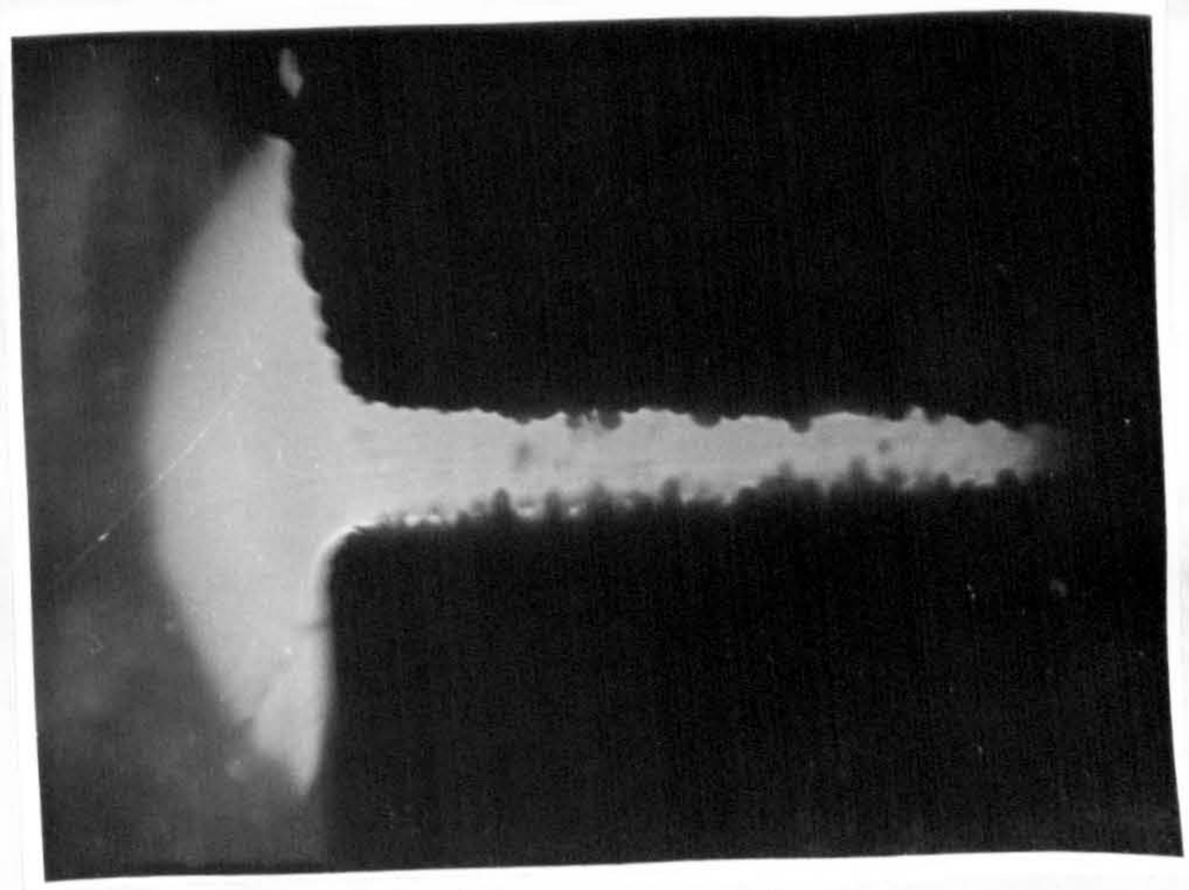

5.2 Low current.

5.3 Limiting current.

Figures 5.4 to 5.7.
Copper/Phosphoric acid.
Gap .050"
Flow 85 ins/sec.
x50.

5.4 No current

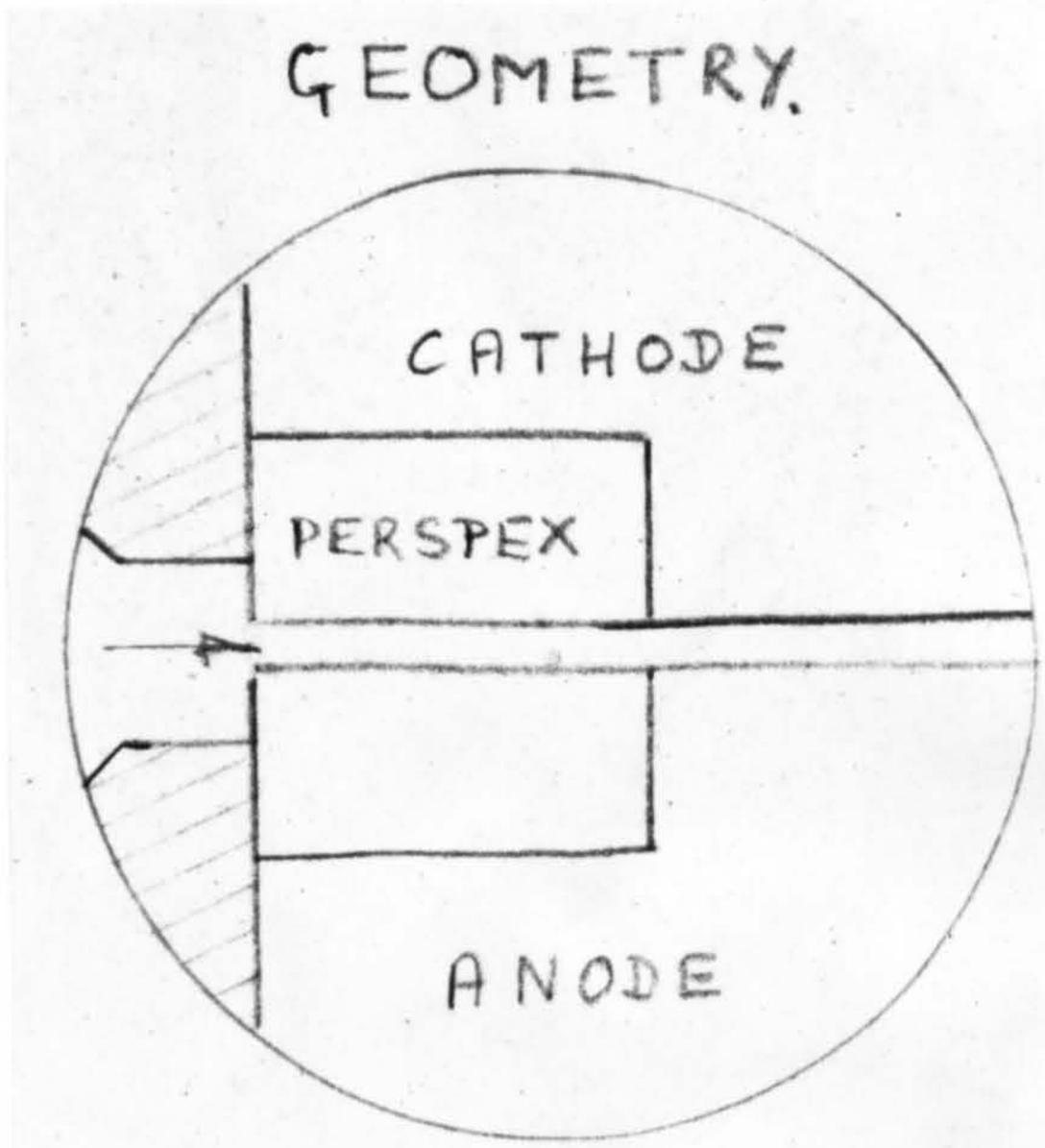

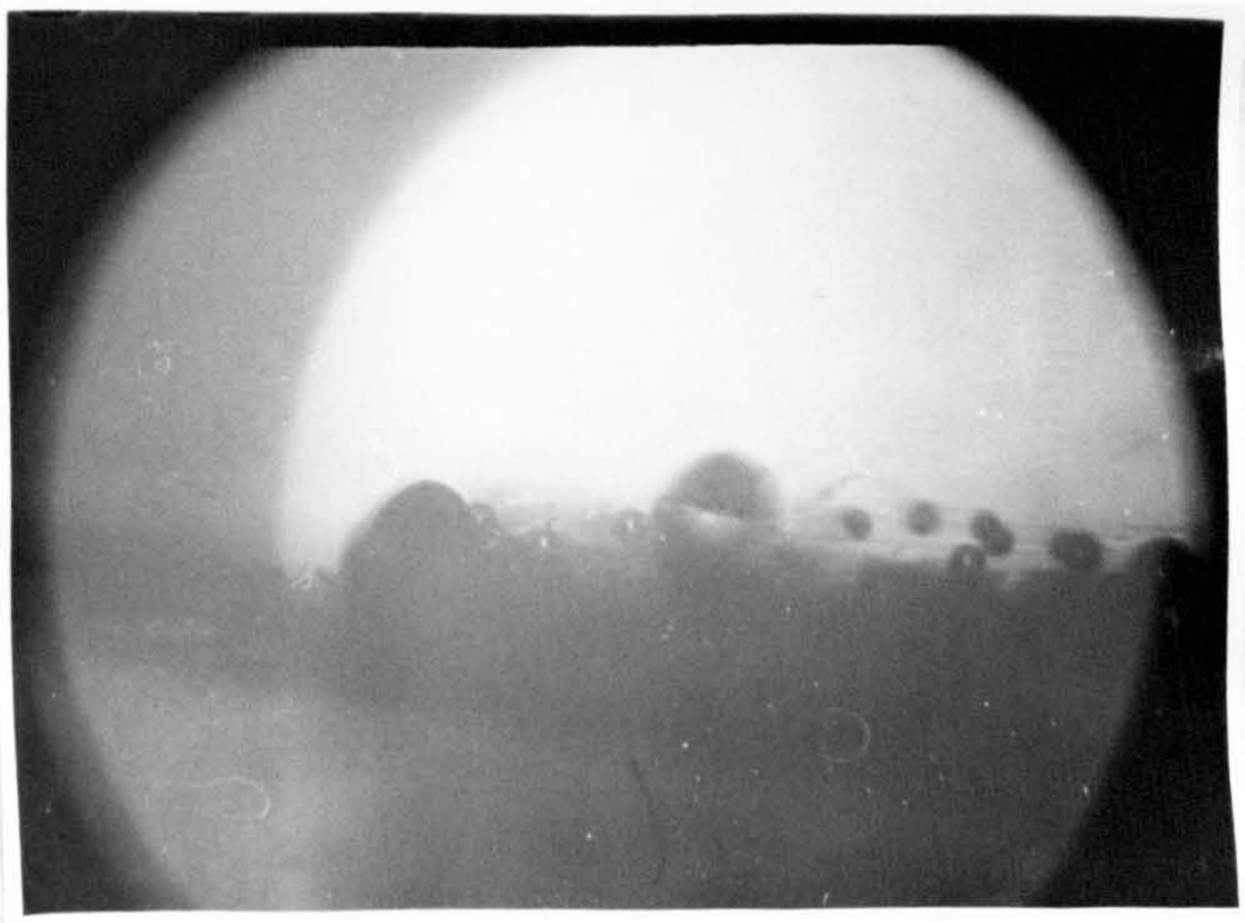

5.5 30 Amps/in^2

5.6 48 Amps/in^2

5.7 70 Amps/ in^2

could be measured. A series of measurements was made at several pressures, the mean bubble size at each pressure is recorded in table 10.2.

It was found that useful photographs could only be obtained at currents up to about half the limiting value, the many bubbles near the electrodes then caused so much scattering of the light that insufficient illumination was available. To obtain photographs of the limiting current regime, it was necessary to reduce the width of the channel by blocking some of the width with perspex to .055", photographs were then obtained of the limiting current regime, and these are contained in Section 10.4.

6. CURRENT DENSITY DISTRIBUTION.

6.1 Segmented electrode design.

A special electrode assembly is required to measure the current distribution along the flow path, and all results are influenced to a greater or lesser degree by the design of the electrode and insulation present. A segmented cathode has to be used,as, if an anode were employed, the insulation between the segments would rapidly become proud and invalidate the results. Two different assemblies were made.

6.2 First Electrode.

The first is shown in Figures 6.1 and 6.2.

A copper bar $\frac{1}{2}$" x $\frac{3}{8}$" x 2" was joined to the main electrode body with 16 pegs of 8 swg resistance wire driven into blind holes, leaving a gap of $\frac{1}{4}$", instrument wires being soldered to the body and between each pair of pegs. The gap was then filled with 'Araldite,' and the top block sawn into eight segments; the sawn gaps were also filled with 'Araldite' The wires were led through holes in a perspex window, made to fit the working section, which was then glued to the fabricated electrode.

Each pair of pegs thus acts as a current shunt measuring the current to its segment of the electrode.

This segmented electrode showed that the method was possible, but had several practical snags that meant that no useful results were obtained. These snags were:-

(1) insufficient sensitivity- shunt resistance was about 1 mΩ, giving signals of 10 mV . maximum. This resistance also proved to be unstable, it was thought to be due to the drive fit connection between the resistance wires and the copper.

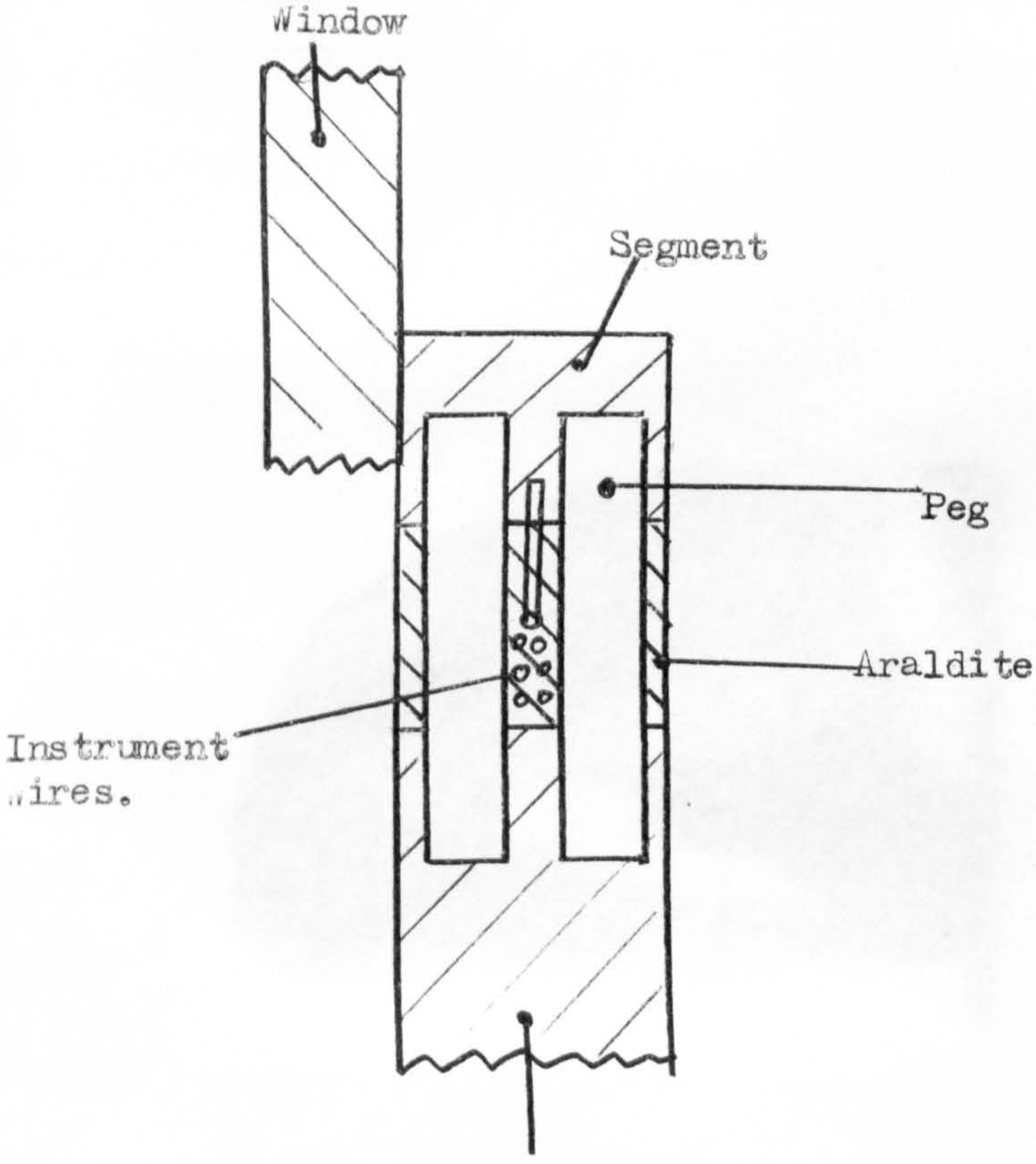

First Segmented electrode.

Figure 6.1 and 6.2

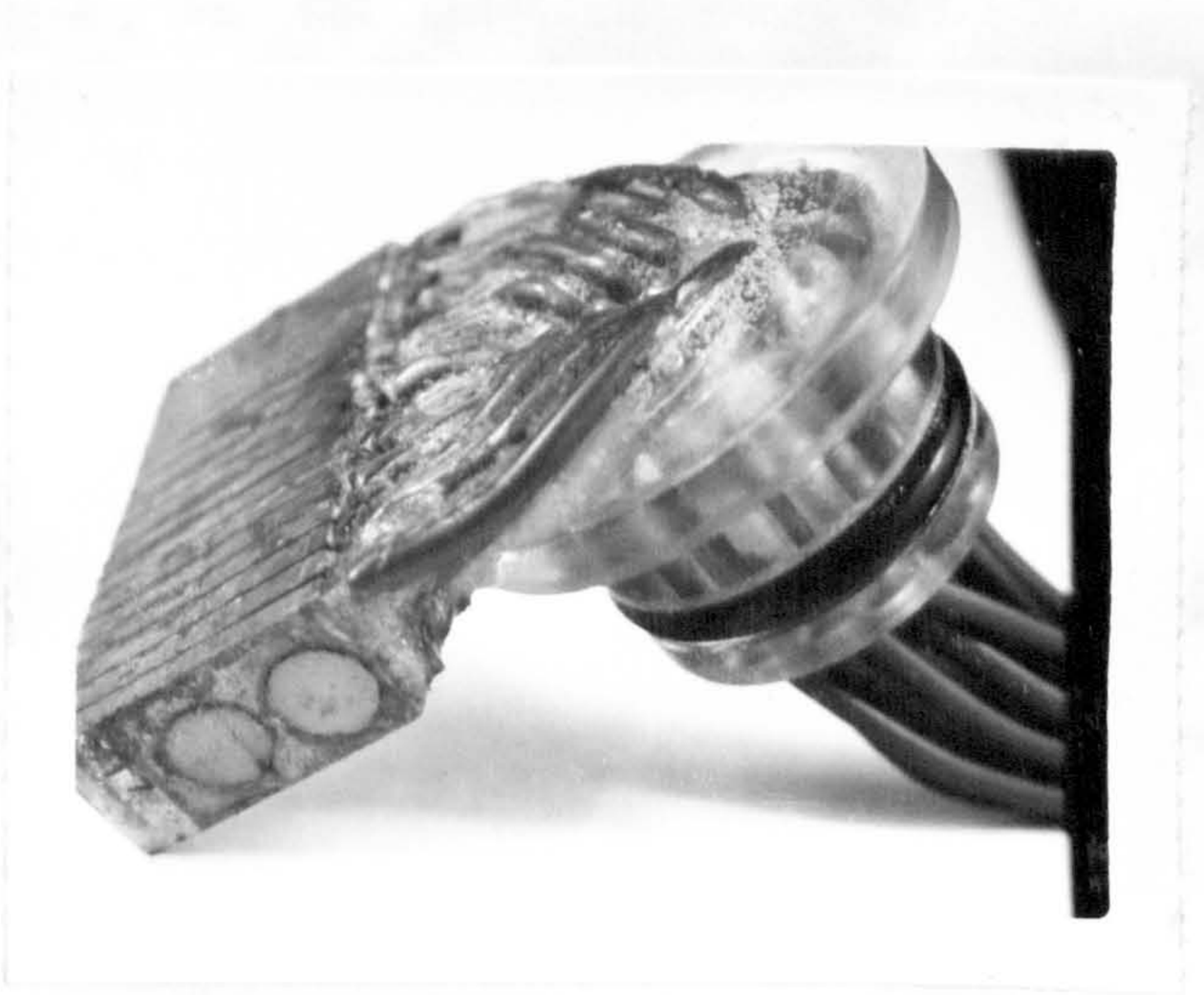

Second segmented electrode.

Figures 6.3& 6.4.

(2) The instrument wires proved fragile and rapidly broke at the point of emergence.

(3) It was difficult to fill the saw cuts with 'Araldite' and obtain a smooth surface.

6.3 Second Electrode.

It was, therefore, decided to employ external shunts to measure the current, and accept the rather larger potential drops in the leads which allow the electrode to depart from the ideal of an equipotential surface. This assembly is shown in Figures 6.3 and 6.4 . 17 brass strips, $\frac{1}{2}$" x 0.1" x 1" had 10 amp insulated leads soldered to one end, and were drilled to take two P.V.C. bolts. They were insulated with P.V.C. tape, bolted together and then wrapped with P.V.C. tape. A perspex plug was made to replace the fixed electrode assembly in the working section, and the leads cemented through this. The whole was inserted into the working section and all but the working face well packed with silicone grease. This electrode was satisfactory though not ideal, since the P.V.C. tape tended to ooze from between the segments and had to be trimmed. The P.V.C. bolt also tended to stretch and allow the segments to fan out. The electrode face was re-machined and no further trouble was encountered from this cause. An external shunt was made up of resistance wire to have resistance of 10 mΩper segment and a current capacity of 10 Amps per segment.

6.4 Results.

Two types of experiment were run. Firstly the current to each segment was measured at various currents, at one flow rate and gap using both copper/phosphoric acid and Aluminium/sodium chlorate systems. The flow was then increased for the critical current case, and the voltage reduced to maintain the same current. These results are shown

in Figure 6.5.

The second type of experiment was to measure the external current voltage characteristic for a selected segment. The results of these experiments are given in Figures 6.6 and 6.7

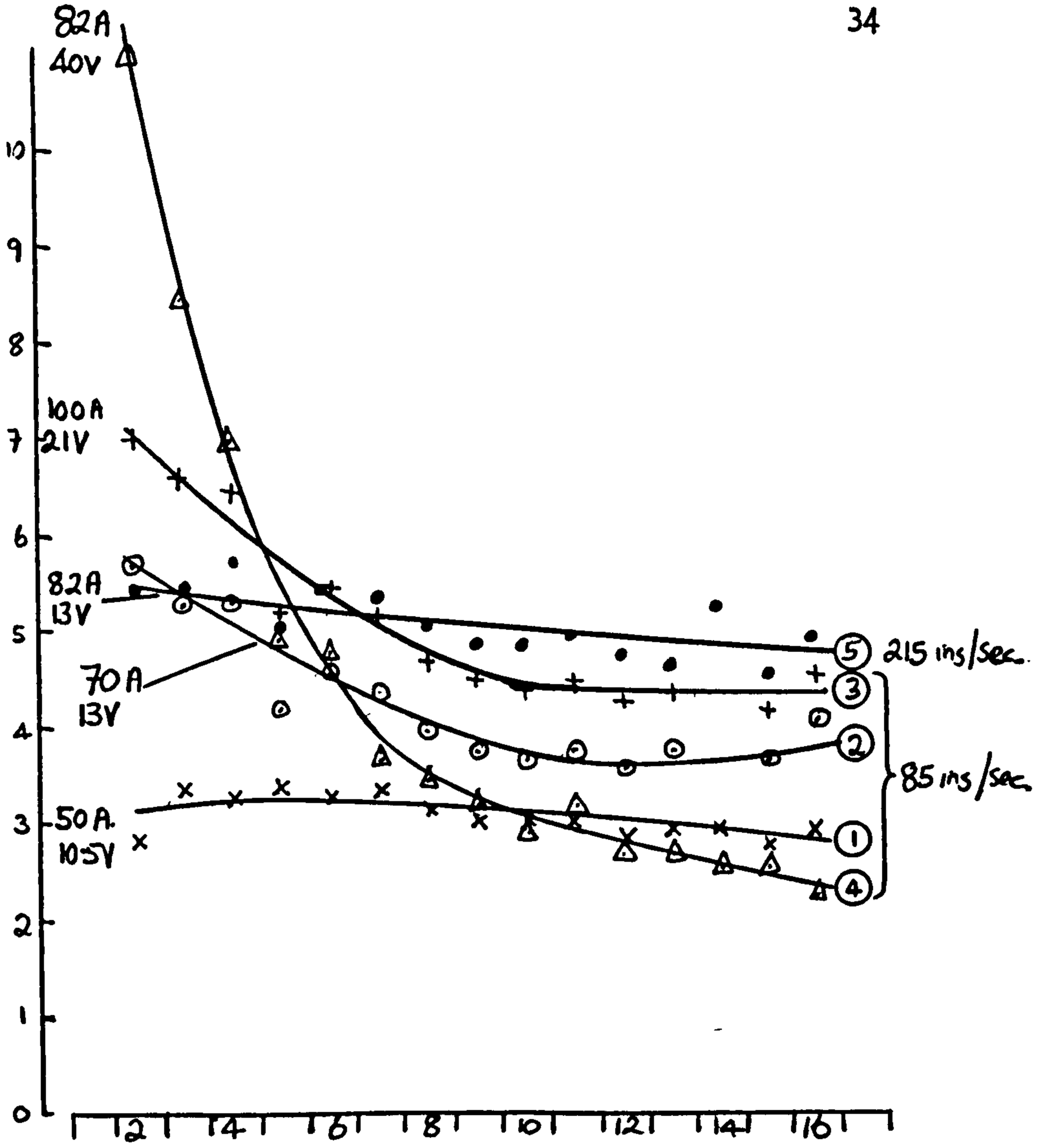

Current distribution
Copper/phosphoric acid
Gap .050"
Total Current, Cell Voltage and flow velocities noted for each curve.

Figure 6.5

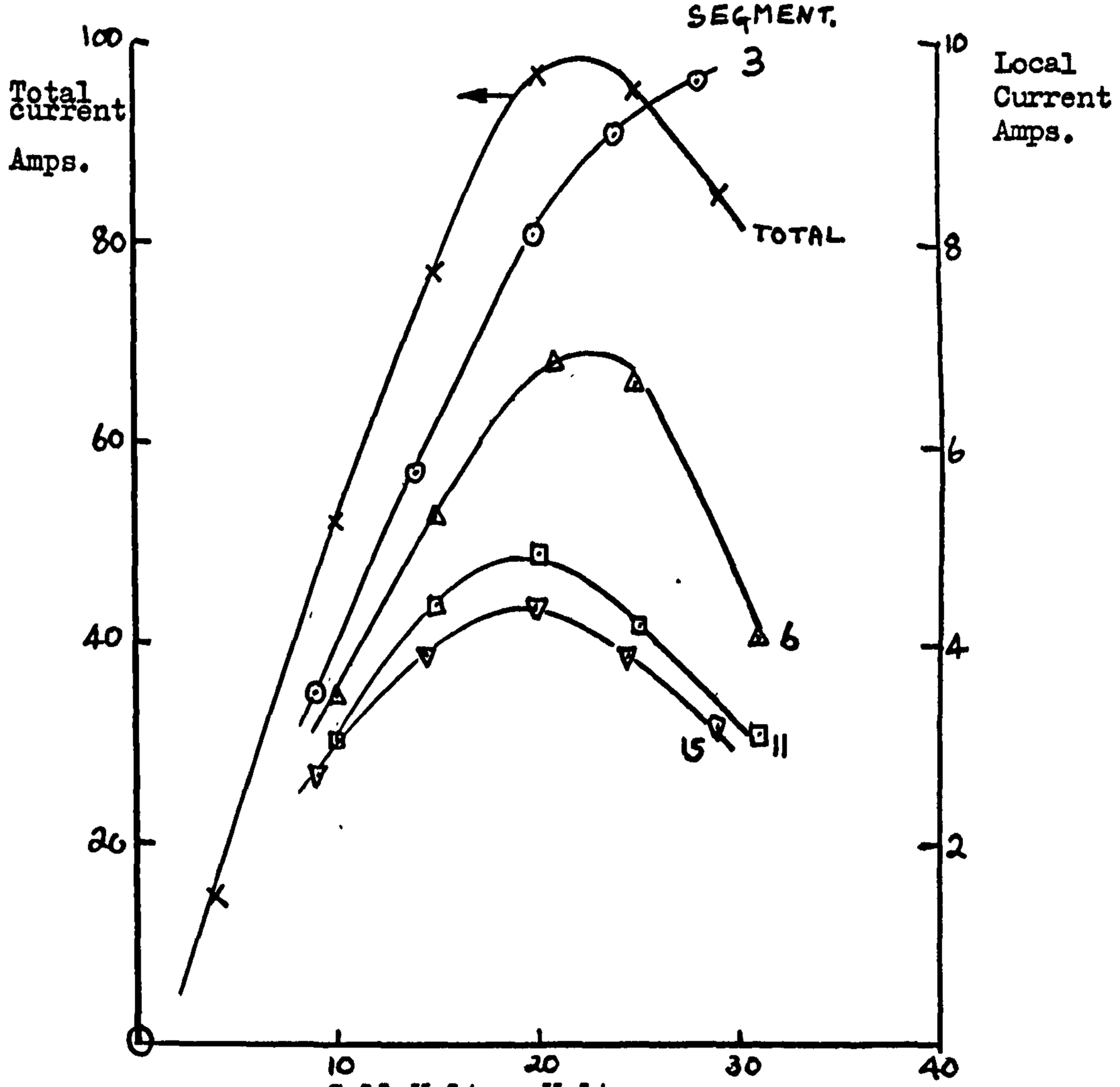

Current Distribution
Copper/Phosphoric Acid
Gap .050" Flow Velocity 85 ins/Sec

Figure 6.6

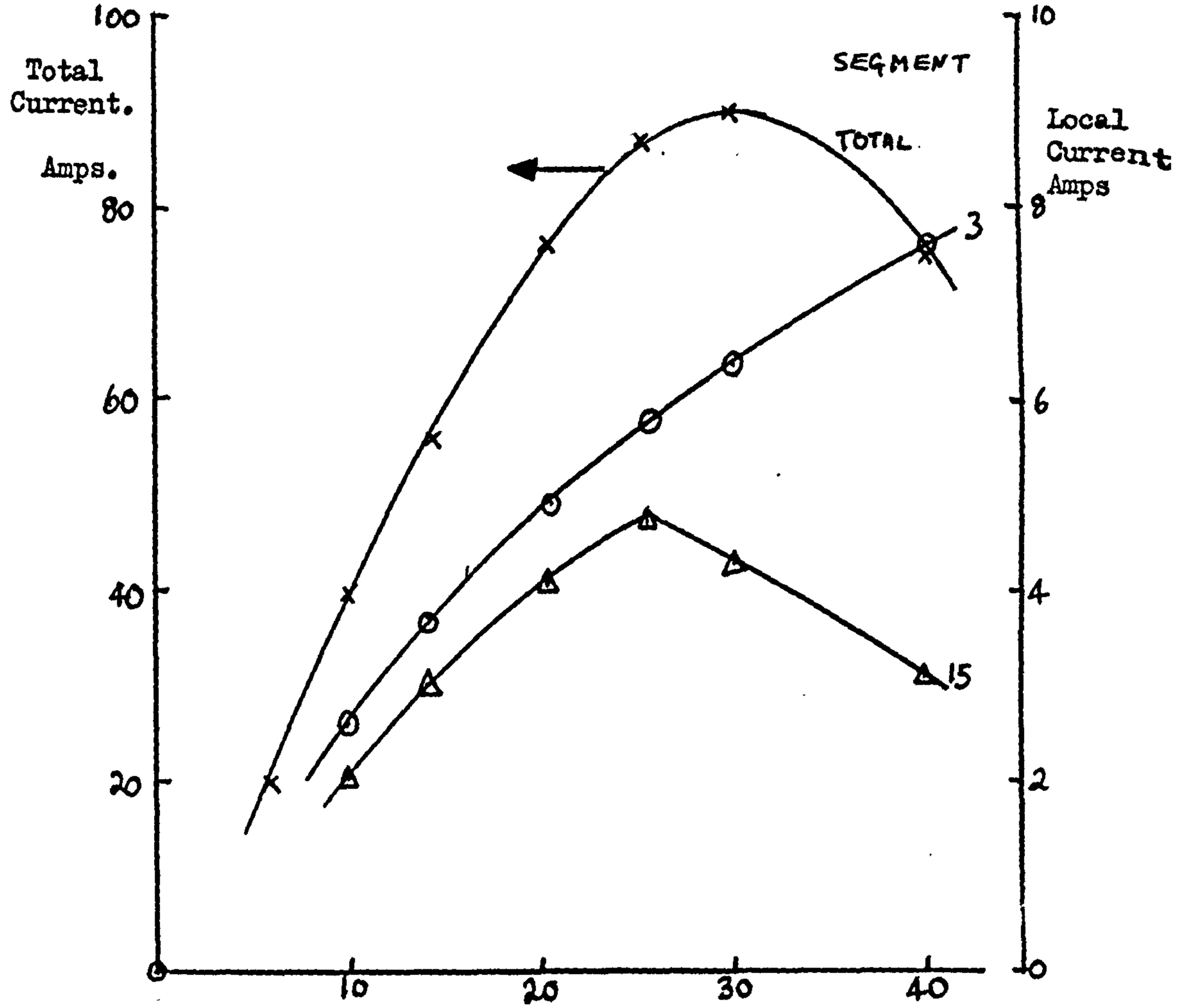

Current distribution
Aluminium/Sodium Chlorate
Gap .050" flow 90 ins/sec

Figure 6.7

7. POTENTIAL DISTRIBUTION

7.1 Problems

The measurement of potential distribution within the gap is one of the most difficult to achieve. The problem in this case is the small scale of the experiment.

To measure the potential distribution across a channel about .050 inches wide full of rapidly flowing electrolyte a measuring probe much smaller than the channel, say .001 inch is required to give reasonable accuracy. The supporting mechanism must also be small enough not to interfere with the flow pattern, either of fluid or current. It is impossible with probes of such dimensions to achieve sufficient mechanical strength to withstand the environment, particularly as the probe must be insulated, which means that the majority of the material is comparatively weak.

Calculations show that a wire of .0005", insulated to .0015 inch could only protrude about .005 inch into the flow without breaking. Since it would by then be suffering considerable deflection it was decided not to attempt to build such a probe, which would be a difficult task.

As an alternative it was decided to make an array of electrodes mounted in the side wall of the channel and measure the potential distribution down the wall of the channel. This may be considerably different from the two dimensional distribution required, but may show important qualitative features of the phenomena.

A further problem is that as the size of the probe is reduced, so the current density rises. This means that for small probes high input impedance volt-meters are required. Using .001 inch diameter wire with an area of about 10^{-6} square inches, a volt-meter having an

input impedance of 1 megohm would produce a current density of 1 amp per square inch when measuring 1 volt. Thus for the measurements intended, which are up to 50 volts, a higher input impedance is required, since the reference electrode should draw no current if it is to give a true reading.

Thus data logging methods using an oscilloscope were abandoned.

7.2 Wall Electrode Assemblies.

Once again , two different electrode assemblies were made. The assemblies are shown in Figures 7.1 and 7.2, and were made as follows:-

A perspex window was made to fit the working section and a hole was milled from the outside leaving about .030 inch wall. For the first electrode assembly .0075 inch holes were then drilled from the inside at .020 inch pitch. For the second electrode .005 inch holes were drilled at .010 inch pitch.

The first electrode was designed to be as easy to make as possible and to determine the error involved in staggering the electrodes in the streamwise direction. This stagger is required because of the need to leave a reasonable amount of material between holes, while providing a fine coverage of the wall with electrodes.

In the first design each hole was threaded with .0024 inch (42 SWG) enamelled copper wire, the other end of this wire was bared and trapped in one of the outer ring of holes by a shouldered peg, to which it was then soldered. It was found that this method was difficult to use and led to many broken wires. The large hole was then flooded with 'Durofix' and the fine wires worked to introduce the glue into the holes to provide a seal.

In the second design a short length of fine wire was soldered to the lead and the junction cemented into an outer hole. The fine wires

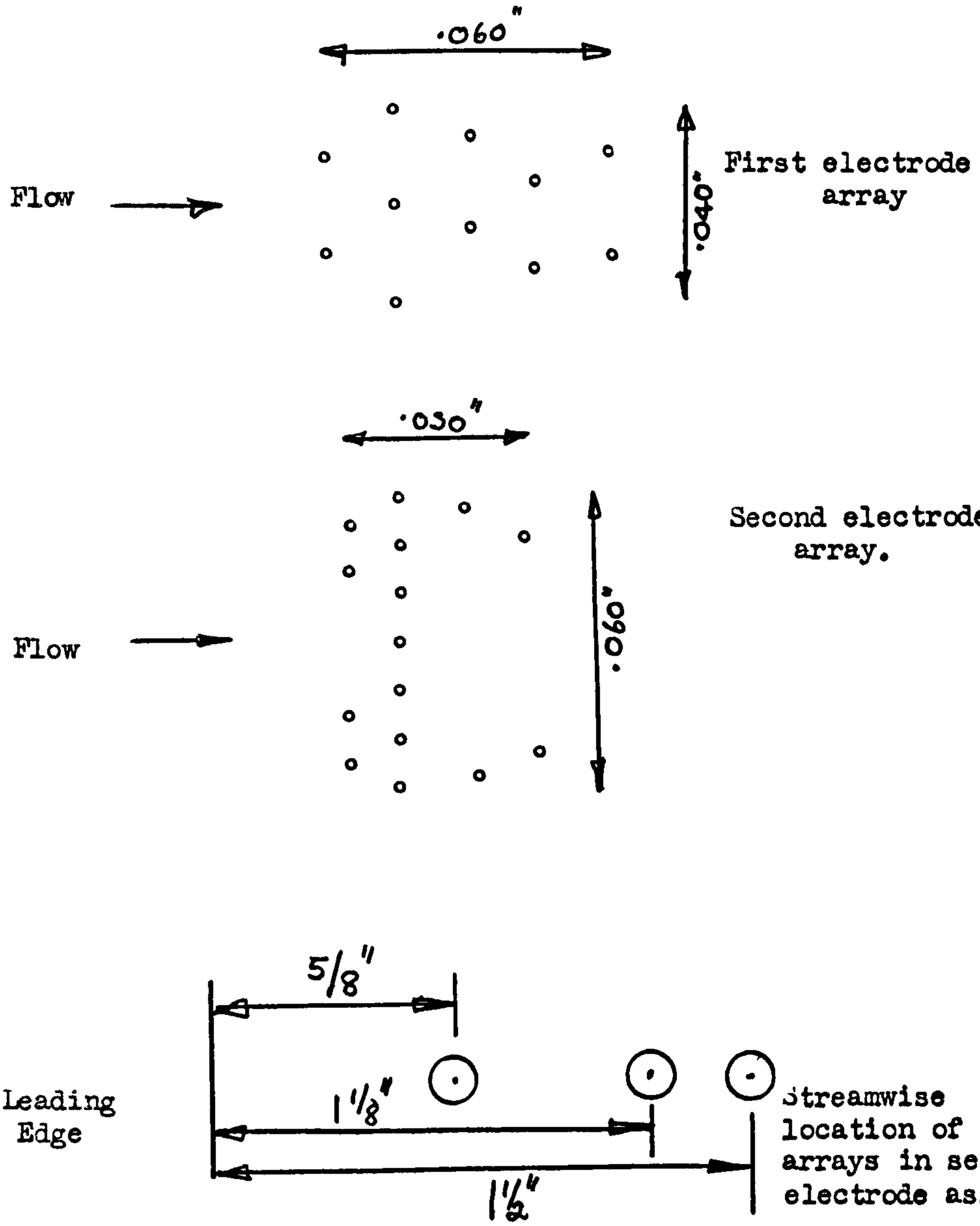

Potential distribution electrode position.

Figure 7.1

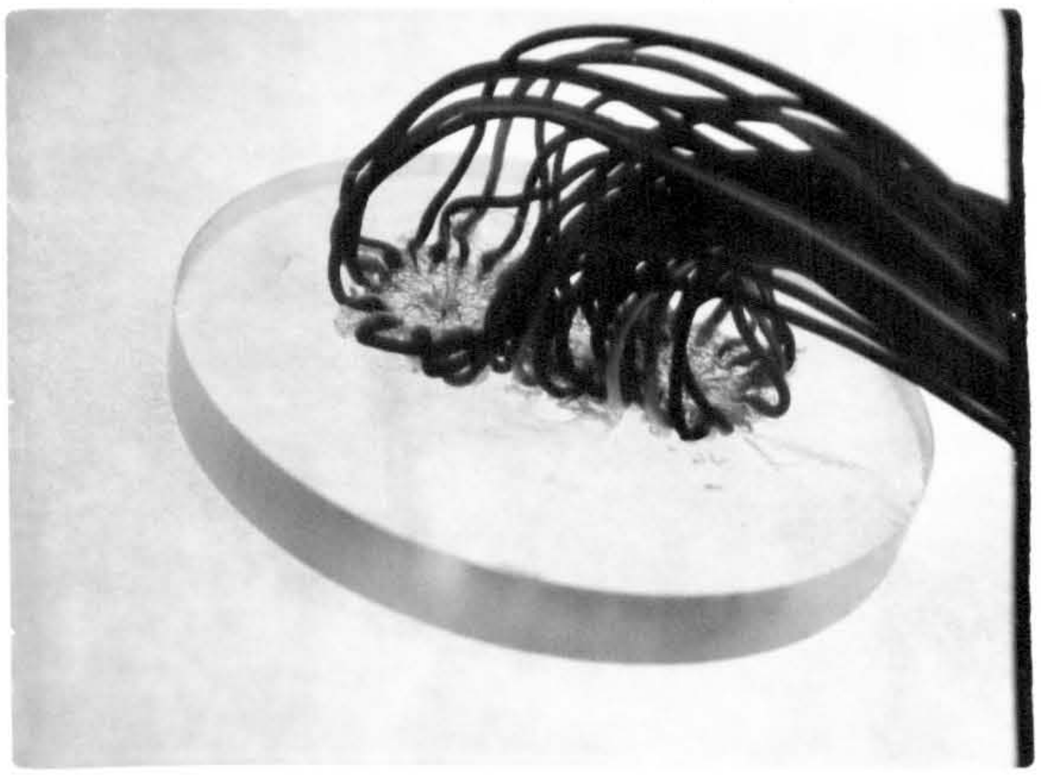

Final potential distribution
electrode assembly.

Figure 7.2.

were then passed through the appropriate small hole and the whole assembly then flooded with several coats of "Durofix" so that the fine wires were completely encapsulated.

The inner faces of the electrodes were then polished on fine emery cloth and the exact positions of each wire end established with a travelling microscope.

7.3 Results.

The potentials were measured with a valve voltmeter having an input impedance of 100 Megohm. This means that when measuring 10 volts a current density exists at the measuring electrode of 20 milliamps per square inch, which is allowable.

The results obtained with the first assembly are shown in Figure 7.3 and should be regarded as preliminary data. They clearly show that there is a negligible error introduced by staggering the electrodes in the streamwise direction. The position of the anode surface in these measurements is variable.

The results also show that attention should be concentrated on the behaviour of the layers adjacent to the anode and cathode, and in particular the latter. The second assembly was, therefore, designed with a concentration of electrodes in the wall region of the channel, and, noting the results of the current distribution experiment, with sets of electrodes up and down stream from the centre. The results of the potential distribution measurements obtained with this assembly are shown in Figures 7.4 to 7.6. They show that the errors involved in the technique are considerable and largely unavoidable.

They do however, show several important features, and it was decided that it would be unrewarding to attempt to improve the

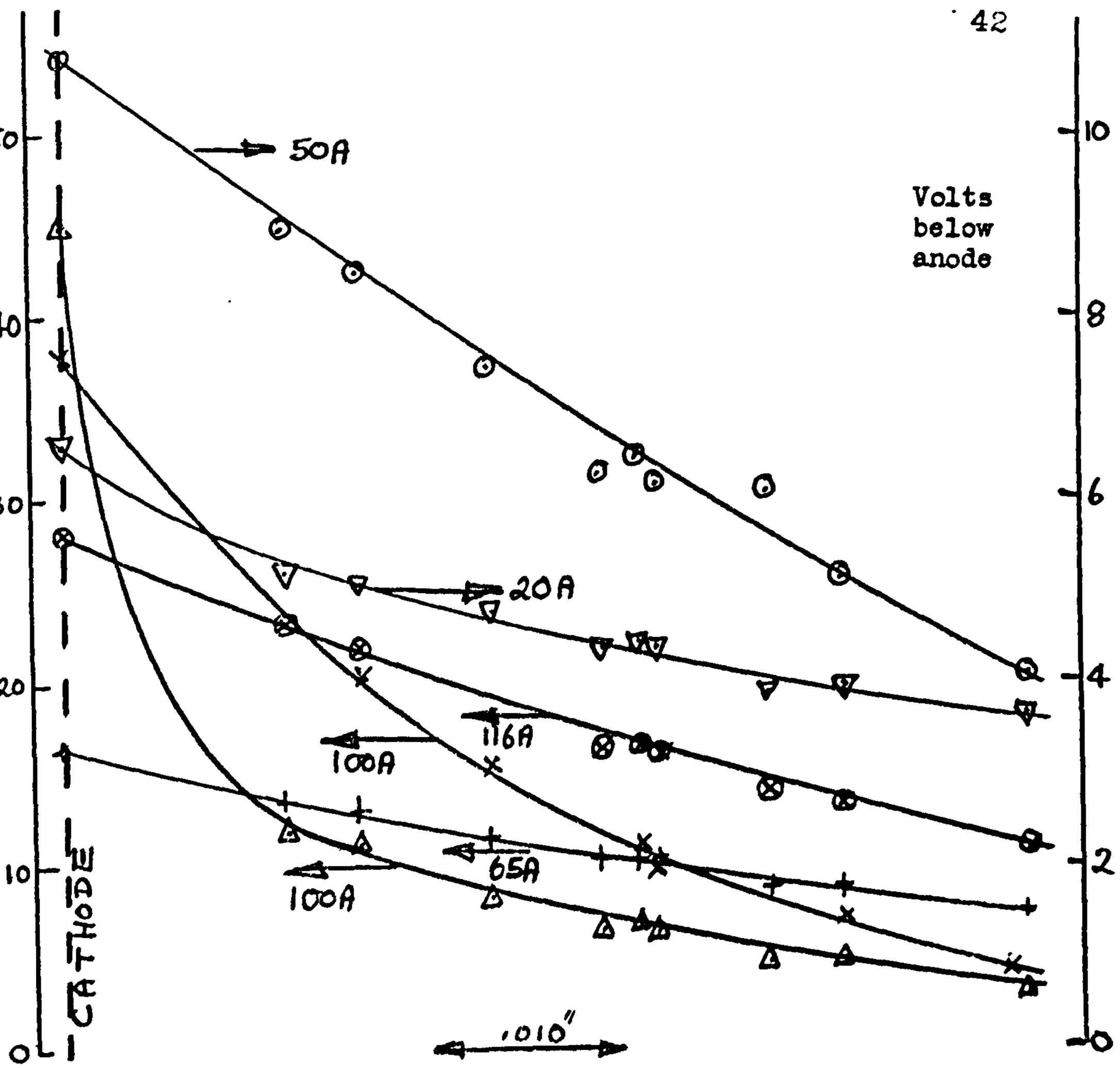

Preliminary Potential distributions
Copper/Phosphoric acid.
Gap .050" to .090"
Flow 2.4 Cu.ins/sec.

116 Amps. is the maximum current for that gap.

The two curves for 100 Amps. are for different gaps, both greater than that for the 116 Amp. curve; their cell voltages are larger than that which gives the maximum current in each case.

Figure 7.2

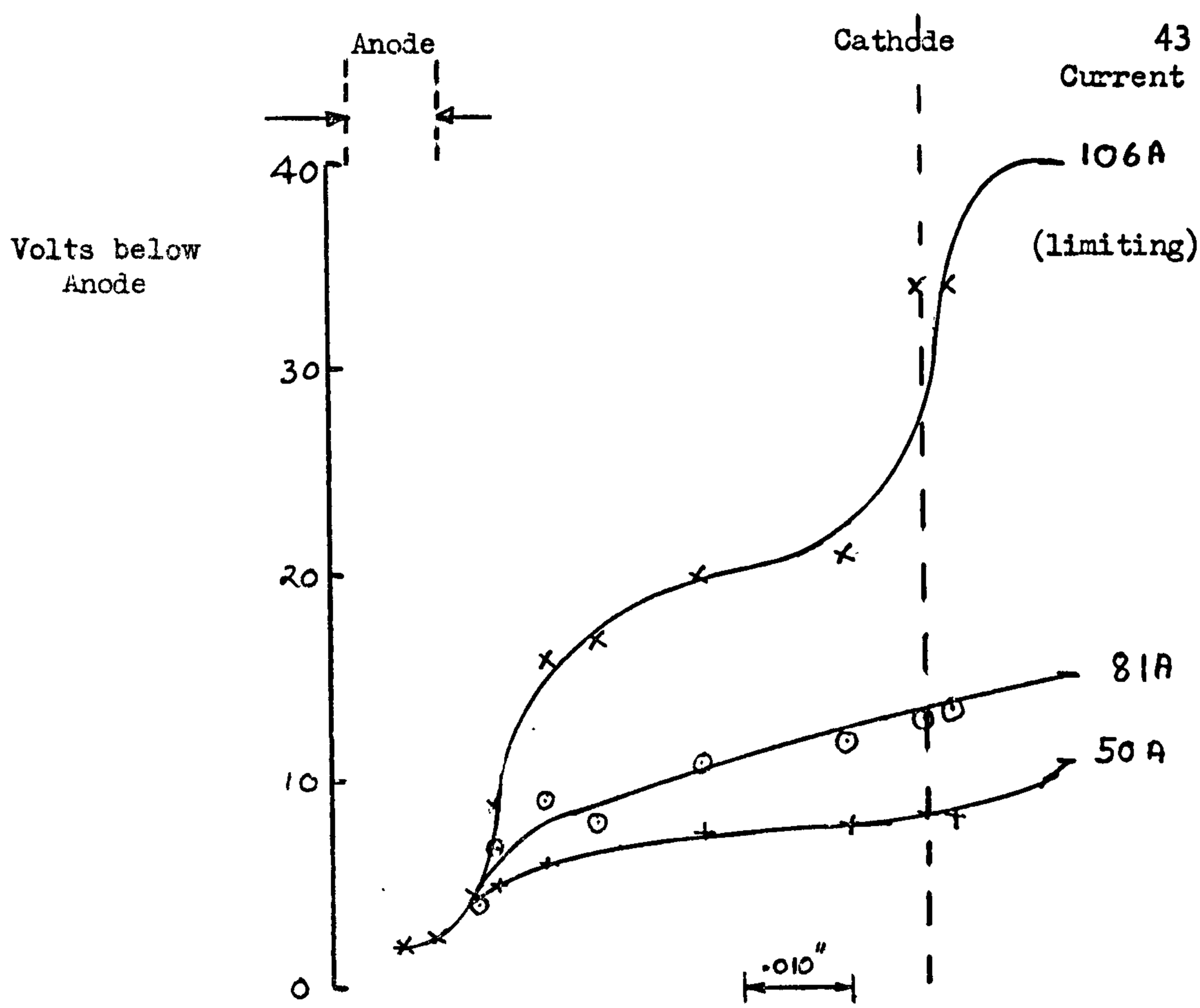

Potential Distribution $\frac{1}{8}$" downstream
Copper/Phosphoric acid
Flow Velocity 85 ins/sec

Figure 7.4

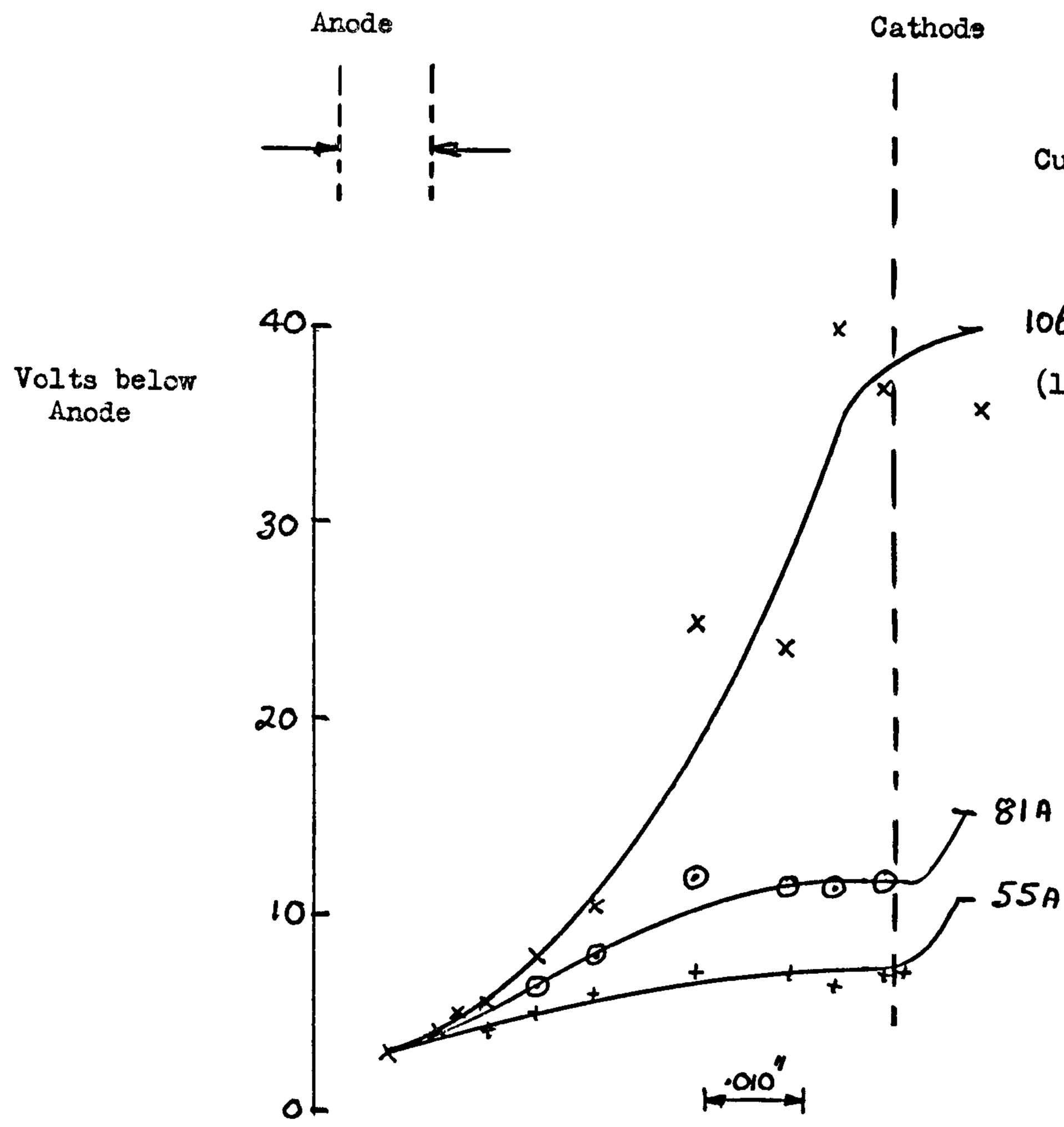

Potential Distribution $1\frac{1}{2}$" downstream
Copper/Phosphoric Acid
Flow velocity 85 ins/sec.

Figure 7.5

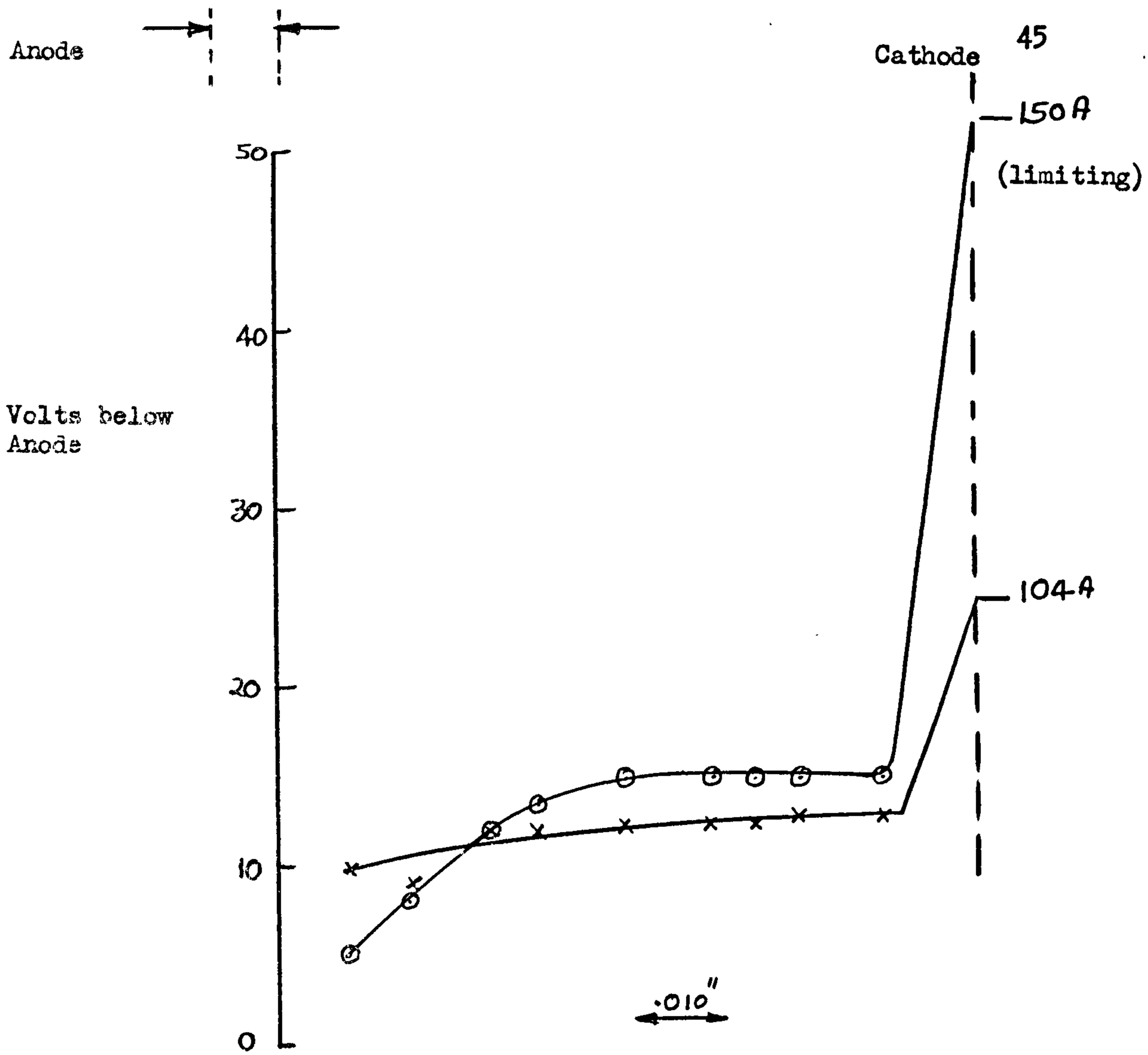

Potential Distribution $1\frac{1}{2}$" downstream
Copper/Phosphoric acid
Flow Velocity 140 ins /sec

Figure 7.6

technique.

The main features are as follows:-

(1) The anode layer appears mainly unaffected by current density increase.

(2) The bulk of the flow is affected in degree only.

(3) The cathode layer undergoes a marked change when the limiting condition is reached.

To clarify this, measurements were taken of the potential difference between selected reference electrodes and the anode and cathode as the current was increased. The results of these experiments are shown in Figures 7.7 and 7.8

These clearly show that the limiting current is produced by a cathodic phenomenon.

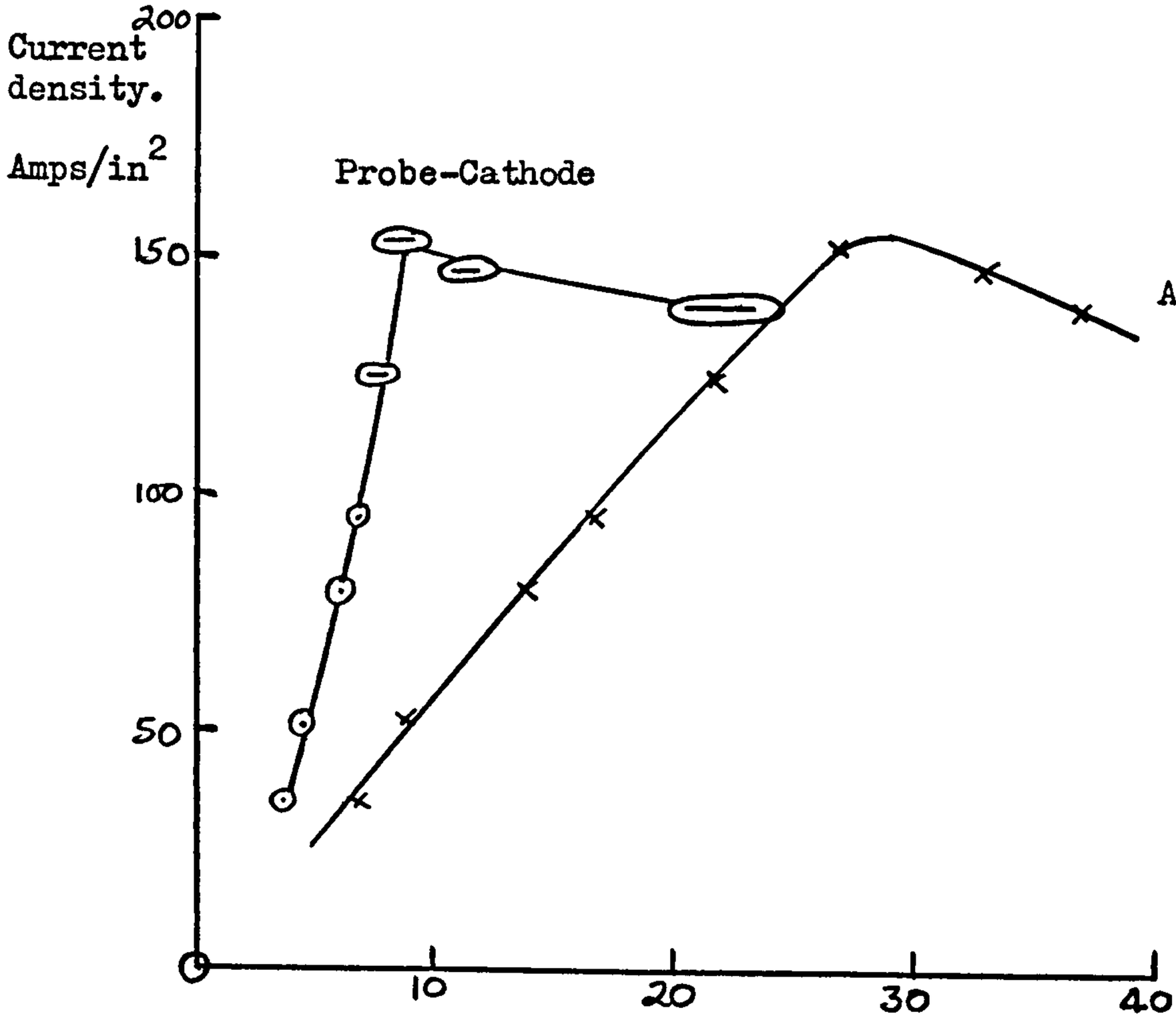

Cathode layer potential drop
Copper/Phosphoric acid
Gap .075" Flow velocity 145 ins/sec

Probe Near Cathode

Figure 7.7

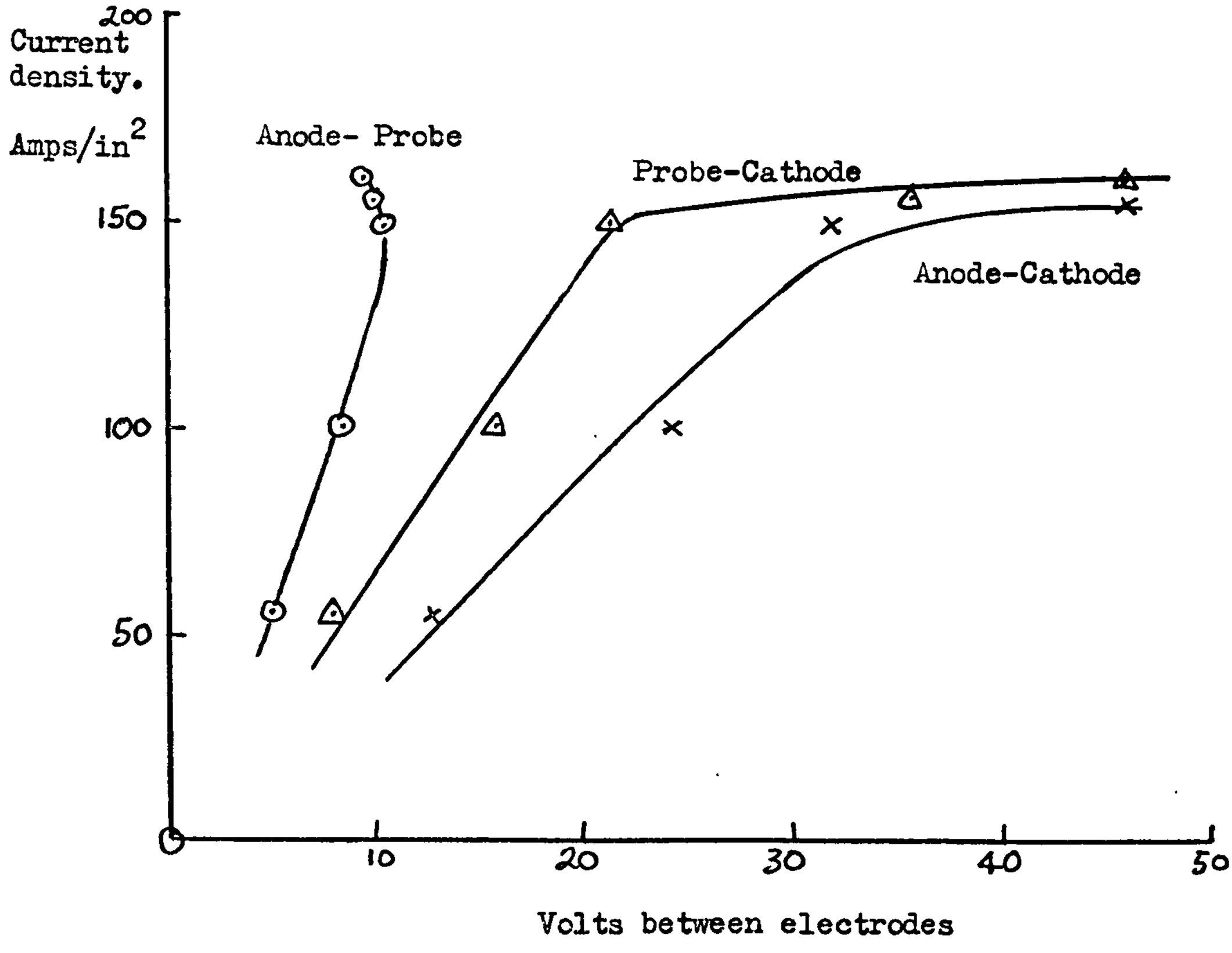

Limiting potential drops
Copper/phosphoric acid
Gap .075" Flow velocity 145 ins/sec
Probe near anode

Figure 7.8

8. POTENTIOSTAT STUDIES

The current- voltage characteristic shown in Figure 4.1 showed two current arrests. The lower of these was thought to be similar to that reported by Hoar (4) , and it was, therefore, investigated using a potentiostatic technique to distinguish between passivation and a polishing plateau.

The usual working section was employed and a reference electrode inserted in the wall just upstream of the electrodes. A 'Witton' potentiostat providing up to 10 Amps was used. The copper-Phosphoric acid system was investigated for comparison with the experiments of Hoar (4) , a copper wire being a suitable reference electrode for this system.

The current - anode voltage characteristic was obtained for various flow rates and gaps, the anode voltage quoted being the potential difference between the anode and the reference electrode.

Figure 8.1 shows a typical set of results for a gap of 0.2" The blurring of the current arrest at high flow rates is thought to be due to a combination of ohmic potential drop included in the anode potential, eddies due to the sharp entry condition, and side wall effects.

Figure 8.2 shows the limiting current plotted against (mean flow velocity) $^{\frac{1}{2}}$ and shows a similar dependence to that found by Hoar (4) with some effect due to gap size.

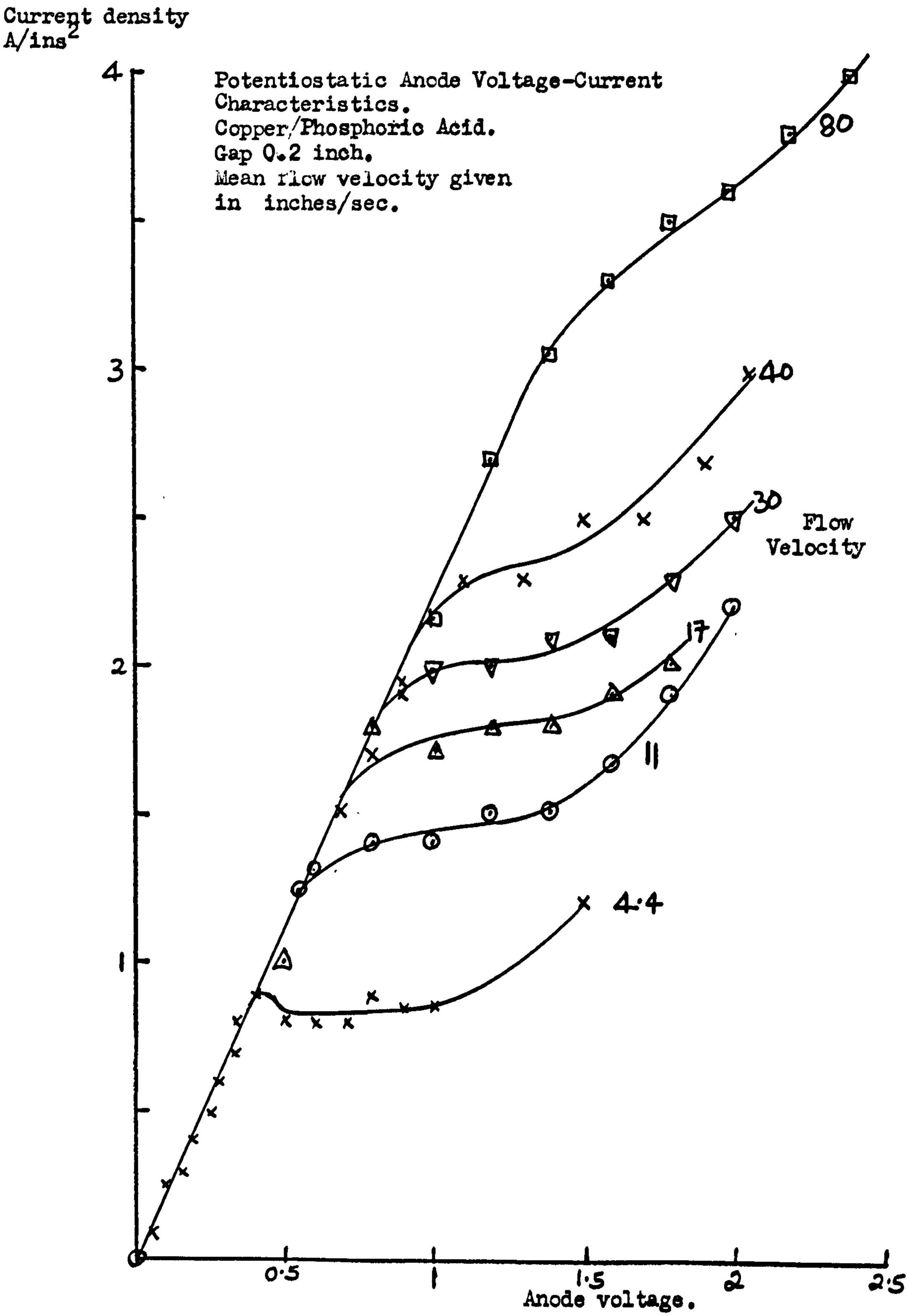
Current density
A/ins²
Potentiostatic Anode Voltage-Current
Characteristics.
Copper/Phosphoric Acid.
Gap 0.2 inch.
Mean flow velocity given
in inches/sec.
4
3
2
1
80
40
30
17
11
4·4
Flow
Velocity
0·5
1
1·5
2
2·5
Anode voltage.

Figure 8.1

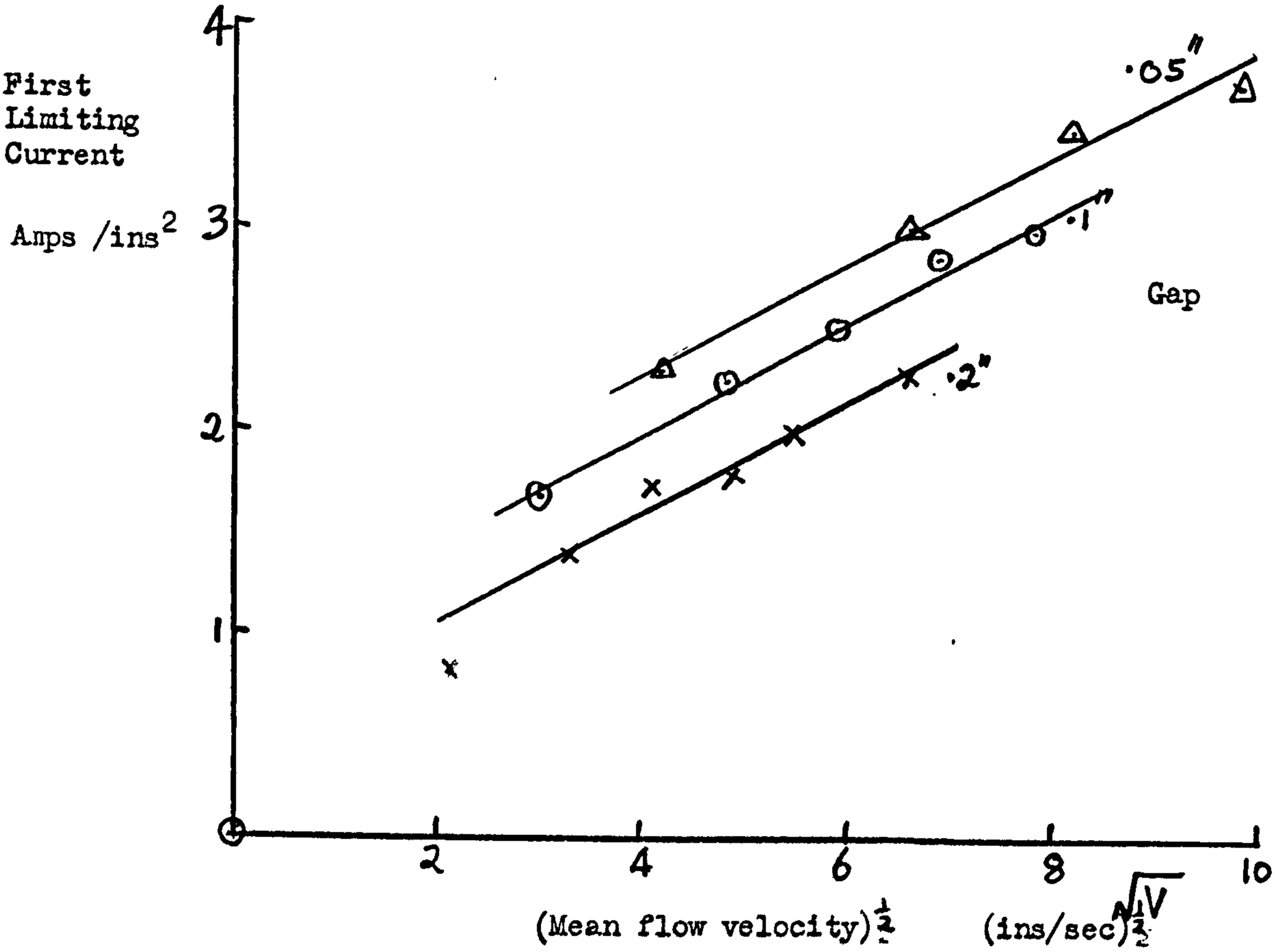

Lower limiting current
Dependence on mean flow velocity
Copper/Phospharic acid.

Figure 8.2

9. DISCUSSION

From the results given in Chapters 4 to 8 the nature of the current limiting process in E.C.M. can be hypothesised, and a qualitative explanation given for the whole process.

9.1 Current limiting process.

As can be seen from Figure 4.1, there are two arrests of current in the external current-voltage characteristic at constant gap and flow rate.

The first occurs at current densities of the order of 1 to 10 Amps per square inch, depending on the flow velocity. This phenomena is that reported by Hoar (4), and is investigated here in the potentiostatic experiments.

The second is the maximum current attainable for each set of conditions, and is of great interest as it is the governing factor involved in increasing the machining rates.

The relevant facts deduced from the results reported in Chapters 4 to 8 are as follows:-

9.1.1 Gas evolution (presumably oxygen) takes place at the anode at all cell voltages above about 2 volts, though the exact voltage depends on conditions.

This is exactly in line with electropolishing experience, for which oxygen evolution is observed at anode voltages above about 1.8 volts. The evolution of gas can be seen to increase in volume with current density(and hence cell voltage, or vice -versa) since the flow photographs show increasing amounts of bubbles present.

9.1.2 From the current density measurement it can be seen that for currents and voltages below the limiting values, the distribution of current density is essentially uniform (Figure 6.5 , curve 1) and

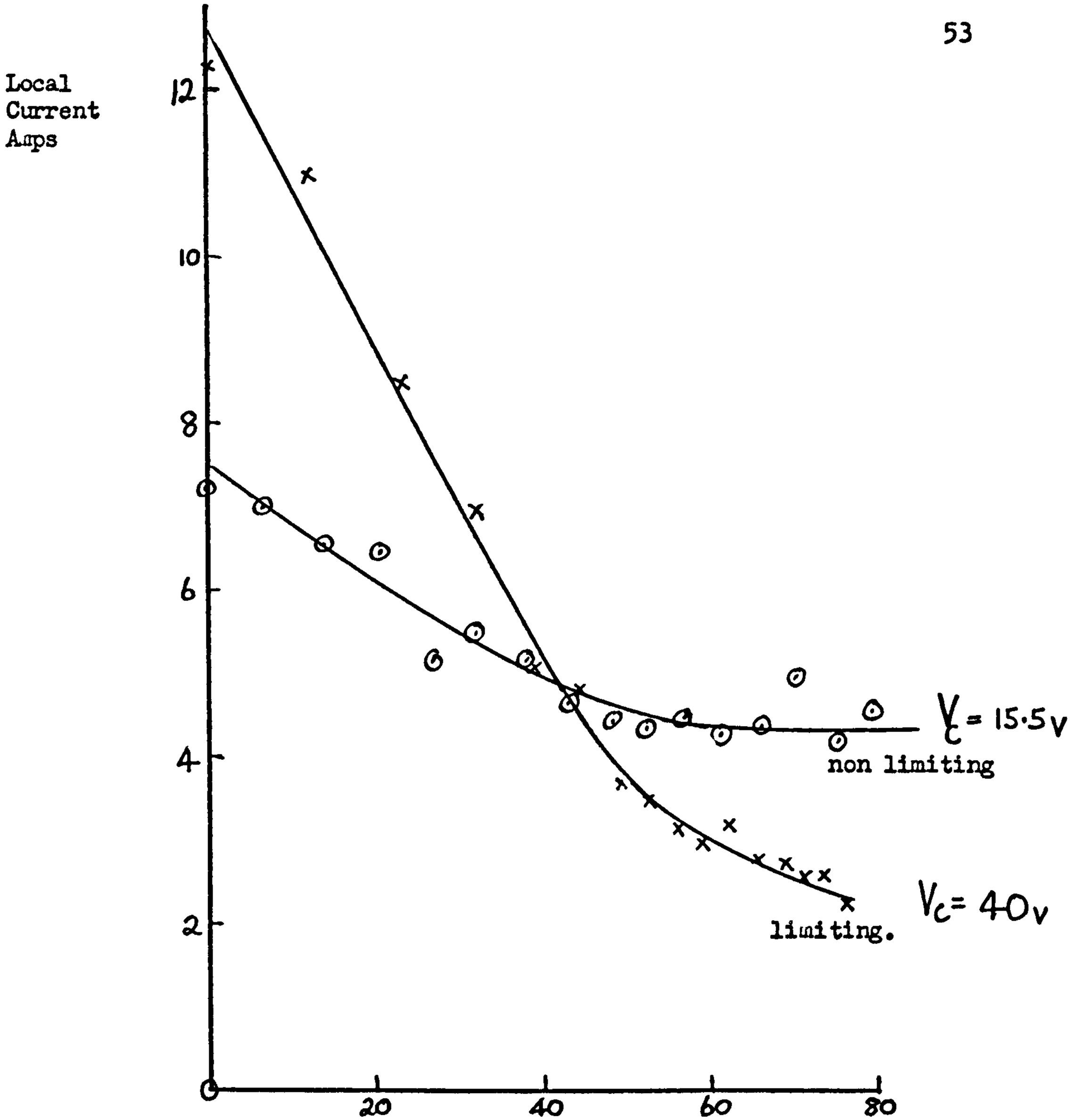

Dependence of local current on upstream condition
Copper/Phosphoric acid system
Data derived from Figure 6.5

Figure 9.1

all segments of the electrode are behaving similarly as the current is increased. As the limit is approached, however, the current density at the downstream end of the channel reaches a limiting valve and then commences to fall (Figure 6.6, segments 15,11.), though the total cell current is still increasing.

The limiting current density condition propagates upstream rapidly(Figure 6.5, curve 3) When about half of the channel is limited the total current reaches the limit and commences to fall (Figure 6.7). As the voltage is further increased the current density on upstream segments continues to rise, while downstream current densities fall (Figure 6.5, curve 4 ; and Figure 6.6 segments 3 and 6)

Thus the limiting phenomenon must be one which depends on the history of the flow.

Figure 9.1, which is taken from the data of Figure 6.5, shows the local current against total current passed upstream of the local segment. It compares two cases which differ only in that one is before the limit, having a cell voltage of 15.5 volts, and the other is after the limit, having a cell voltage of 40 volts. This shows that it is not just the volumetric concentration of hydrogen that causes the trend as suggested by P.E.R.A (5) but rather the detailed distribution of the hydrogen, in particular in the region of the cathode.

9.13. From the potential distribution plots of figures 7.4. to 7.7. it can be seen that the limiting phenomenon occurs closer to the cathode surface than the instrumentation will discern. It would also appear that the stirring of the electrolyte by the cathode gas boundary layer reduces the resistance of that part of the channel. This result is somewhat surprising as the addition of non conducting gas

bubbles to an electrolyte normally increases the resistance(Meredith & Tobias (6)).

It would be wrong to place too much emphasis on this last point, however, as the effect may arise from errors introduced by the positioning of the electrodes flush in the wall, since the effect we are measuring will be sensitive to the influence of a wall.

9.1.4 Hypothesis

All the preceeding evidence leads to the hypothesis that the current limiting process in E.C.M. is a crisis in the cathodic evolution of hydrogen. A reasonable model could be one in which a thin layer of hydrogen is formed next to the cathode, effectively shielding it from the electrolyte. Such a layer would be periodic in nature, and could be governed by factors controlling its stability. These factors would basically be the distribution and magnitude of the bubbles present, and their interfacial properties. Thus surface tension, pressure, temperature, hydrodynamic conditions, and previous history may be expected to effect the process. The history effect has already been shown in Figure 9.1 The effect of pressure and temperature will be basically to change the total volume of hydrogen present, plus any effect on solution properties that may be caused. As a check on the hypothesis, therefore, further experiments were made in which the static pressure was varied, and also surface tension altered by the addition of a surfactant. These experiments are reported in Chapter 10.

9.2 Current Voltage Characteristic

Figure 9.2 shows a copy of the XY recorder trace of the external machining characteristic of cell current against cell voltage. The hypothesis developed to explain the limiting current phenomenon is

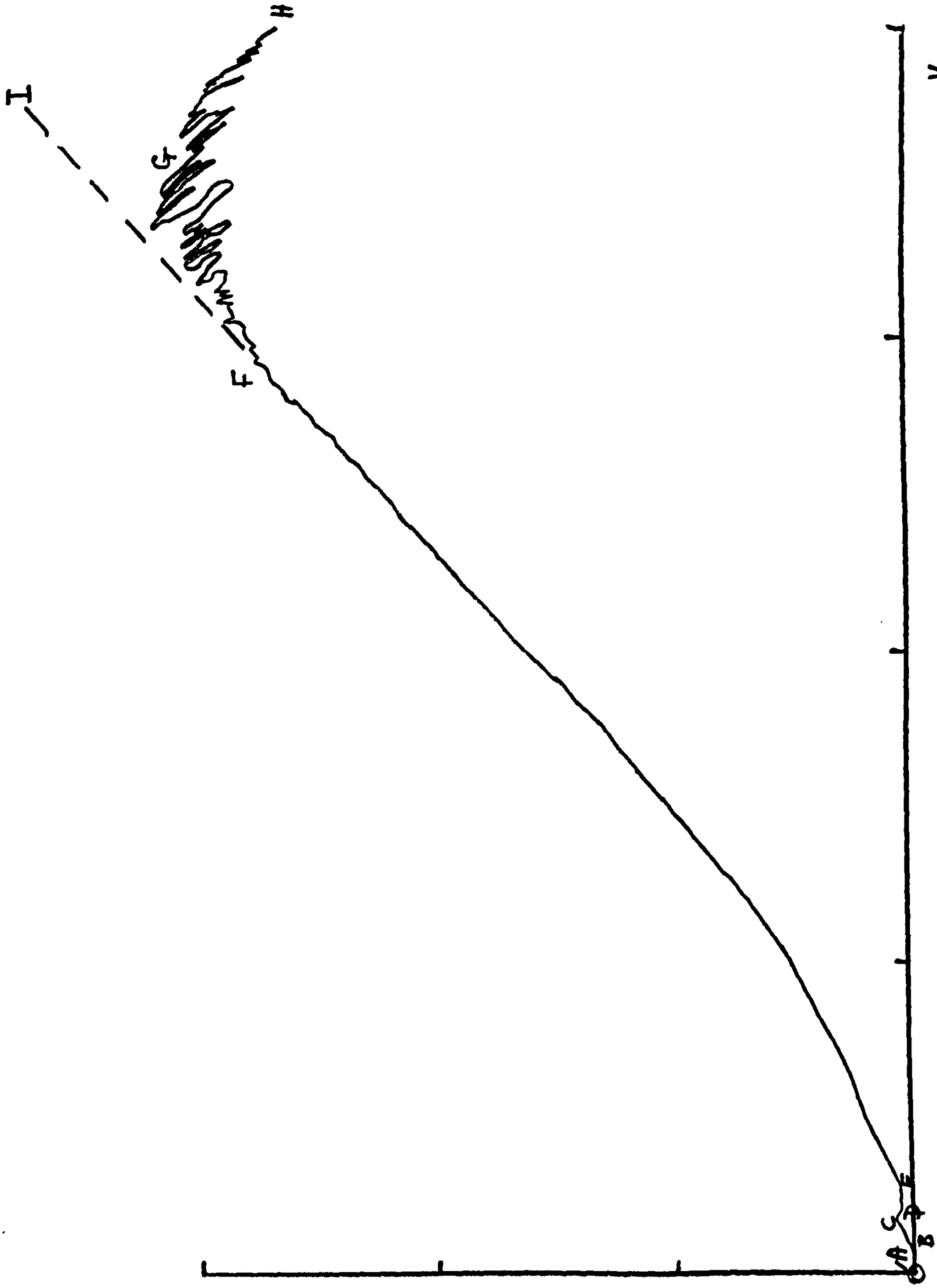

Figure 9.2.

here extended to include the whole machining curve.

Region AB is due to the dissolution of particularly vulnerable metal atoms, probably those at grain boundaries in grains standing proud of the mean surface, and thus having low binding energies. At B the reversible dissolution potential of the metal is achieved and bulk removal of the material commences. In the region BC, from comparison with the experiments of Hoar (4), the dissolution takes place leaving an etched finish due to preferential attack at grain boundaries.

The inflexion at C and the limiting current DE are attributed by Hoar and others to the growth of a thin film (a few molecules) of a compound, probably a copper oxide, on the surface of the metal. The mechanism determining the current is now probably one of ion transport through this film, though which ion is involved is not clear.

Experiments on thicker films on 'valve' (sic) metals by Davies et al (7) and Vermilyea(8) and on aluminium by Francis(9) show that the mobilities of electrons, anions and cations in these films are very specific to the film, and depend not only on the metal but on the electrolyte and forming technique.

Similar films also account for the passivity of some metals in particular solutions and work on these by Bockris et al(10) and Ammar & Darwish (11) for nickel are indicative of the difficulties, both in experimental technique and interpretation, involved in the detailed analysis of one particular case.

Work by Valeev and others (12 , 13, 14) has brought to light several important features of the film responsible for the polishing phenomenon. Their shadowgraph measurements (Valeev, 12) indicate that the anodic diffusion layer contains, at the wall, a highly super-saturated solution of copper.

Their experiments on the photo-electrochemical effect (13 , 14) lead them to the hypothesis that this effect is produced by the same mechanism that produces the polishing effect.

A paper by Hoar et al (4c) summarises and collates much, but not all, of the current theory of the existence, properties and behaviour of all types of anodic films.

From these considerations it is clear that a film of some sort exists on the surface of the metal, and this produces the polishing effect. Metal/electrolyte systems that do not exhibit such an arrest can be expected not to produce satisfactory machining. Those that produce passivating films can be expected to produce no machining at all, while those that dissolve without the formation of a film will machine, but with an etched surface with grain boundary attack. Much evidence in support of this has been collected by many workers in E.C.M., notably in the work of Turner at Nottingham University(15) where several effects have been investigated. The conclusion that can be drawn from this is that the ideal of one universal electrolyte is unlikely to be achievable commercially, since many different electrolytes are required for the successful polishing metals. Work by Hopkins et al (16)on thinning by polishing of electron transmission microscopy specimens of rare earth metals has indicated that a universal electrolyte may be possible in the laboratory if the process were developed for the machining of 'perfect surface' test specimens.

The technique does, however, involve low temperatureand possibly explosive chemicals.

The increase in current in the region EF is brought about by the evolution of oxygen. Some of the current goes directly into

evolving oxygen, but the gas produces very effective mixing conditions in the diffusion layer. This may be expected to lead to a thinning of the layer and a tendency to reduce the concentration of metal at the anode surface. Since this surface is the oxide film/electrolyte interface such a tendency must lead to an increased rate of dissolution of the underlying metal, either by an increased field, or a field induced ion mobility change, or a thinning of the film, or any combination of these effects. The difficulties involved in any attempt to determine which of the latter effects dominate must make the task virtually impossible.

It would be expected that this general increase in current would continue to I if the anodic reaction continued to dominate the characteristic, but in the region of F the control of the process passes to the cathode and the crisis of hydrogen evolution already described.

Further experiments were carried out at this stage to investigate the crisis and the anodic avolution of gas in the region EF., and these are reported in Chapter 10.

10. Experiments to Investigate Crisis Hypothesis.

10.1. Cathodic Potentials.

A cathode was constructed with wire reference electrodes flush in the surface in an attempt to measure the cathodic crisis more accurately, 20 S.W.G. silk covered copper wire was cemented in .055" holes with "Durofix" and finished flush with the electrode surface.

In practice the potentials measured at these electrodes showed fluctuations larger than their mean values and hence were of little value.

This is attributed to two causes. Firstly the region around the probe differs from the ideal equipotential surface, having a copper electrode at zero potential surrounded by a band of insulation. Secondly the size of this different area is of the order of the size of the bubbles present, when ideally it should be much smaller.

10.2 Effect of the addition of Surfactant

The surface tension of the electrolyte was reduced by the addition of approximately 0.15% "Teepol" to it. The machining characteristics with and without surfactant are compared in Figure 10.1, the limiting current density being reduced to about 55% of its previous value. The surface tension of the two electrolytes was compared with water by the capillary rise method, the accuracy of these measurements being uncertain. The results gave the surface tensions of water acid and acid + Teepol to be 72, 65 and 47 Dyne- cm^{-1} respectively, the former being a very reasonable value for water.

Thus the addition of surfactant to the acid reduces the surface tension to 72% of its original value. The correlation between surface tension and limiting current is discussed in Chapter 11.

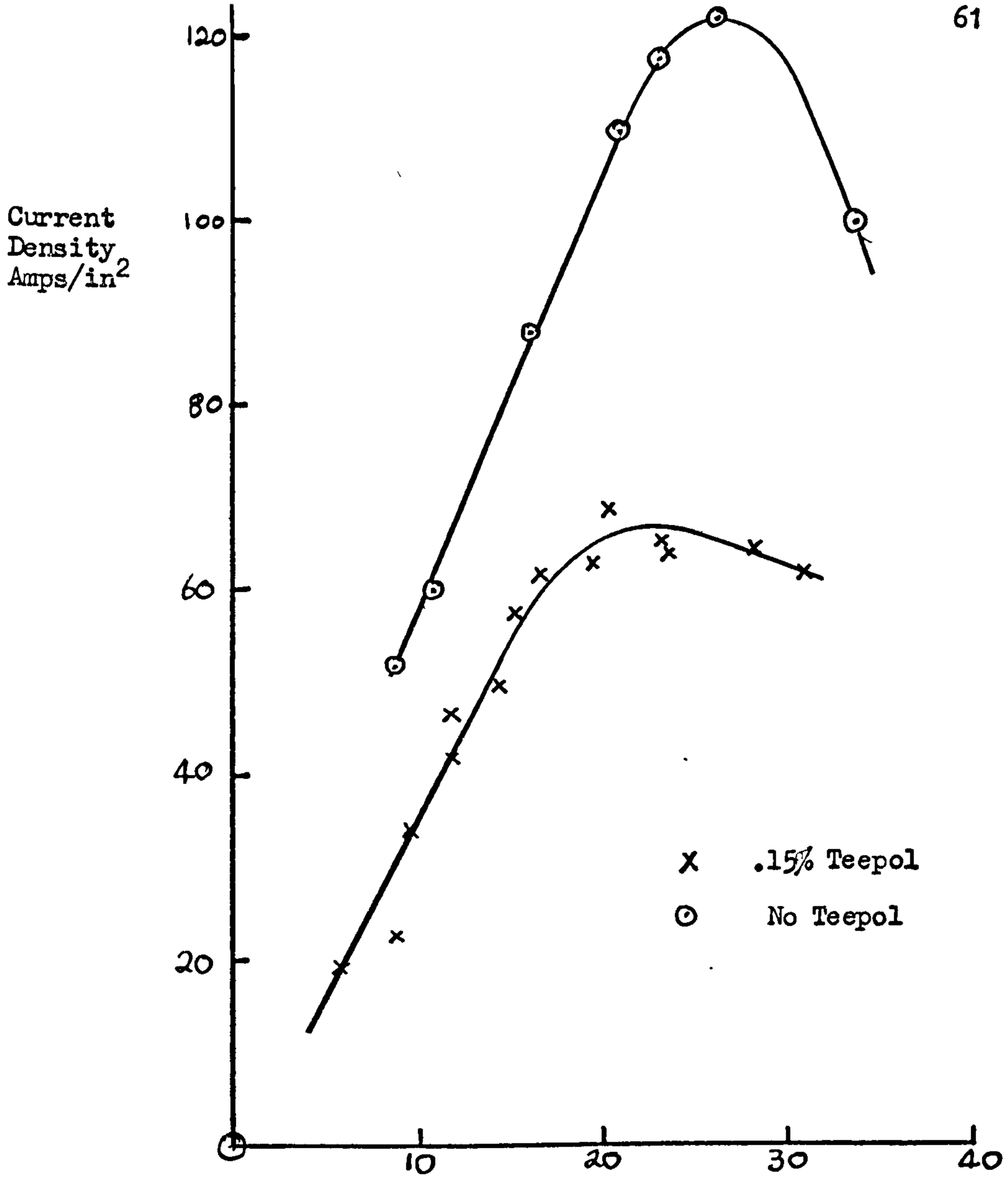

Effect of Surfactant
Copper /Phosphoric acid
Gap .050 ins Flow Velocity 84 ins /sec.

Figure 10.1

10.3. Pressure Effects.

The effect of pressure was investigated by applying a static back pressure to the system, and also by reversing the pump so that the working section was on the suction side. By these means pressures over the range 5 to 120 p.s.i.a. were obtainable. The limiting current was measured using the X-Y recorder technique for a range of pressures at otherwise identical conditions. At each pressure photographs were taken of the bubble boundary layer at low currents, and the size of bubble determined. The results of these experiments are recorded and analysed in table 10.2. The dependence of both bubble size and limiting current on $(\text{pressure})^{\frac{1}{3}}$ is examined for comparison with the theory of Levich(22) P.465 on the breakup of bubbles.

TABLE 10.2

p Absolute Pressure p s i a	I Limiting Current Amps/in^2	d Bubble Diameter Ins x 10^{-3}	d x p$^{\frac{1}{3}}$	I/p$^{\frac{1}{3}}$	I x d
4.8± .5	100	9.5	19	59	0.95
15±3	145	8.5	21	59	1.23
45	185	7	25	52	1.39
65	220	6	21	54	1.32
90	250	5	22	56	1.25
115	150	4.5	21	53	1.12

Copper/Phosphoricacid
Gap .050 ins
Mean Flow velocity 90 ins/sec

10.4 Photographic Experiments.

A special machining channel was constructed with a gap of .050" , .055" wide. Photographs were taken of this at all conditions through the crisis, using the same technique as that used in Chapter 5. Sufficient illumination was available to obtain useful results; typical photographs are shown in Figures10.3 to 10.7 They clearly show the high void ratio involved in the crisis, but do not help in clarifying the mechanisms involved.

10.5 Gas Evolution and Process Efficiency

Since it has been shown that a gas is evolved at the anode during metal dissolution at the high rates encountered in E.C.M. it is clear that some care is required when considering the "efficiency" of the process. To clarify the situation three different efficiencies will be defined and used here as follows:-

Faradaic efficiency Number of coulombs theoretically required to dissolve a particular weight of metal taking each component of the alloy, at its lowest normal valency, in parallel/Total number of coulombs passed to dissolve the metal less those coulombs required for gas evolution.

Gas Efficiency Total number of coulombs passed less those coulombs required for gas evolution/total number of coulombs passed

Overall efficiency = Faradaic efficiency x Gas efficiency.

Most measurements of efficiency reported to date are of overall efficiency though the basis of the calculation is frequently not stated. If it is assumed that the Faradaic efficiency of a given electrode/electrolyte system is constant, though for some metals such as aluminium this may well not be so (Straumanis et al (23) , then the overall and Gas Efficiencies will be proportional and can be compared.

Figures 10.3 to 10.7.

Photographs at 1" downstream from entry of narrow channel.
Copper / phosphoric acid.
Magnification x70.
Crisis occurs at a cell voltage between 20 & 30v.

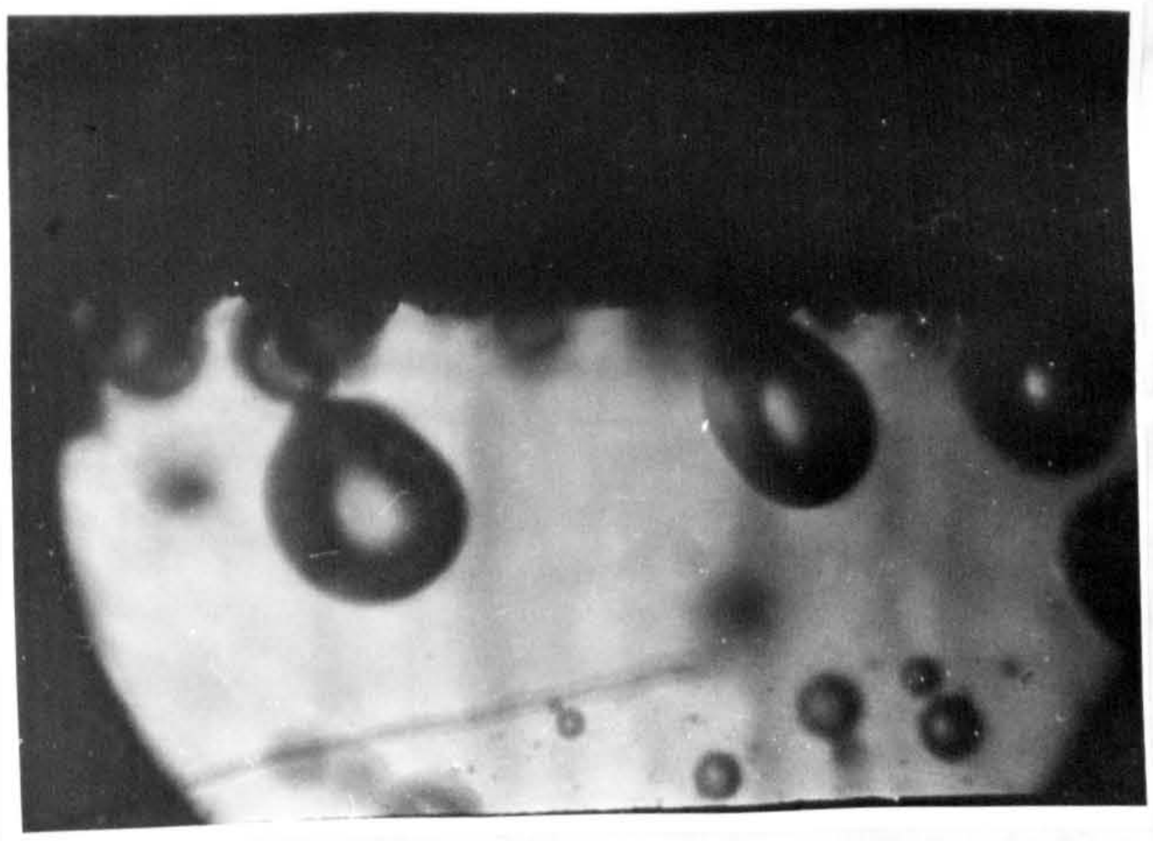

10.3. Vc=5v.

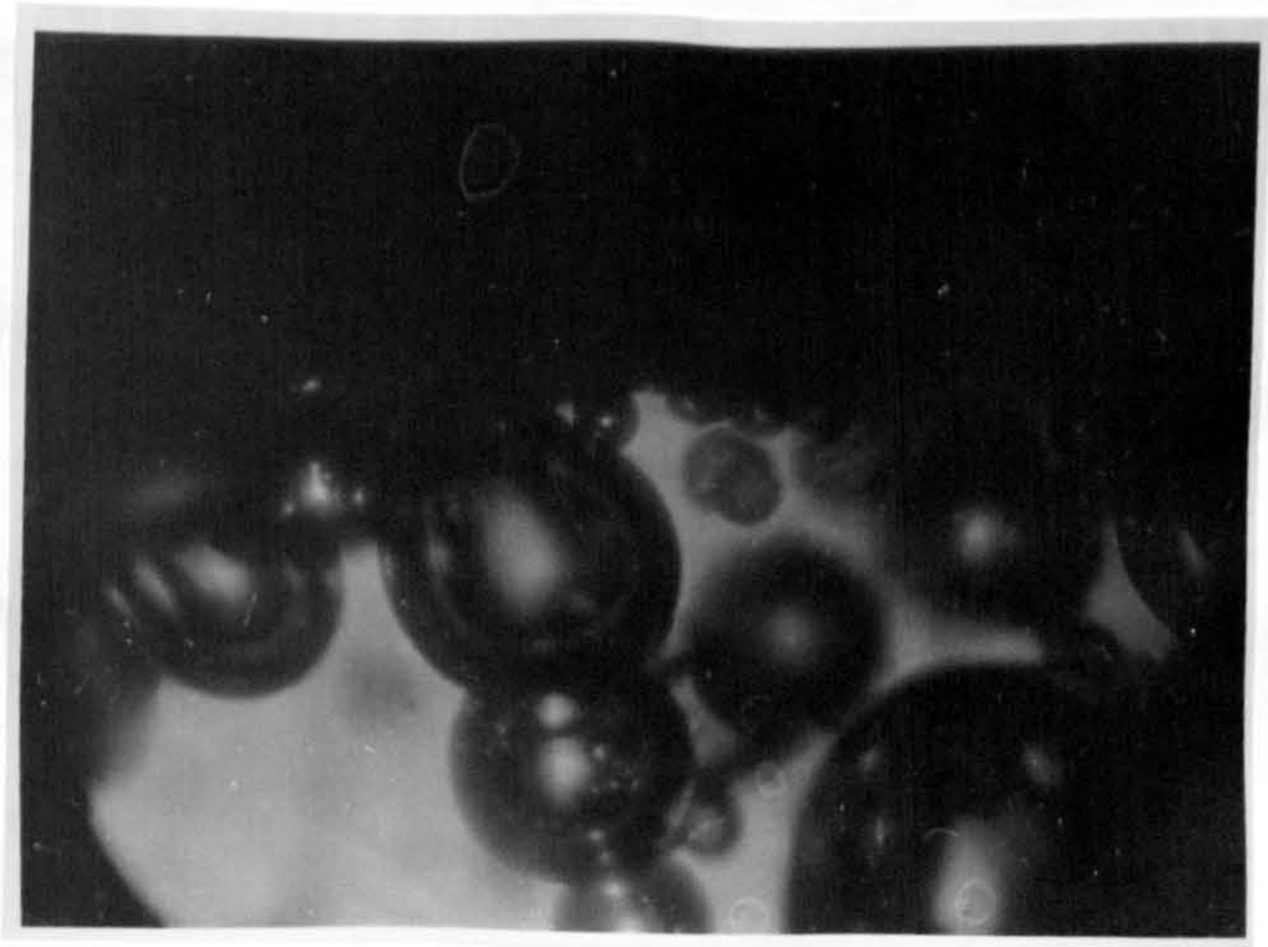

10.4. Vc=10v.

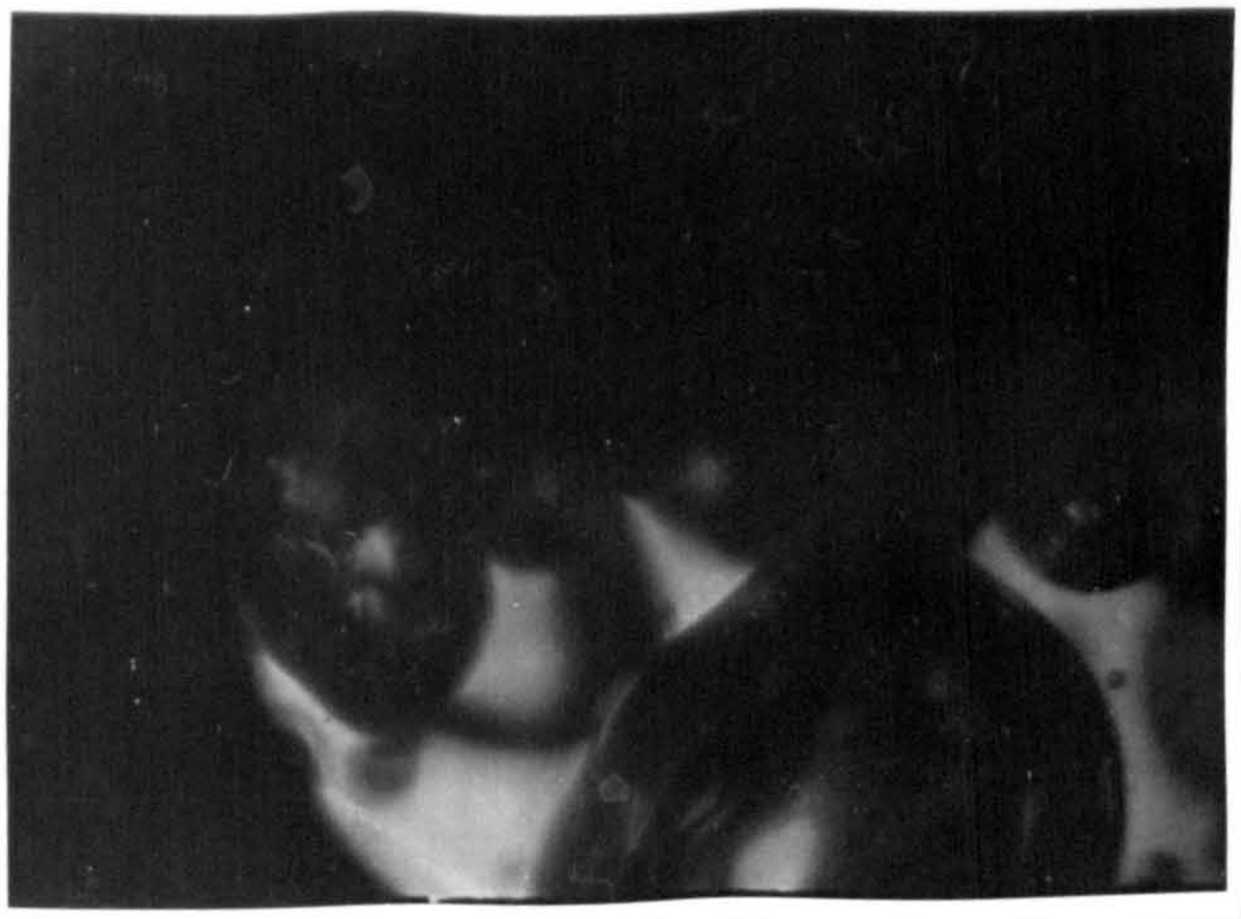

10.5. Vc=19v.

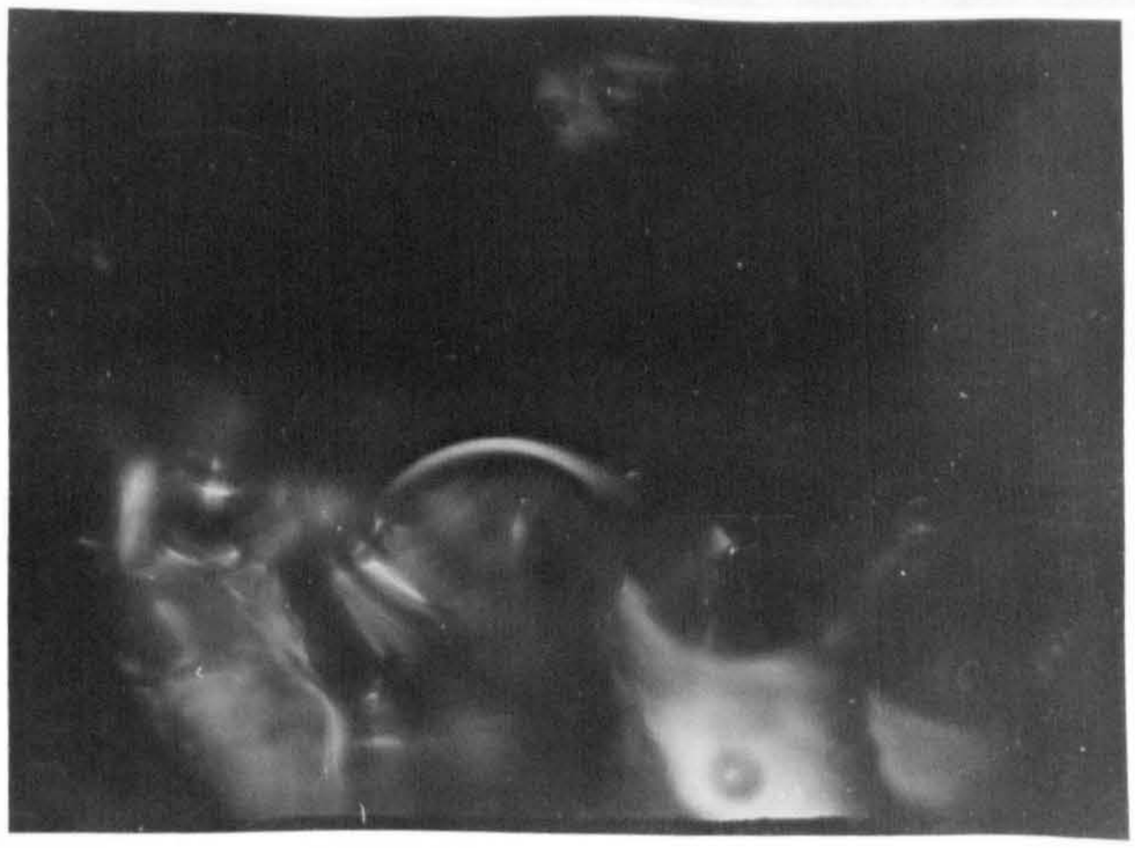

10.6. Vc= 24v.

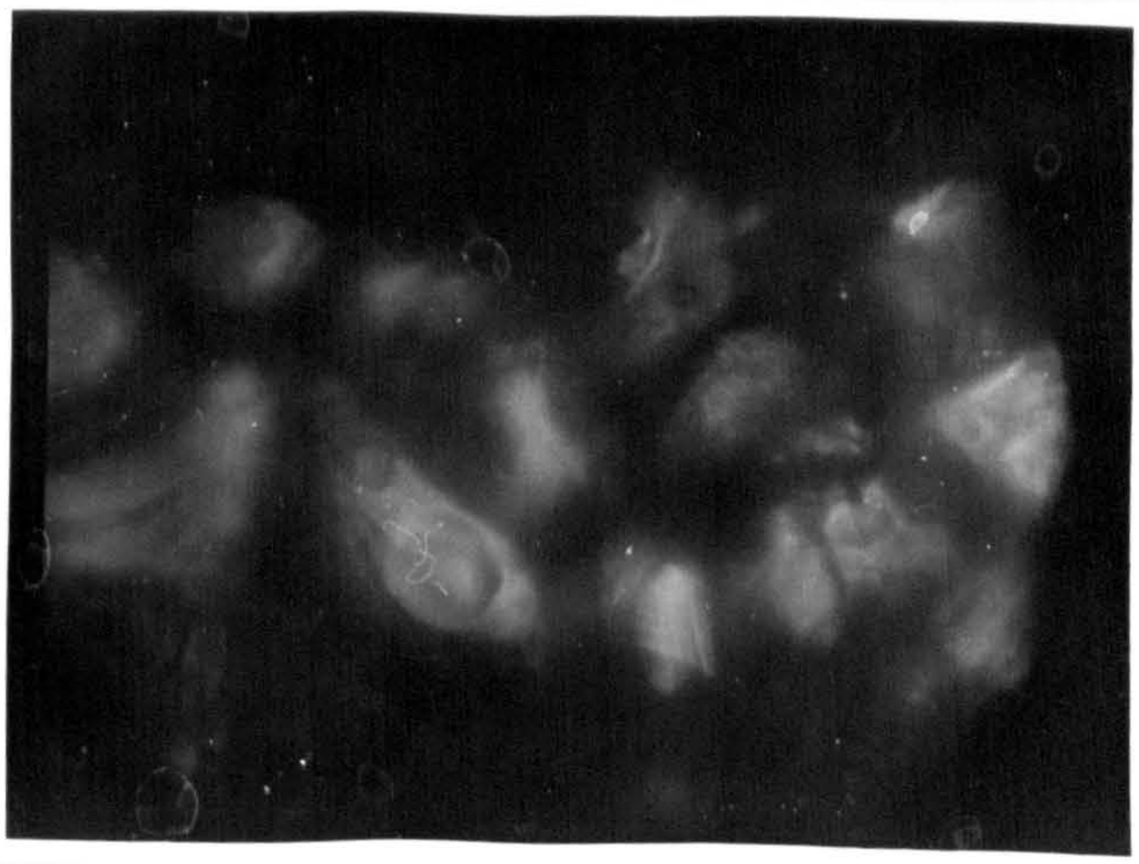

10.7. Vc= 39v.

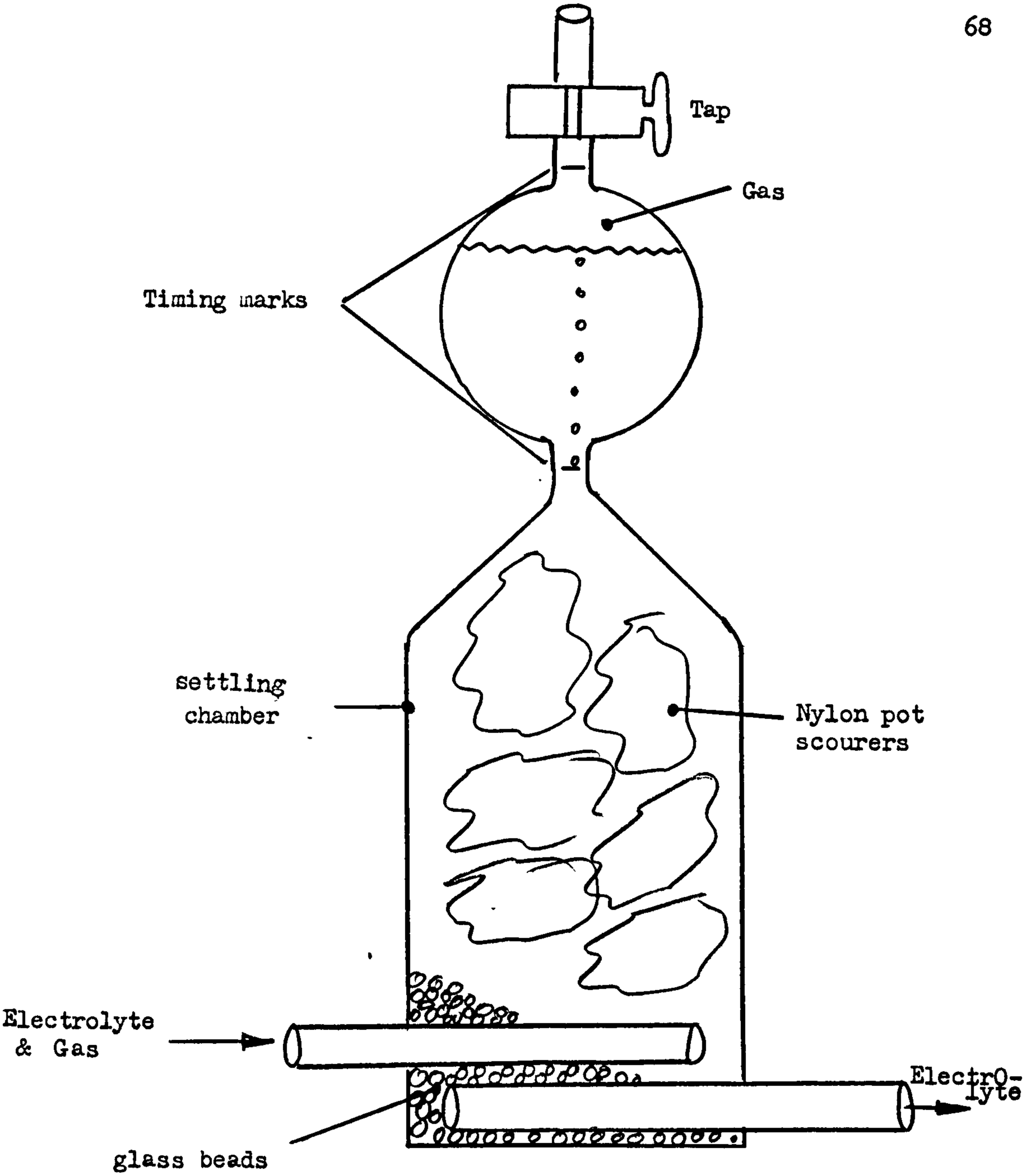

Gas Separation apparatus
Construction one piece glass
(inlet would be better at top of settling chamber)

Figure 10.8

This assumption is particularly dubious in the case of alloys when the valencies are often uncertain.

The Gas efficiency was measured during machining in the normal working section by separating the gas evolved from the electrolyte. This was done by introducing a large chamber in the outlet pipe in which the gas could rise in the slow moving fluid. The apparatus is shown in Figure 10.8. Under some flow conditions the bubbles produced are very small and, having low rise velocities, are difficult to separate. The apparatus is far from ideal and could be developed to reduce the considerable errors experienced due to some of the bubbles passing through with the fluid.

Several systems were investigated; the copper/phosporic acid system, and copper, aluminium and mild steel with sodium chlorate and sodium chloride as the electrolytes. The current- voltage characteristics of these systems are shown in Figures 10.9 to 10.12; The current was held at a particular value, and the gap maintained constant while the time taken to fill the upper flask was measured. The pressure of the gas in the flask was measured at the end of each run with a manometer; the temperature was assumed to be that of the electrolyte in the tank.

From the time taken to fill the flask at a given current the "gas efficiency" can be calculated as follows;-

Number of coulombs passed = current x time = C

This number of coulombs will liberate $\frac{C \times 11.2}{96,500}$ litres

of hydrogen at S.T.P.

The volume of oxygen (or other gas) evolved is then calculated by subtracting the theoretical volume of hydrogen from the volume of the gas in the flask corrected to S.T.P. Assuming that the

gas evolved at the anode is oxygen, the number of coulombs required to evolve v litres of oxygen at S.T.P. is $\frac{v \times 96,500}{5.6}$ coulombs (Q)

The gas efficiency is $\frac{C-Q \times 100\%}{C}$.

Since some gas was lost due to poor separation this efficiency was sometimes negative. This is clearly in error, but in the absence of a reliable method of correcting for the lost gas the results are plotted as obtained in Figure 10.13. to 10.15.

A correction was, however, applied to some early results on the copper/phosphoric acid system to allow for a gas leak in the apparatus which, due to a sub-atmospheric pressure in the flask, produced readings indicating efficiencies greater than 100% .

The results for low currents were corrected on the assumption, justified by visual observation, that no gas was evolved at the anode, and hence the gas efficiency should be constant at 100%.

The leak was assumed to produce a constant rate of loss of gas ' w '. The time 'T' taken to fill the flask of volume 'V' is given by $\frac{V}{T} = q - w$ where q is the rate of evolution of gas.

Now for very low currents $q = k \times I$ since only cathodic hydrogen evolution occurs.

hence $k I - \frac{V}{T} = w$

and from the intercept of an I vs $1/T$ plot, a correction is obtained which is then added to all values of $1/T$ for that series of experiments to produce corrected values of T. At very low currents this produces a constant value of gas efficiency of 85%, thus indicating that some 15% of gas may be lost due to inefficient separation.

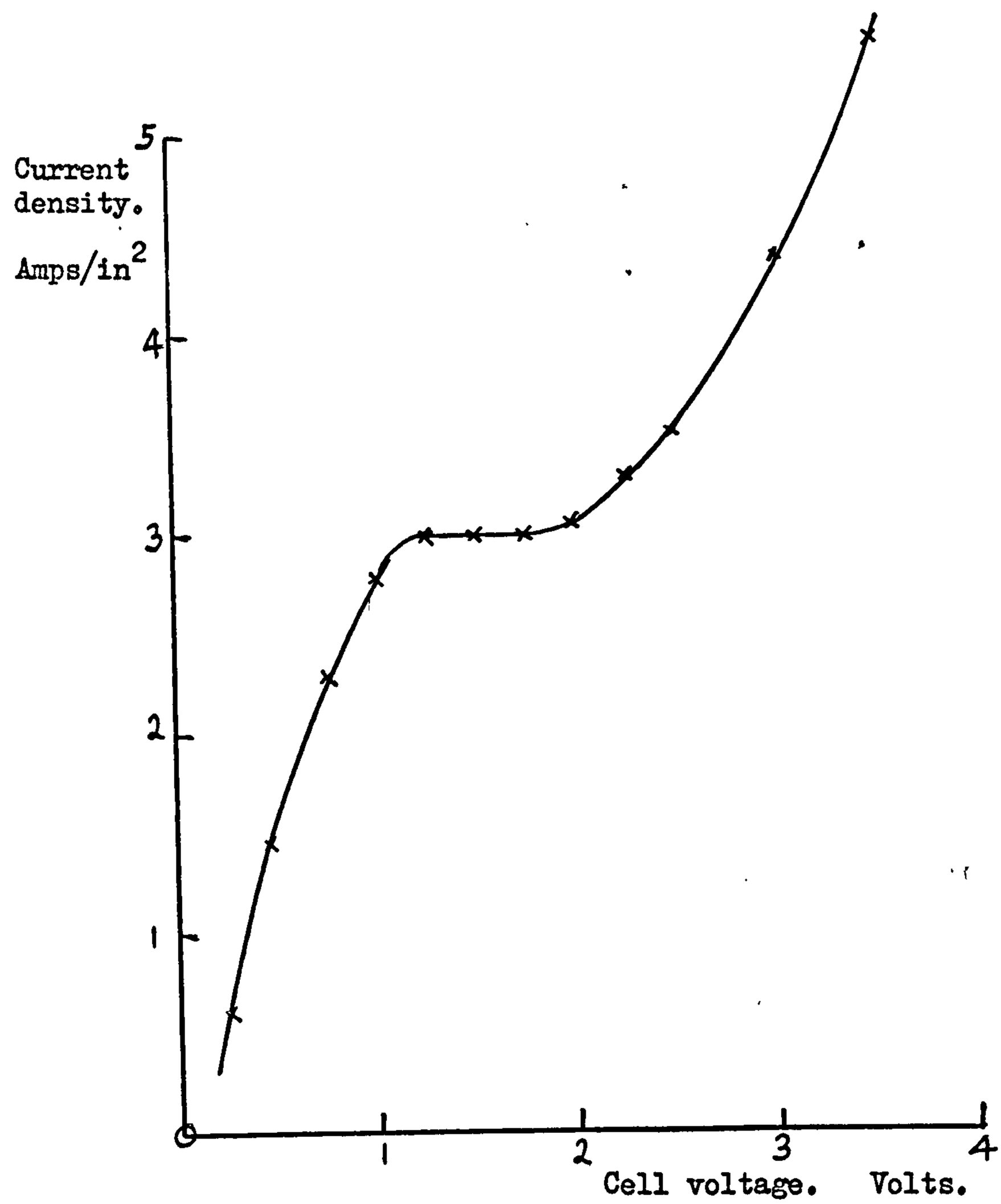

Cell voltage-current.(Galvanostatic).

Copper / phosphoric acid S.G.= 1.14.

Gap .050 ins. Flow velocity 40 ins/ sec.

Figure 10.9.

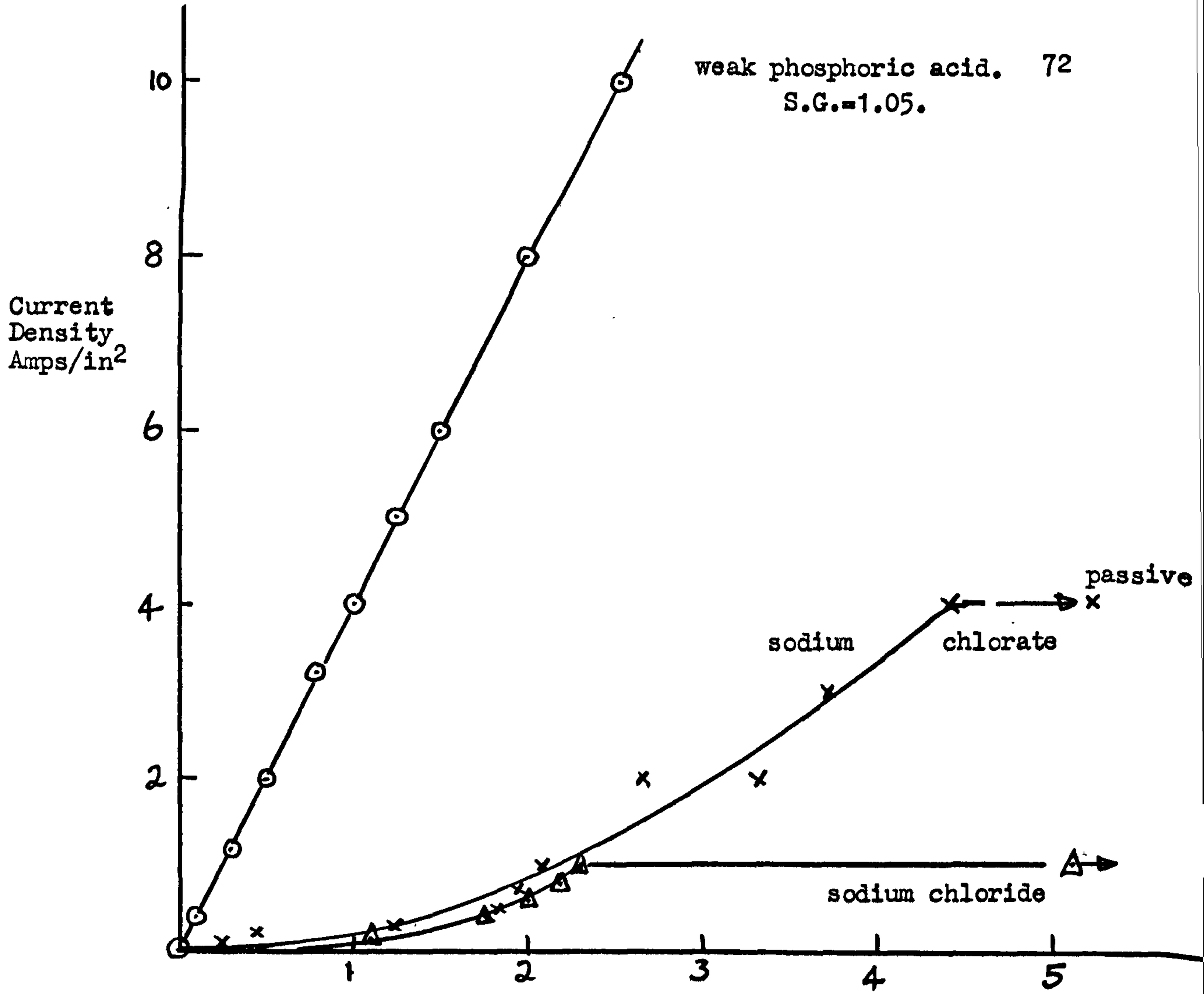

Cell Voltage - Current (Galvanostatic)
Copper in various electrolytes
Gap .050 ins Flow Velocity 40 ins /sec.

Figure 10.10

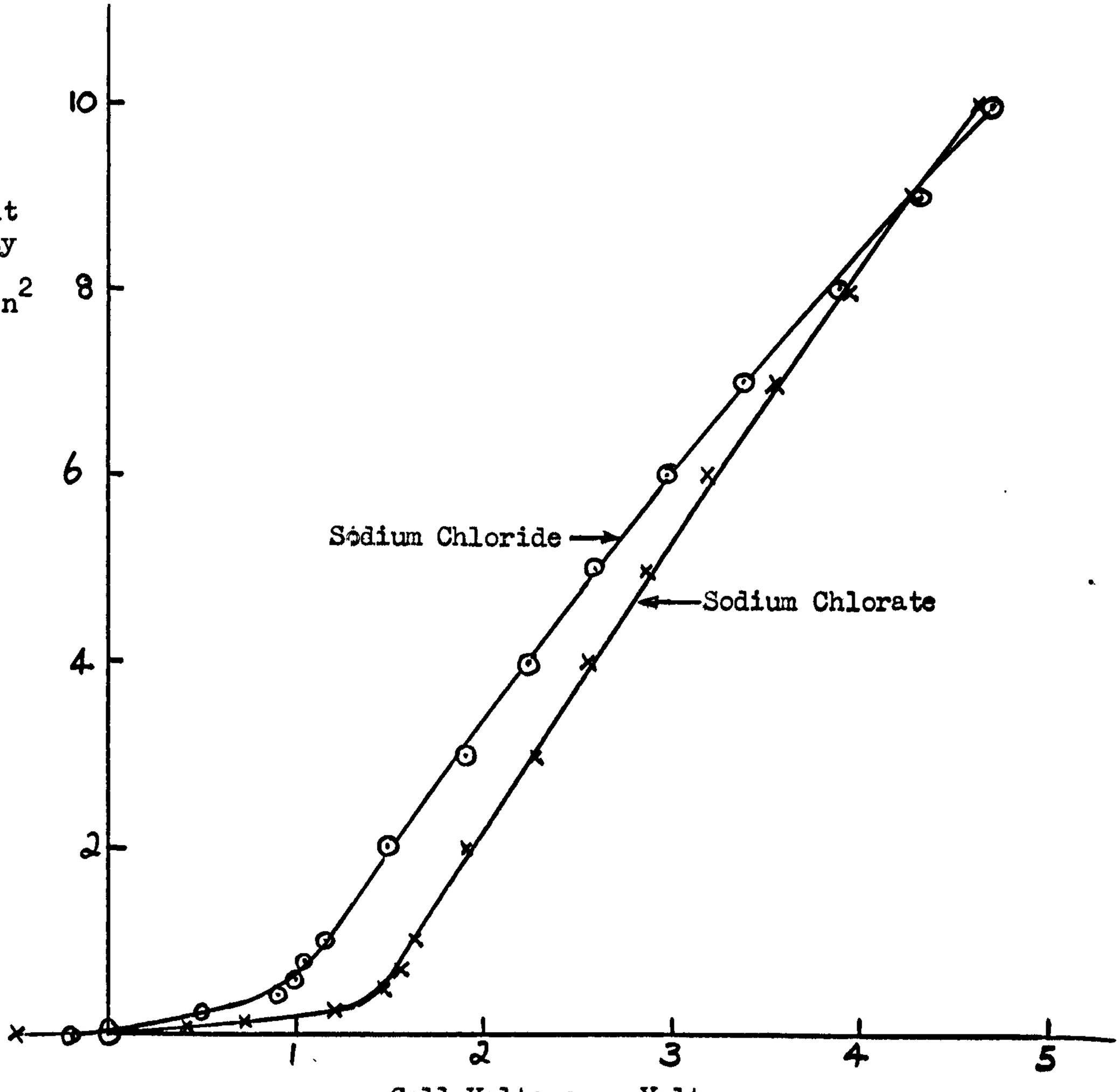

Cell Voltage-Current(Galvanostatic)
Aluminium/Sodium Chlorate & Sodium Chloride
Gap .050 ins. Flow Velocity 40 ins/sec

Figure 10.11

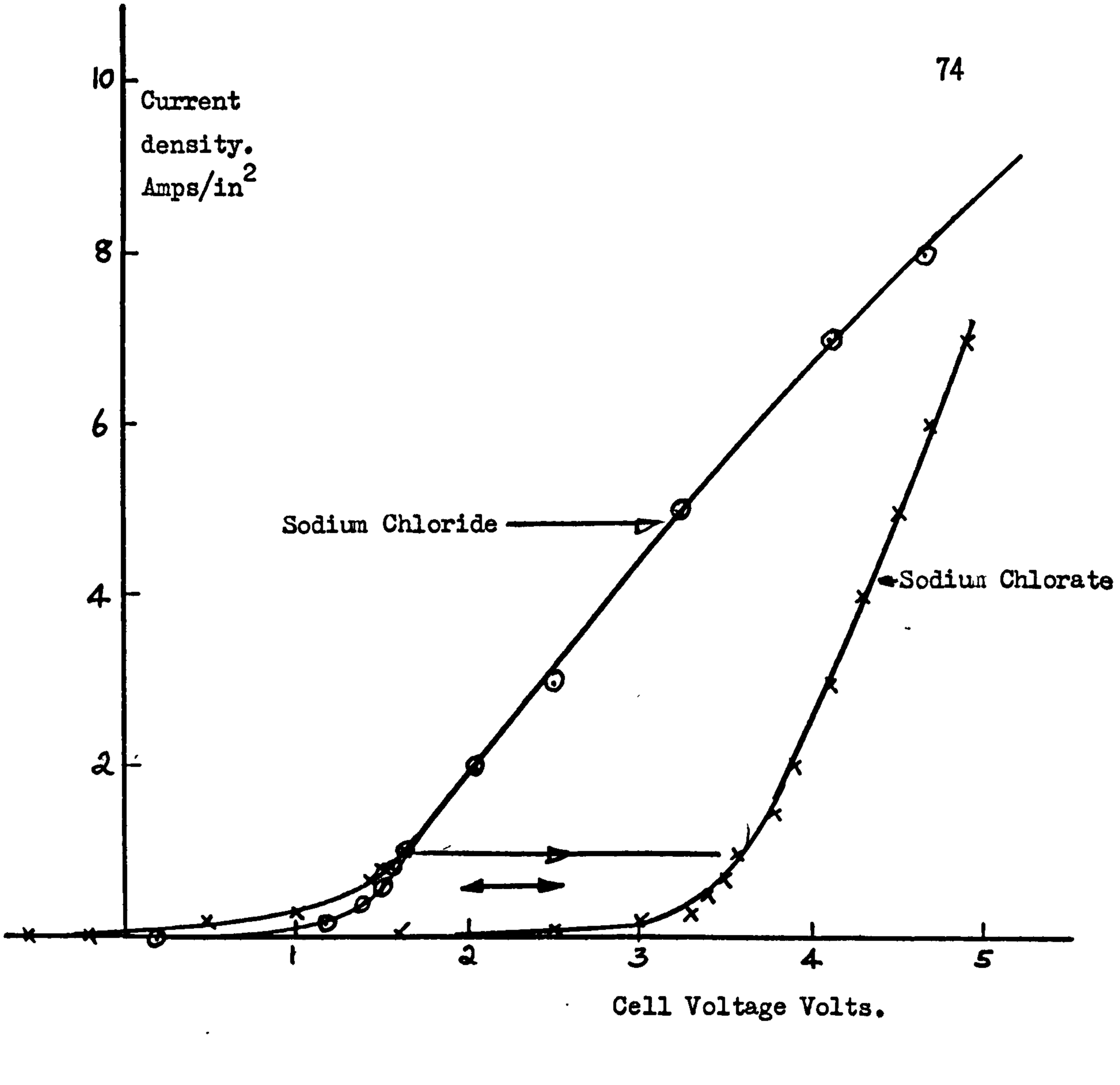

Cell Voltage - Current (Galvanostatic)
Mild Steel in sodium Chlorate & chloride
Gap .022ins Flow Velocity 85 ins/sec

Figure 10.12

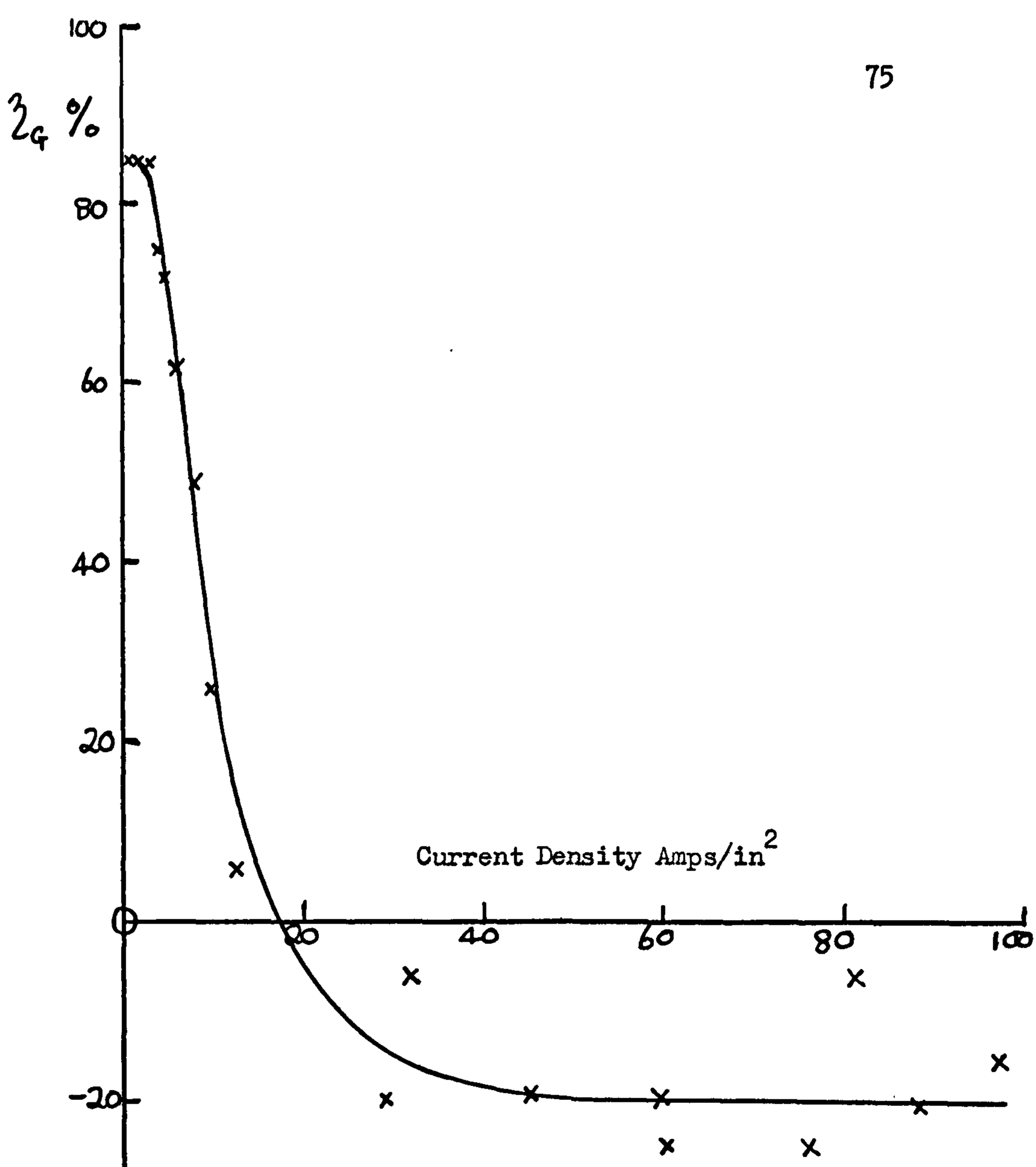

Gas Efficiency
Copper in strong phosphoric acid
Gap .050 inch Flow velocity 90 ins/sec

Figure 10.13.

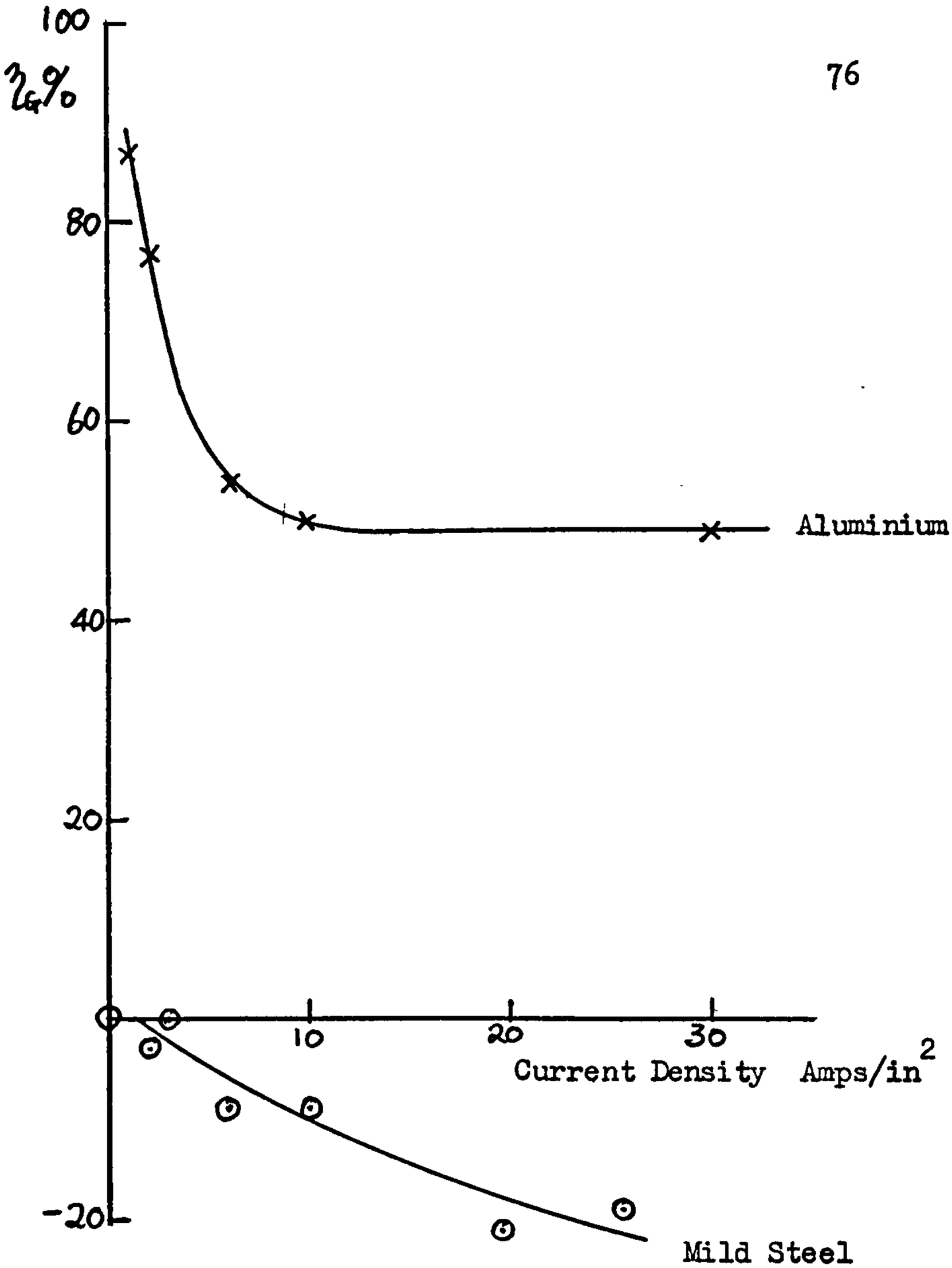

Gas Efficiency
Sodium Chlorate Solution
Gap .050 inch Flow Velocity 90 ins/sec

Figure 10.14.

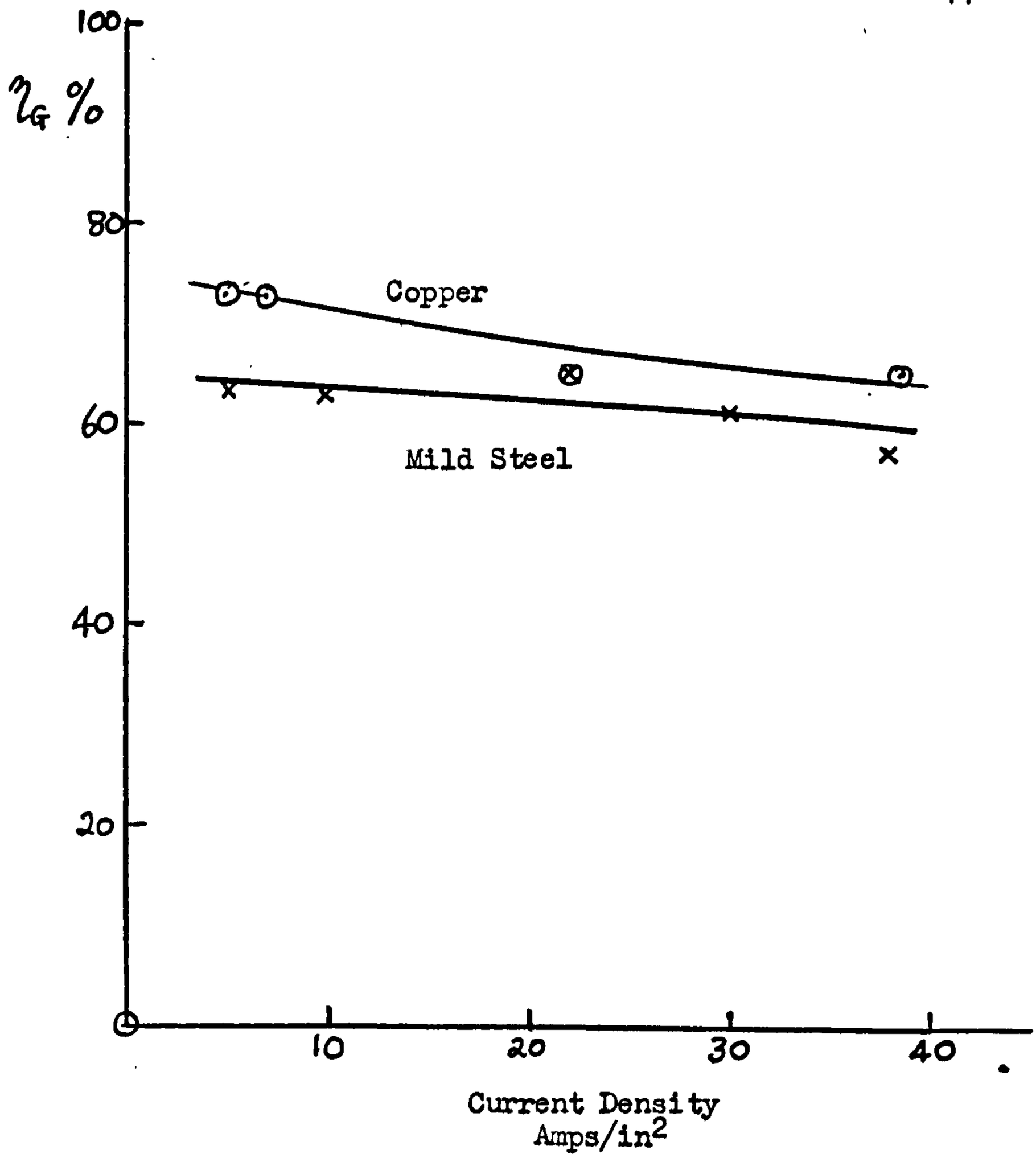

Gas Efficiency
Sodium Chloride Solution
Gap .050 inch Flow Velocity 90 ins/sec

Figure 10.15.

11. DISCUSSION.

11.1 Crisis Hypothesis.

It will now be shown how the results of the experiments detailed in the previous chapter confirm and clarify the hypothesis of the controlling processes of electrochemical machining.

From the results of the experiments on the variation of limiting current and bubble size with pressure, given in Table 10.2, it is clear that a correlation exists between the limiting current and the bubble size. Now the mass of gas in a bubble is proportional to ρd^3, hence the results show that the mass of gas in each bubble is invariant with pressure; the size of the bubbles, however, varies, and hence to account for the increased current the number of bubbles involved must rise. From the work of Levich (22,p465.) on the breakup of bubbles we can theoretically expect the diameters to be proportional to σ/p,$^{1/3}$ unfortunately no data is available on the variation of bubble size with surface tension. The current required to evolve a bubble must be proportional to the mass of gas contained in it, and hence the limiting current data of Table 10.2 can be interpreted as showing that the number of bubbles involved in the crisis is inversely proportional to their diameter at constant pressure.

The simplest model of the crisis would be one in which a layer of bubbles is formed on the electrode, the geometry of the layer depending on the bubble diameter; such a layer will lead to a constant degree of shielding of the electrode surface by bubble arrays of different sizes.

This leads to the prediction that the number of bubbles involved should be inversely proportional to their diameter squared. Theories of constant void ratio predict inverse proportionality to diameter cubed. If the crisis is supposed to be due to a limited number of bubble nucleation sites being used at a maximum(constant) rate, then there would be no dependance on bubble diameter.

Suppose however, that each bubble departs from the site at a constant velocity U , then the maximum bubble generation rate is U/d, the current will be proportional to the total mass of gas evolved i.e. a constant x Pd^3 x U/d. Since $d p^{\frac{1}{3}}$ has been found to be a constant we then find $I = k \times \frac{U}{d}$ where k and U are constants, the limiting current is inversely proportional to bubble diameter. This would agree with the pressure experiments. For the surfactant experiments this model would predict $I = k \times d^3 \times \frac{U}{d}$ at constant pressure, if $d = k^1 \times \sigma$ then $I = k\sigma^2$; the limiting current is proportional to surface tension squared, thus predicting a reduction to 52% of its former value compared with 55% experimentally.

The photographic evidence of figures 10.3 to 10.7 shows that whatever mechanism is involved the void ratio at the crisis is high throughout the channel, but does not help in defining the mechanism involved. This mechanism proposed appears reasonable; further experimental evidence for a wider range of pressure, surface tension, and hence bubble sizes,would be useful.

11.2 Gas Evolution.

The gas evolution experiments provide further evidence in favour of the theory of the control of the E.C.M. process by stirring of the anode layer by gas evolution.

The"gas efficiency"was introduced as a measure of the coulomb

efficiency of the process. It does not involve the valency of the metal cut which is often open to doubt, and is the ratio of the coulombs available for metal removal to total number of coulombs passed. From the systems investigated the following general observations can be made.

(1) The high values of gas efficiency at high current densities are associated with etched finishes, the lower values with better finishes, though nearly complete passivation can be accompanied by either a good or a very rough finish.

(2) The rise in gas efficiency at low currents is associated with the approach to reversible dissolution without anodic gas evolution.

(3) All the systems investigated show similarly shaped curves, tending to a constant value of efficiency at high currents. A similar result was obtained by McGeough (3) using a weight loss technique of cutting rate measurement for cast iron in sodium chloride. This behaviour may or may not be general, the model proposed by Hoar(4) and modified to include gas evolution in chapter 9 of metal solid(oxide?) film- supersaturated electrolyte stirred by gas evolution is so complicated that the prediction of such an effect is difficult.

The results of these experiments show that all the published cutting efficiencies must be viewed with suspicion as they do not allow for the evolution of oxygen. It is clear that a further series of experiments is needed combining improved gas evolution rate measurements with weight loss measurements to clarify the actual metal removal rates and Faradaic efficiencies.

12. THEORETICAL WORK

As stated earlier it was clear that E.C.M. conditions could not be approximated by the normal assumptions made in convective mass transfer analysis. The differences are (1) Very high degrees of supersaturation of metal ions at the electrode, leading to non-constant viscosity, density and diffusion coefficients. (2) Gas evolution.

The latter was only proved to exist during this investigation and will produce effects much larger than the former. Gas evolution will effect the process by removing some highly supersaturated solution to a region of lower concentration. The model required to describe this could be similar to that proposed by Han & Griffith(19) for nucleate pool boiling, but experimental evidence will be required to determine the exact form of the model.

12.1 The effects on convective mass transfer by high supersaturation of the electrode layer are examined theoretically in this chapter.. This work was done before the evidence of significant bubble evolution was obtained, and though of little direct interest to E.C.M., it is included for completeness.

The configuration taken was that of a semi-infinite flat plate in an infinite fluid in uniform steady motion.

Consider the laminar boundary layer equations, and the diffusion equation, allowing viscosity to vary with the concentration of the diffusing species. From the Navier Stokes equations, including variable viscosity, making the normal boundary layer approximation we obtain :-

$$v_x \frac{\partial v_x}{\partial x} + v_y \frac{\partial v_x}{\partial y} = \frac{1}{\rho} \frac{\partial}{\partial y}\left(\mu \frac{\partial v_x}{\partial y}\right) \quad -- \quad (1)$$

$$\frac{\partial v_x}{\partial x} + \frac{\partial v_y}{\partial y} = 0 \quad -- \quad -- \quad -- \quad (2)$$

The diffusion equation in the boundary layer case reduces to

$$v_x \frac{\partial c}{\partial x} + v_y \frac{\partial c}{\partial y} = \frac{\partial}{\partial y}\left(D \frac{\partial c}{\partial y}\right) \quad -- \quad (3)$$

If we now introduce the stream function ψ such that $v_x = \frac{\partial \psi}{\partial y}, v_y = \frac{-\partial \psi}{\partial x}$, then Equation (2) is satisfied identically, and consider a similarity parameter $\eta = kyx^{-\frac{1}{2}}$ where $k = \frac{1}{2}\sqrt{\frac{U_o}{\nu_o x}}$, and express ψ as a function of η i.e.

$$\psi = k_1 x^{\frac{1}{2}} f(\eta) \quad \text{where } k_1 = \sqrt{\nu_o U_o}$$

then we find that $v_x = kk_1 f'$ $\qquad v_y = \frac{k_1}{2x^{1/2}}(\eta f' - f)$

$$\frac{\partial v_x}{\partial x} = -\frac{k k_1 \eta f''}{2x} \qquad \frac{\partial v_x}{\partial y} = \frac{k^2 k_1 f''}{x^{\frac{1}{2}}}$$

$$\left(f' = \frac{\partial}{\partial \eta}[f(\eta)]\right)$$

Now we require to know the dependence of the viscosity and diffusion coefficient upon concentration; These are taken as

$\mu = \mu_o e^{\eta c}$ (24, Stokes & Mills) and $D\mu = \text{const}$ (25, Robinson & Stokes)

The former was fitted with reasonable accuracy to data for copper in phosporic acid, the latter is taken for simplicity, its validity in concentrated solutions is doubtful, but there is little data available for these solutions. Making these assumptions we find

$$\frac{\partial}{\partial y}\left(D \frac{\partial c}{\partial y}\right) = D_o e^{-\eta c}(c'' - \eta c'^2)\frac{k^2}{x}$$

$$\frac{\partial}{\partial y}\left(\mu \frac{\partial v_x}{\partial y}\right) = \frac{k^3 k_1 \mu_o e^{\eta c}}{x}(f''' + \eta c' f'')$$

substituting in equations (1) and (3) we find that they reduce to

$$\left.\begin{aligned} fc' + \frac{e^{-\eta c}}{Sc}(c'' - \eta c'^2) &= 0 \\ ff'' + \frac{e^{+\eta c}}{e/e_o}(f''' + \eta c' f'') &= 0 \end{aligned}\right\} \qquad (4)$$

where $Sc = \frac{\nu_o}{D_o}$

Now in the region very close to the wall where the large variations in concentration occur the fluid motion will be governed by a balance of viscous forces, in equation (4) the ff'' term, which arises from the inertia forces, is small, and hence variation in density will be unimportant. In the outer regions of the boundary layer the concentration is nearly constant and hence variations in density will be small; hence take $\rho/\rho_o = 1$

now put $\ln(\phi) = \quad - Zc$

then the equations (4) become:-

$$\left.\begin{aligned} f\frac{\phi'}{\phi} + \frac{\phi''}{Sc} &= 0 \\ \frac{f'''}{f''} &= \frac{\phi'}{\phi} - \phi f \end{aligned}\right\} \qquad (5)$$

The solution is required to these equations with the set split boundary conditions, at $\zeta = 0$; $\phi = e^{-ZC_{sat}}$ $f = 0, f' = 0.$ and at $\zeta \to \infty$, $f' = 2$, $\phi = e^{-ZC_\infty}$.

12.2. Data

Numerical values for the various properties involved were taken as follows:-

Phosphoric acid of 1.55 gms/litre concentration is saturated with cupric ions at 93gms/litre, and can be supersaturated by anodic dissolution to 330 gms/litre. Valeev (12)

The value of Z in the relations $\mu = \mu_o e^{ZC}$ where C is in gms/litre was found to be .0077 by fitting the data of Zembura(18) for 20N. phosphoric acid and copper.

The Schmidt number Sc was evaluated from the data of Edwards and Huffmann(17) for moderate concentrations of

phosphoric acid.

$D \approx 8 \times 10^{-6}$ Cm^2/sec ($[H_2PO_4]^-$ ion)

$\nu \approx .041$ Cm^2/sec

$S_c \approx 5000$

12.3 Solution.

The problem was solved by digital computation using an iterative Runge-Kutta method. The programme was written in algol for an Elliot 803 computer and is given in Figure 12.1.

Solutions were obtained in the range of parameters

$$1000 < Sc < 9000$$

$$.5 < ZC_w < 3$$

$$0 < ZC_\infty < 1.25$$

The general form of solution is given in Figure 12.2 showing the variation of ZC and f' with ζ . The most interesting part of the solution is the rate of the reaction at the wall, in this case the current. This is given by

$$\left(D \frac{\partial c}{\partial y}\right)_{wall} = \frac{Do}{2}\sqrt{\frac{U_o}{\nu \sigma x}} \left(c' e^{-ZC_w}\right)_{wall}$$

Hence $J = k\left(ZC' e^{-ZC}\right)_{wall}$ where $k = \frac{Do}{2Z} \times \sqrt{\frac{Uo}{y_o x}}$

It was found that, as with the constant property solution, J was nearly proportional to $(Sc)^{-\frac{1}{3}}$

Table 12.3 gives the particular solutions obtained.

```
begin real a,c,e,f,h,k,l,m,q,r,s,t,x,y,Sc,
        aa,N,A,B,C,D,E,F,Y,G,H,K;
switch d:=build,cut,stop,start,end,go;
integer i,z;  array L,M,P,Q[1:3];
read Sc,Y,G,H,aa,z,K;
go:L[1]:=L[2]:=G; L[3]:=G*(1-aa); M[1]:=M[3]:=H;
         M[2]:=H*(1-aa);  i:=1;
start: a:=L[i];c:=M[i];   y:=exp(-Y);
print freepoint(4), Sc,y,a,c,K;
x:=e:=f:=0; h:=.01;
build:k:=h*a*(1-h*Sc*f/y/2); q:=-Sc*f*a/y;
 r:=-Sc*(f+h*e)*(a-h*Sc*f*a/y)/(y+h*a);
cut: if z>1then print freepoint(4),
x,sameline,ff s3??,e;
if x>4.4 then goto stop;
l:=h*(e+h*c/2); m:=h*c*(1+h/2*(a/y-y*f)); s:=c*(a/y-y*f);
t:=(c+h*s)*((a-h*Sc*f*a/y)/(y+h*a)-(y+h*a)*(f+h*e));
x:=x+h; f:=f+l; e:=e+m; c:=c+h/2*(s+t);
if a/y<.001 then goto cut;
if z>1 then print sameline,freepoint(4),
ff s3??,-ln(y),ff s3??,-a/y;
y:=y+k; a:=a+h/2*(q+r);
if a/y>.01 then goto build else
         begin Q[i]:=-ln(y); a:=0; y:=exp(-K); h:=.1;
                goto cut;end;
stop: P[i]:=e; if z>3 then goto end;
i:=i+1;if i<3.5 then goto start;
C:=(P[1]-P[2])/aa/M[1]; B:=(P[1]-P[3])/aa/L[1];
A:=P[1]-B*L[1]-C*M[1];
F:=(Q[1]-Q[2])/aa/M[1]; E:=(Q[1]-Q[3])/aa/L[1];
 D:=Q[1]-E*L[1]-F*M[1];
G:=((2-A)*F-K*C+D*C)/(B*F-E*C);
 H:=((2-A)*E-K*B+D*B)/(C*E-F*B);
N:=abs(G-L[1])/10/G+abs(H-M[1])/10/H;
aa:=aa*N; print aa; if aa<.00001 then z:=4;
        goto go;
end: end;
```

FIGURE 12.1.

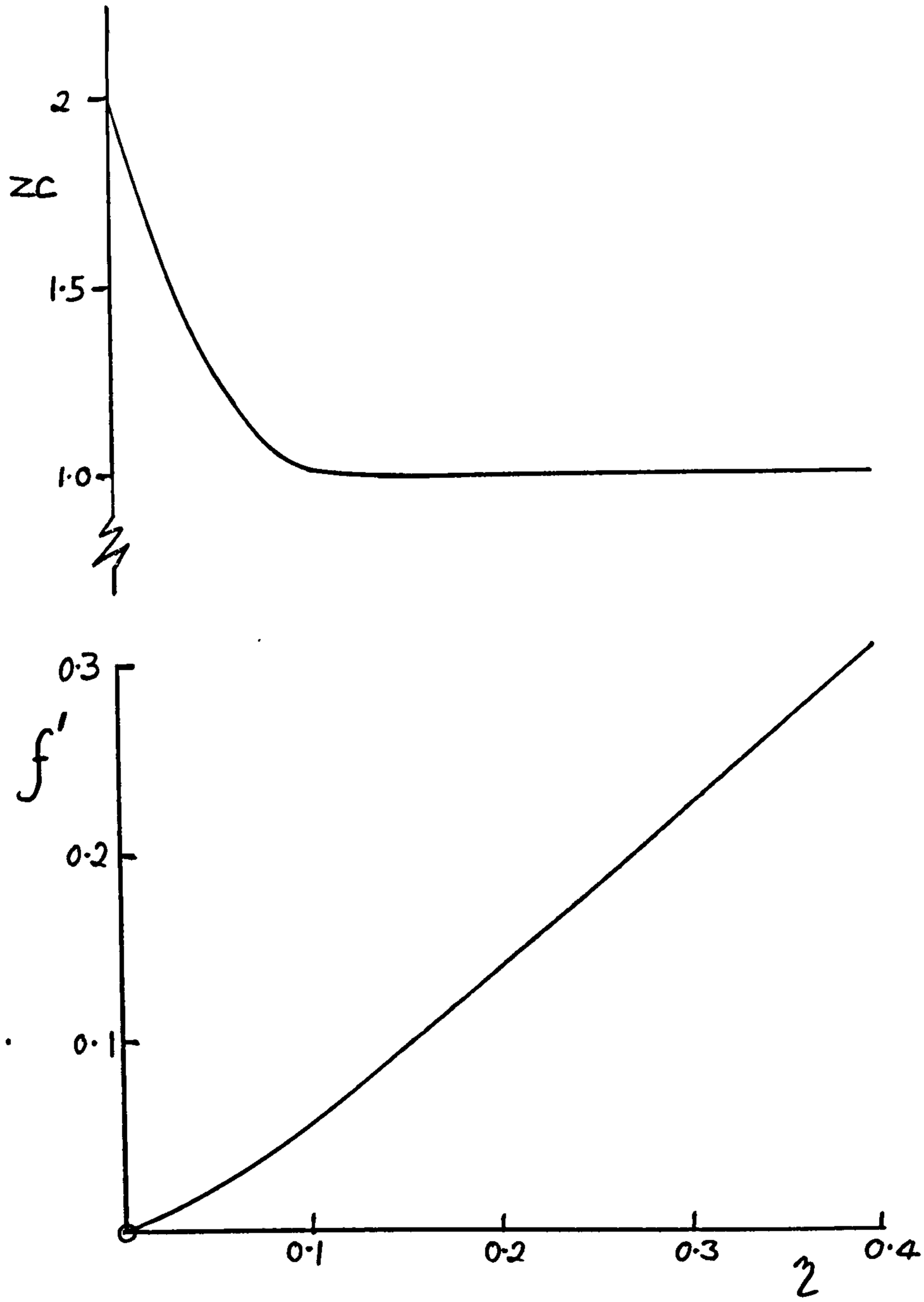

Variation of zc and f' with z.

Sc = 5000.

Figure 12.2

TABLE 12.3

Sc	ZCw	ZC_∞	$\left(\frac{z c' e^{-zc}}{Sc^{\frac{1}{3}}}\right)$ WALL
9000	2	0	.455
7000	2	0	.456
5000	2	0	.457
3000	2	0	.459
9000	1	0	.368
7000	1	0	.369
5000	1	0	.370
3000	1	0	.371
1000	1	0	.373
5000	3	0	.475
5000	2.5	0	.469
5000	2	0	.457
5000	1.5	0	.430
5000	1	0	.370
5000	.5	0	.246
5000	2	1.25	.150
5000	2.	1	.161
5000	2	.75	.217
5000	2	.5	.283
5000	2	.25	.362
5000	2	.1	.416
5000	2	0	.457
5000	1	.6	.316
5000	1	.5	.323
5000	1	.4	.332
5000	1	.3	.340
5000	1	.2	.349
5000	1	.1	.359
5000	1	0	.370

These results are plotted in Figure 12.4 which also includes the constant property solution (Levich § 22).

Though interesting, this solution does not bear directly on E.C.M., and ignores the effect of any electric field which will exert a considerable influence on the high concentration gradients experienced.

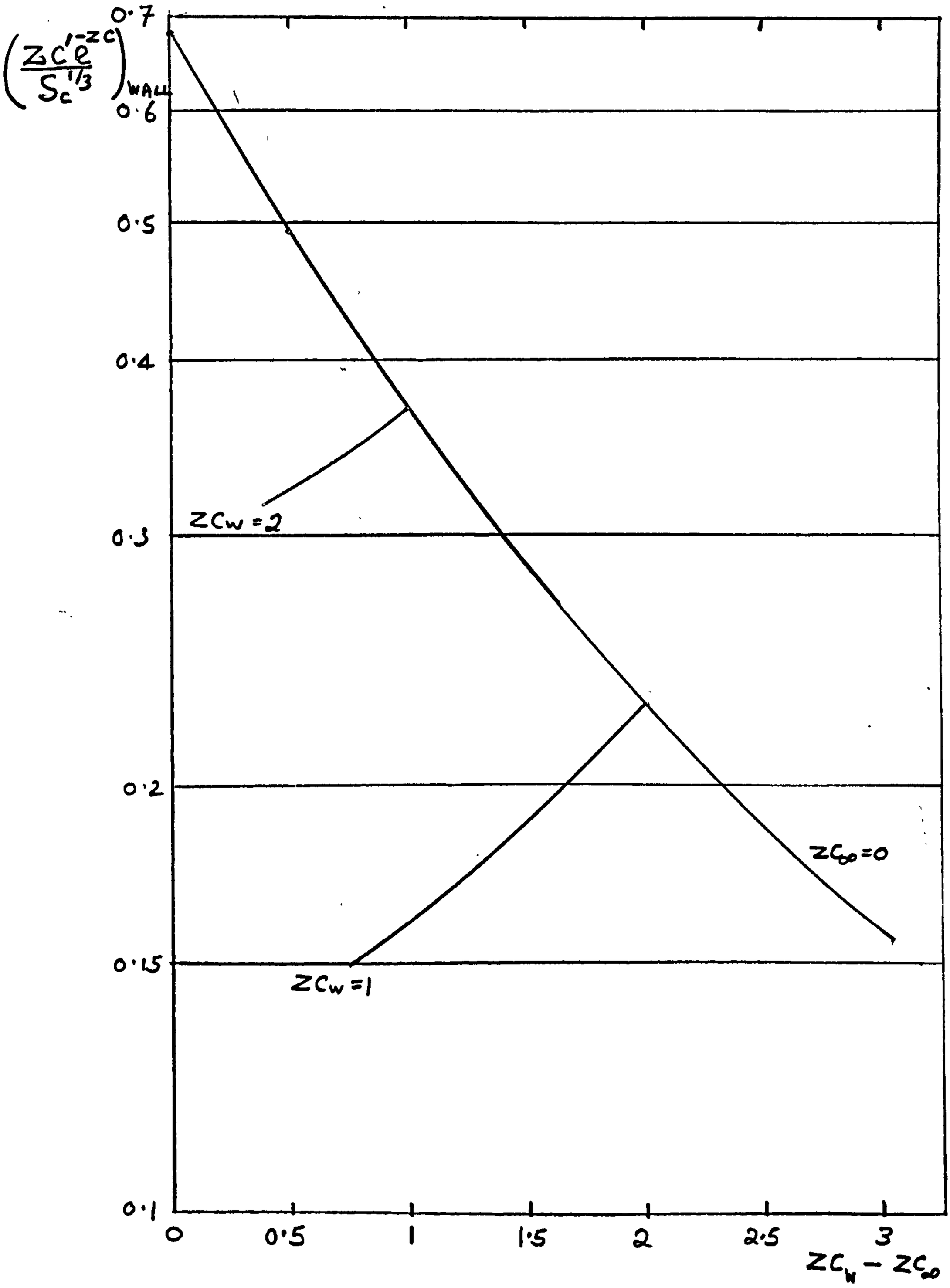

Variation of current at wall with zc_w and zc_∞

Figure 12.4

13. CONCLUSIONS AND SUGGESTIONS FOR FURTHER WORK

13.1. Conclusions

The main achievements of the work contained in this thesis can be summarised as follows. It has been shown that the current - voltage characteristic of the E.C.M. process is a complicated one containing two limiting currents. The lower is deduced to be the electropolishing limiting current, associated with the formation of a thin film, probably of an impure oxide, on the anode surface. The higher has been shown by photography, potential and current distribution experiments, and further tests with surfactant and pressure variation to be due to a crisis of cathodic hydrogen evolution. The shape of the characteristic curve has been explained qualitatively throughout, and detailed mechanisms suggested for the important features.

13.2. Relevance to Industrial E.C.M.

The results of this investigation provide some information of immediate industrial importance

(1) The use of surfactants such as "Teepol" must be avoided.

(2) High flow rates lead to more uniform current distributions.

(3) High static pressures throughout the gap also lead to more uniform current distributions.

(4) Arcing is caused by reaching the limiting current, which should be avoided.

13.3. Further Work.

The theoretical work included in Chapter 12 was found to have been founded on incorrect assumptions of the dominating features of E.C.M. Work is now in hand on an analysis of the mass transfer to an electrode in the presence of gas evolution.

To provide date for theoretical work, experiments are needed on the effect of gas evolution on the mass transfer process. Data is available for "static" fluid (Duffield, 20) but not for channel flows.

A study of the characteristic curve for other metal-electrolyte combinations, in particular for alloys such as brass, nimonics and steels, together with studies of the transient behaviour of the current when the anode voltage is switched rapidly from one value to another, would be an important contribution; some work is in hand at the University of Nottingham on these lines.

Further investigation into the effect of variation of surface tension of the electrolyte might produce useful results for industrial application, and an investigation into the possibility of using low temperatures (between 0 and -100° C) in the laboratory looks a promising line of research. (16,21)

Assessments of the exact proportions of the available current going into metal removal and gas evolution, and the Faradaic efficiency of metal removal, are of immediate industrial importance. Work on the latter is proceeding at the University of Nottingham, but at present no work is being done where both metal removal rate and gas evolution rate are measured simultaneously. This omission needs rectifying.

REFERENCES

General (Chapter 1)

Faust. C.L. E.C.M. of Metals
Trans. Inst. Metal Finishing 41, 1.1964 p.1

Ho,S. Researches on E.C.M. Process
J. Mechanical Lab. of Japan. 9, 2, 1963 p.34
10 , 2, 1964 p.33
11, 1, 1965 p. 8

Kleiner.W.B., E.C.M. production made practical by good tooling and controls.
S.A.E. Journal 72, 11, 1964 p.66

Batelle Memorial Institute.
DM/C Memoranda 28 1959

Cole.R.R. Basic research in E.C.M.
Int. J. Production Research 4, 2, 1965 p.75

Particular

1. Tegart.W.J. The electrolytic and chemical polishing of metals
Pergamon 1956

2. Bayer.J., Final report on Electrolytic machining development 1964
ML - TDR- 64-313.

3. McGeough.J.A., Thesis. University of Glasgow 1966.

4. a.Hoar.T.P. & Rothwell.G.P., The influence of solution flow on anodic polishing. Copper in aqueous o-phosphoric acid.
Electrochimica Acta 9, 135 1964.

4.b as above Magnesium in ethanolic o-phosphoric acid 92
and nickel in aqueous sulphuric acid.
Electrochimica Acta 10, 403, 1965

c. Hoar,T.P., Mears.D.C., & Rothwell,G.P.,
The relationship between anodic passivity,
brightening and pitting.
Corrosion Science 5, 279 1965.

5. P.E.R.A. Report No. 144.

6. Meredith.R.E., & Tobias.C.W. in: Advances in
Electrochemistry and Electrochemical
engineering. Vol.2. p 15
Interscience 1962

7. Davies.J.A., Domeij,B., Pringle.J.P.S., & Brown.F.,
The Migration of metal and oxygen
during anodic film formation.
J. Electrochem. Soc. 112, 7, 1965. P.675

8. Vermilyea.D.A., Electronic conduction in anodic films
J. Electrochem. Soc. 112., 12.1965, p.1232

9. Francis,H.A., Direct Observation of the Anodic
Oxidation of Aluminium
J. Electrochem.Soc. 112, 12, 1965, p.1234

10. Bockris,J. O'M. ,Reddy,A.K.N., & Rao.,B.,
An ellipsometric determination of
the mechanism of passivity of Nickel.
J. Electrochem,Soc. 113, 11, 1966.p.1133

11. Ammar I.A., & Darwish,S., Potentiostatic behaviour
of passive nickel in sulphuric acid.
Electrochimica Acta 11 1966. p.1541

12. Valeev, A. Sh., & Chibizova,G.P.,
Anodic dissolution of copper investigated
by a shadowgraph method.
Russian J. Physical Chem. 39, 1965, 6.p.790

13. Valeev, A.Sh., & Grechukhina,T.N.,
Relationship of structural changes in the
surface of copper during anodic solution
to the semi-conductor properties of the
film that arises.
Izv. Akad. Nauk. S.S.S.R. Ser.Khim. 11 1965. P.1942

14. and " " " " " " " " P.1946

15. Turner,T.S., & Cuthbertson,J.W. Electrochemical Machinery.
Production engineer 45, 5, 1966.p.270
and " " 46, 1, 1967, p.2.

16. Hopkins,E.N., Peterson,D.I., & Baker.H.H.,
A Universal electropolishing method I.S. 1184.

17. Edwards, O.W., & Huffman,E.O., Diffusion of aqueous
solutions of phosphoric acid at 25°C.
J. Phys.Chem. 63 1959,p.1830

18. Zembura,W. & Michalik.W.,
The Limiting current during electrolyte
polishing of copper in a 20N. $H_3 PO_4$
solution.
Bull. Acad. Polonaise. Sci. V 11. 1957.p.1073

19. Han,C.Y., & Griffith.P.,
Mechanism of heat transfer in neucleate
pool boiling.
Int.J.Heat & Mass transfer. 8 6., 1965. p.887

20. Duffield.P.L., Diffusion controlled electrolysis at a porous electrode with gas injection Thesis. Imperial College 1966.

21. Krichmar,S.I., Anodic dissolution of copper Russ.J., Physical Chemistry.39. 4. 1965. p.433

22. Levich.,V.G., Physiochemical Hydrodynamics Prentice Hall 1962.

23. Straumanis.,M.E., et al. The Valency of aluminium ions and the anodic disintegration of the metal.1965. AD. 610 — 194.

24. Stokes,R.H., & Mills,R., Viscosity of Electrolytes and related properties. p 66. Pergamon. 1965.

25. Robinson, R.A., & Stokes, R.H.. Electrolyte solutions. p44. Butterworths 1959